Very Large Telescope

Paranal Science Operations

CRIRES User Manual

Doc. No. VLT-MAN-ESO-14500-3486

Issue 83.2, Date 19/12/2008

R. Siebenmorgen, A.Smette 19/12/2008
Prepared . . . .
                                                    Date   Signature

G. Marconi
Approved . . . .
                                                    Date   Signature

C. Dumas
Released . . . .
                                                    Date   Signature

This page was intentionally left blank

Change Record

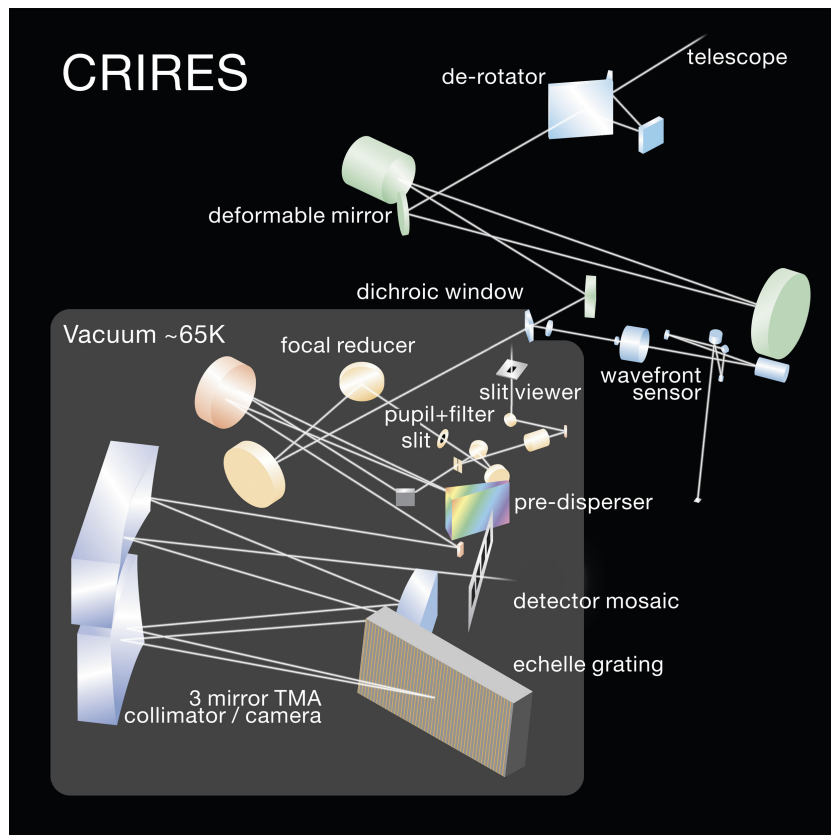| Issue/Rev.	Date	Section/Parag. affected	Reason/Initiation/Documents/Remarks
79.1	29/08/06	all	RSI,ASM: First release, issued for P79 Phase1
79.2	08/09/06	all	ASM: Sec. 11, corrected wavelength table
79.3	20/12/06	all	RSI, ASM, comments DMD
79.4	21/12/06	14,15	ASM, minor editorial corrections
80.1	05/03/07	0,1	ASM, corrected layout figure and description
		3	added a web-link
		6	corrected detector gain
			added comments on a non-linearity correction method
			minor updates and corrected typos
		5	updated limiting mag. in noAO
		8	added subsection on entrance window transmission
			updated sensitivities
		10	updated overheads
		11	added 3 recommended DIT values, updated text
		12	updated
80.2	12/03/07	0,8.1,10.3	corrected typos
		7.2,14.2	added paragraph on gas-cell
			and generic offsets template
80.3	20/03/07	15	corrected J band wavelength ranges
80.4	26/03/07	15	corrected missing entries in Table 4
80.5	07/05/07	1	corrected description
	21/05/07	14.2	new observation template
	05/06/07	7.2	added link to N2O line list; 1st results on RV accuracy
	09/06/07	0,1,7.4	corrected slit length and slit viewer f-o-v
	09/06/07	14.1.1	corrected typo in RA offset
	09/06/07	12	daytime wavecal only for $\lambda < 2400$ nm
	19/06/07	1.4,6.4	contact information, odd-even
	19/06/07	8.4	add important note on intermediate slit
	20/06/07	17,18	new section 17, update §18
	20/06/07	11.1,14.1	added comments on ext. objects, moving targets
	20/06/07	9.3	added comments on std stars
	20/06/07	14.2	added gas cell P2PP parameter description
81.1	31/08/07	8.4	updated
	31/08/07	8.2	Added Fig. 21: comparison UVES vs CRIRES
	31/08/07	10.3	Table 3 (overheads) updated
	31/08/07	15	Slightly changed captions
	01/09/07	6.4	Added links to method and reference frames
	01/09/07	9.1	Added link to ETC
	01/09/07	11.2.1	Added para.: choice of a SVGS in crowded field
	01/09/07	8.2	Added para. on slit loss due to diff. refraction
	01/09/07	11.4	Added requirement for fc
	02/09/07	5, 7.5	Figures added (AO performance, resolving power)
	02/09/07	11.5	Add a para. on airmass

81.2	19/11/07	11.2.4, 14.2, 14.2.5	Added SpectroAstrometry template
	20/11/07	14.1.2	Change default value of SEQ.NGS.USELASTSKY to T
	21/11/07	1.5	New section: NEWS
	21/11/07	10.1	Added: specific comments for SM (telluric OBs)
	22/11/07	14.2.4	Expanded description of generic offsets template
	18/12/07	Table 1	Dark current values corrected
	18/12/07	7.2	Changed comment regarding gas-cells
	27/12/07	Tables 4a-5h	Wavelength settings updated
	27/12/07	§7.5, 8.4,9.1, 9.2.1	typos corrected
	27/12/07	§9.2.3, 10.2, 11.1, 11.2.1	typos corrected
	27/12/07	§11.2.4,10.1,13.1, 14.1, 5	typos corrected
	27/12/07	§11.5.3, 5.1	clarified
	27/12/07	§7.3, 5.2	updated
	28/12/07	§5.1.2	AO star bright mag. limit updated
82.1	20/01/08	§7.2	updated available gas-cells
	20/01/08	§19	added section
	03/03/08	§7.1	updated: new configuration table
	03/03/08	§8.4	updated
	03/03/08	§11.7	numbering changed
	03/03/08	§11.6	new sub-section on water vapor
	03/03/08	§14.1.6	updated
	03/03/08	§18	updated
82.2	19/06/08	§10.2	ETC updated: precipitable water vapor
	19/06/08	Table 3	incl. overhead for derotator motion in spectroastrometry
	19/06/08	§9.1,Fig.24	added a fig. with water vapor only transmission
	23/06/08	§7.2	ThAr fibers, CO gas-cell and visitor gas-cells
	23/06/08	§14.2.2 14.3.5	Updated for the use of CO gas-cell
	23/06/08	§1.5	Updated
	23/06/08	§2.1, 11.2.5	Updated for ThAr fiber
	25/06/08	§12	calibration plan updated
	25/06/08	§14.1.6	added note regarding slit width
	25/06/08	§7.1	Added note: vacuum wavelength are used
	25/06/08	§11.4	Added note regarding multiple stars
83.1	29/08/08	Tab. 8a	updated with CO gas-cell for order 24
	29/08/08	§1.5	news updated
	29/08/08	§19.1	checklist updated
	29/08/08	§7.2.1	update on identification of ThAr lines
	29/08/08	§7.4	added not regarding slit width
83.2	19/12/08	§7.2.2	radial-velocity measurements: added
	19/12/08	§7.5	spectral resolution: updated
	19/12/08	§6.5	linearity: added
	19/12/08	§14.1.2	WFS last sky measurements: updated
	19/12/08	§8.2	limitations due to differential refraction: removed
	19/12/08	§1.3,11, 19.2	P2PP links: updated

Abbreviations and Acronyms

AO	Adaptive optics
APD	Avalanche photo-diode
BOB	Broker of observation blocks
CPL	Common Pipeline Library
CRIRES	Cryogenic high-resolution infrared echelle spectrograph
DM	Deformable mirror
DMO	Data management and operations division
ESO	European Southern Observatory
ETC	Exposure time calculator
FC	Finding chart
FoV	Field of view
FWHM	Full width at half maximum
NGS	Natural guide stars
NIR	Near infrared
NIST	National Institute of Standards and Technology
OB	Observation block
P2PP	Phase II proposal preparation
PSF	Point spread function
QC	Quality control
RTC	Real time computer
RTD	Real time display
SDD	Software Development Division
SM	Service mode
SNR	Signal-to-noise ratio
SR	Strehl ratio
TIO	Telescope and instrument operator
TTM	Tip-tilt mount
USD	User support department
VLT	Very large telescope
VM	Visitor mode
WF	Wave front
WFS	Wave front sensor

Overview

CRIRES

telescope

de-rotator

deformable mirror

dichroic window

Vacuum ~65K   focal reducer

slit viewer

wavefront sensor

pupil+filter
slit

pre-disperser

detector mosaic

echelle grating

3 mirror TMA
collimator / camera

Calibration system	halogen lamp, IR-emitter, ThAr, N_2O gas cell
Adaptive optics	60-actuator curvature sensing MACAO system
Slit length	$\approx 31\,''$
Slit width	$0.05\,''$ – $3.0\,''$: recommended $0.2\,''$ – $0.4\,''$
Echelle grating	40×20cm, 31.6 lines/mm, 63.5^o blaze angle
Resolving power	$100,000$ ($0.2\,''$); $50,000$ ($0.4\,''$ slit)
Wavelength range	0.95μm $\leq \lambda \leq 5.4\mu$m
Free spectral range	$\lambda/70$
Detector science array	4096×512 pixels using 4 Aladdin III detectors
Pixel scale	$0.086\,''$
Slit viewer: filters	J, H, K + 2 H neutral density
Slit viewer: detector	Aladdin III array
Slit viewer: field-of-view	$\approx 36\,'' \times 43\,''$
Slit viewer: pixel scale	$\approx 0.045\,''$
Pre-disperser	ZnSe prism

This page was intentionally left (almost) blank

Contents

1 Introduction

The cryogenic high-resolution IR echelle spectrograph – CRIRES – is the infrared (0.95μm – 5.4μm) high–resolution spectrograph located at the Nasmyth A focus of UT1 (Antu). It provides long–slit (31 ʺ) spectroscopy with a spatial sampling of 0.086 ʺ. Spatial resolution and signal–to–noise ratio can be maximized by the optional use of a MACAO adaptive optics system equipped with an optical (R band) wavefront sensor.

The main optical elements consist of a prism acting as a pre–disperser and a 31.6 lines/mm echelle grating. Total spectral coverage per individual wavelength setting is $\sim \lambda/70$ thanks to an array of four Aladdin III detectors. Acquisition and guiding are performed by means of a slit viewer equipped with an additional Aladdin III detector and a series of 5 filters (J,H,K and two neutral density H filters).

CRIRES has been designed to exploit the enormously enhanced sensitivity provided by a spectroscopic instrument with a large detector array at an 8m telescope. The quantitative and qualitative improvements of observational capabilities affect all scientific applications aiming at fainter objects with higher spatial (extended sources), spectral and temporal resolutions. Indeed, CRIRES provides:

- High-resolution spectroscopy in the 1-5 μm range at the VLT. This instrument employs the largest available grating for a spectral resolving power of up to $\approx$100,000 (for 2 pixel Nyquist sampling) with a 0.2ʺ slit;

- Spectral coverage maximized through four 1024 x 512 pixel InSb detector arrays in the focal plane;

- Spectral imaging using a 31ʺ long slit;

- Adaptive Optics to maximize the signal-to-noise ratio (SNR) and spatial resolution.

Functionally, the instrument can be divided into four units:

1. The fore-optics unit provides field de-rotation, cold pupil and field stops, curvature sensing adaptive optics, and slit viewing.

2. The prism pre-disperser isolates one echelle order and minimizes the total amount of background entering the high-resolution unit.

3. The high-resolution unit comprises the collimator, the echelle which is tilt-tuned for wavelength selection, the camera and the science detectors.

4. The calibration unit outside the cryogenic environment contains the light sources for wavelength calibration and detector flat-fielding.

1.1 Science drivers

Thanks to CRIRES, new phenomena and objects are now available for spectroscopic studies. Some highlights are:

- *Extra-solar planets*:

- – radial velocities
- – spectroscopy of CO, CH_4

- *Solar system*:

  - – Giant planets, Titan: H_3^+, CH_4, CH_3, NH_3, HCN, ...
  - – Terrestrial planets: CO, HCL, HDO, H_2O, ...
  - – Mars: imaging spectroscopy of CO depletion at 40km resolution
  - – Io: volcanic activity (SO_2)
  - – Pluto, Charon, Triton: CO, CH_4 search
  - – Comets: H_2O abundance, temperatures, velocities

- *Stars*:

  - – stellar evolution and nucleosynthesis: CNO abundance
  - – stellar mass
  - – stellar radii
  - – stellar winds and mass loss
  - – atmospheric structure and oscillations
  - – magnetic field structure

- *Star formation and ISM*:

  - – accretion and outflows
  - – ISM chemistry and cloud structures: H_3^+, H_2O, CH_4, ...

- *Extragalactic astronomy*:

  - – AGN: velocity structure of the broad and narrow line region, [FeII], H_2 lines in low extinction regions, H recombination
  - – fine structure lines

1.2   Structure and scope of the User Manual

The CRIRES user manual is structured as follows:

- Part I provides a technical description of CRIRES and its adaptive optics system (AO).

- Part II details the instrument performance.

- Part III describes the commonly used observing techniques in the infrared, summarizes the CRIRES observing modes and provides guidelines for Phase 2 preparation.

- Reference material is given in Part IV. It includes a description of the calibration plan, the data format, the template reference guide and the defined wavelength settings.

- Finally, Part 19 provides a number of recommendations written to increase the chances that a program is executed successfully.

1.3   More information on CRIRES

All CRIRES related manuals are available on the CRIRES instrument web pages together with the most updated information on the instrument:

<p align="center">http://www.eso.org/instruments/crires/</p>

Both Service and Visitor mode Observation Blocks (OBs) should be prepared with the latest version of the Phase 2 Proposal Preparation tool (P2PP), available at:

<p align="center">http://www.eso.org/sci/observing/phase2/P2PP/P2PPTool.html.</p>

Information for the preparation of Service mode observations with CRIRES are available at:

<p align="center">http://www.eso.org/sci/observing/phase2/SMGuidelines.html#CRIRES</p>

Visiting astronomers do not need to submit Observation Blocks in advance of their observations. However, they should prepare them before arriving at the observatory or, at the latest, at the observatory the nights before their observing run. They will find further instructions on the Paranal Science Operations web page and the Paranal Observatory home page:

<p align="center">http://www.eso.org/paranal/
http://www.eso.org/paranal/sciops/</p>

Reference frames, static calibration frames, information regarding the CRIRES pipeline and quality control can be found at:

<p align="center">http://www.eso.org/observing/dfo/quality/
http://www.eso.org/observing/dfo/quality/index_crires.html</p>

1.4   Contact Information

In case of specific questions related to Service Mode observations and proposal preparation please contact the ESO User Support Department:

<p align="center">usd–help@eso.org</p>

For Visitor Mode observations please contact the Paranal Science Operations Team. For general information, use

<p align="center">paranal@eso.org</p>

For specific questions regarding the use of CRIRES, use:

<p align="center">crires@eso.org</p>

1.5   News

Since the release of User Manual v83.1   The announced major change to the instrument control and observing software was successfully implemented in November 2008, although still incomplete at the time of issuing this manual. The missing parts will be implemented in February and March 2009.

Since the release of User Manual v82.2 :

- the CRIRES_spec_cal_Wave template was modified to make use of a variable neutral density filter : this allows optimal illumination of the ThAr lines while avoiding the risk to introduce remanence by the brightest lines..

During P82, a major change to the instrument control and observing software will take place. Implementation of differential refraction correction is one of the advantages visible to the users, allowing to keep the object properly centered while observing at high airmass and with a reference wavelength different from the effective wavelength of the slit viewer filter. §8.2 will be updated once appropriate tests are performed.

In January 2009, an intervention is foreseen. At the time of issuing this Manual, the following actions are planned: (a) replace the cryo-coolers by another model to avoid vibrations affecting the VLTI (currently, the cryo-coolers are switched off during a VLTI-UT run; therefore, CRIRES cannot be used neither during a VLTI-UT run nor a few days after); (b) slightly lower the location of the science detector mosaic which would allow to offer a longer slit length; (c) installation of metrology fibers that would allow to guarantee a better reproducibility of the wavelength settings both in terms of wavelength range and spectral dispersion.

Since the release of User Manual v82.1 :

- version 1.7.0 of the CRIRES pipeline is available: `http://www.eso.org/projects/dfs/dfs-shared/web/vlt/vlt-instrument-pipelines.html`;

- a CO gas-cell is available;

- an intervention took place in April 2008; it consisted in

  1. replacing the carriage by a faster translation table;

  2. moving the ThAr lamp mounted on the carriage to a location close to the baffle where it feeds a set of fibers through a neutral density filter. The end of these fibers are fixed on a connector located on the carriage. In this way, a lot of scattered light is eliminated and spectrograph distortion can be estimated for each ThAr spectrum;

  3. installation of an AO fiber for AO calibrations, until then performed using a pinhole;

  4. an encoder has been installed to control the intermediate slit therefore increasing its reproducibility;

  5. the location of sensors and the values of control loop parameters have been modified to increase the thermal stability of the instrument; a reproducibility of less than 2 pixels has been achieved once the instrument is stable in temperature.

- unfortunately, a detaching Sheldal tape (initially used to decrease possible scattered light) started to vignette the entrance slit, limiting the field first to 12″, then 8″ after a VLTI run during which the cryo-coolers were switched off to limit the amount of vibrations felt by the VLTI. As a consequence, a new intervention took place in June 2008. The tape has been completely removed. Comparison with the value measured before the intervention indicates that no increase in the amount of scattered has been observed.

- the CRIRES_spec_cal_Wave template was modified to make sure that the ThAr fibers are properly centered in the slit (temperature effects can slightly modified the MACAO optics located in the light path)..

- the ETC has been modified in various aspects, most notably by allowing the choice of sky and transmission spectra for different amount of precipitable of water vapor in the atmosphere.

Since the release of User Manual v81.1

- a first version of the CRIRES pipeline is available: `http://www.eso.org/projects/dfs/dfs-shared/web/vlt/vlt-instrument-pipelines.html`

- a new science template is offered, to apply the spectro-astrometric technique: see §11.2.4

- an intervention took place in December 2007; it consisted in

    1. replacing the slit viewer detector with a new, cosmetically better one; this should decrease the number of bad pixels that affect secondary guiding for faint targets;

    2. replacing the entrance slit jaws; the new slit jaws have sharper edges and show a much improved parallelism, leading to a more constant resolution along the slit;

    3. the temperature setting of the instrument has been changed slightly (70 K, instead of 65 K) to improve the temperature stability of the instrument; as a consequence, the wavelength configuration table has slightly changed: users wishing to use the standard wavelength settings should refer to the reference wavelengths listed in Tables 4a to 4h or 5a to 5h. Note that these tables now include two new columns referring to the *unvignetted range*, i.e., the spectral range over which the illumination could be reproduced to better than 1%, despite the lack of reproducibility of the intermediate slit (mainly) and other optical elements.

Part I

The instrument

2 Cold part: the spectrometer

The CRIRES instrument design is presented by Käufl et al. 2004, SPIE 5492, 1218; a summary is presented in the following subsections.
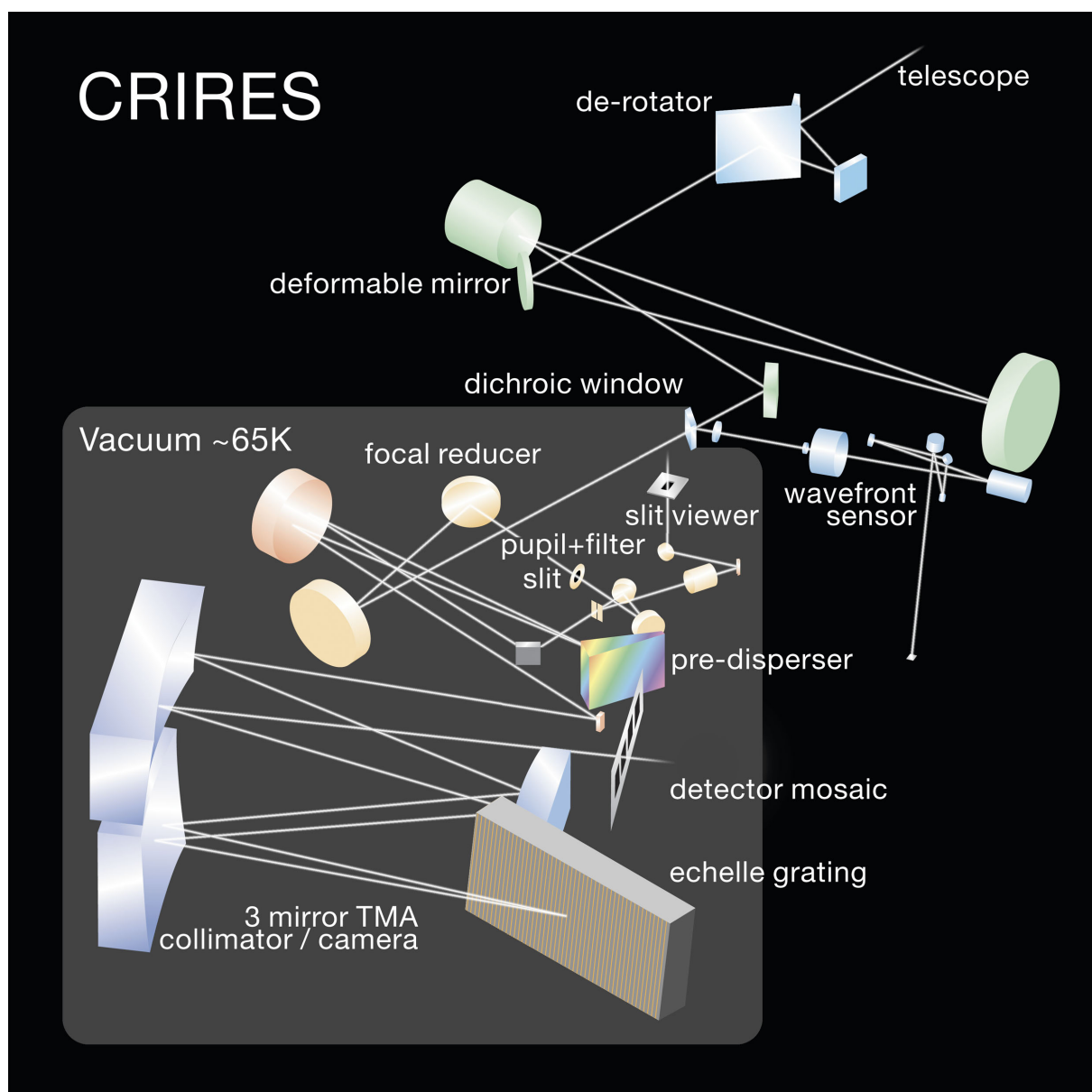

Figure 1: Layout of the CRIRES optical design.

2.1 Optics

The optical layout of CRIRES is shown in Fig. 1. Light enters from the direction of the telescope Nasmyth focus, either via the telescope or from the calibration unit after insertion of a calibration mirror in the light-path.

The calibration unit itself consists of an integrating sphere illuminated by a continuum, Halogen lamp for flat-fielding and, together with a gas–cell, for wavelength calibration. An IR-emitter lamp used for technical tests is also located in the integrating sphere. The integrating sphere provides uniform illumination of the entrance slit of the spectrometer and its flux can be adjusted by a moving baffle.

A carriage can then insert one of the following elements in the light path: (i) a gas-cell either for wavelength calibrations when used with the halogen lamp, or for accurate radial-velocity measurements, similar to the way the iodine cell is used in UVES; (ii) a pinhole used for calibration purposes; (iii) an AO fiber for MACAO calibrations; (iii) a set of fibers fed by a Thorium–Argon lamp used for wavelength calibration. This carriage has also a free position, with no optical element.

Light then goes through a 3 mirror de-rotator which can be used to counteract the telescope field rotation for observations with a slit fixed relative to the sky. On the other hand, for point sources, it can also maintain the slit aligned along the parallactic angle to accommodate the differential atmospheric refraction between the R band used by the adaptive optics system and the IR band used for observations and slit viewer guiding.

Next, the adaptive optics (AO) system concentrates the light on the spectrograph's entrance slit. The AO wavefront sensor uses the visible light reflected by the dichroic (which serves also as entrance window) while the infrared light enters the cryogenic spectrograph. Further details of the AO system can be found in Sect. 3 of this manual. CRIRES can be used without adaptive optics, in which case the AO module just acts as relay optics and the spatial resolution is given by the natural seeing.

The spectrograph itself is housed in a vacuum vessel. Following the input window, a pupil image is formed at the position of a cold stop which limits thermal background. Light then either passes through the slit or is reflected to the slit viewing camera. Light passing through the slit enters the prism spectrometer where it is dispersed and then exits through an intermediate slit sized to limit the wavelength range passing into the high resolution section to a single order. The high resolution spectrograph consists of a 40×20 cm, 31.6 lines/mm, 63.5^o. blaze echelle grating plus a TMA (three mirror anastigmat) which acts first as a collimator and then as a camera to image the spectrum on the four Aladdin detectors effectively forming a 4096×512 array.

2.2 Mechanics

CRIRES is stationary at the Nasmyth A focus of VLT-UT1 (Antu). The instrument is mounted in a 3 m–diameter, 1 m high vessel. Including its support structure, the total weight of the instrument is 6.2 t, spread between 2 t for the warm part or AO system and 4.2 t for the cold part. The optics inside the cryo-vessel is cooled to ~ 70 K. The detectors are stabilized at ~ 25 K within 0.1 K. A main design feature of CRIRES is its cryogenic mechanisms which are required for scanning the pre-disperser prism and echelle grating.
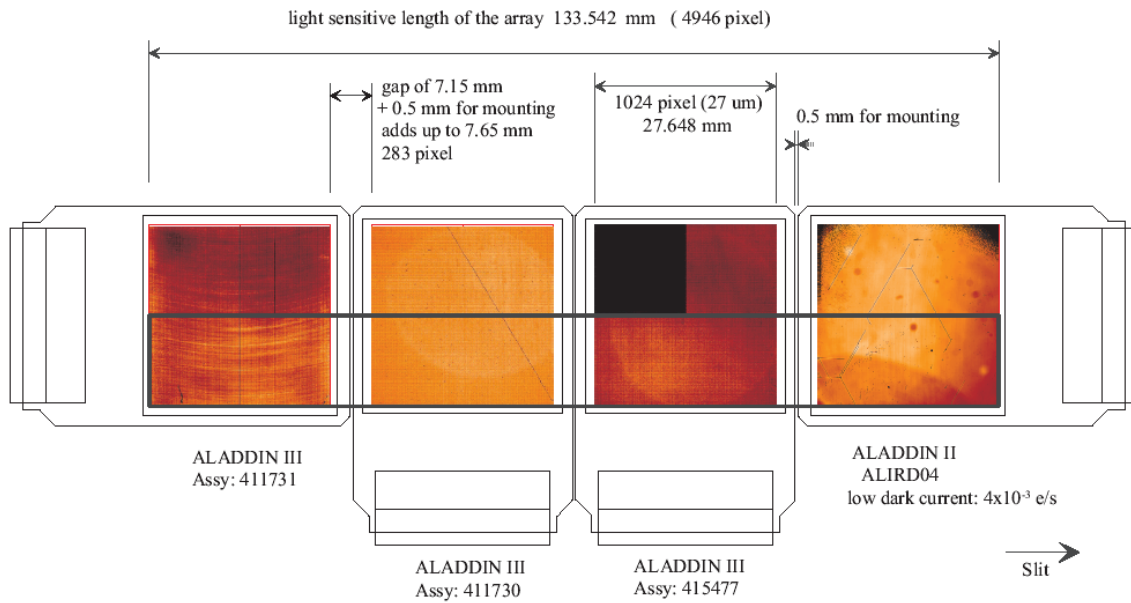
Figure 2: Layout of the mosaic of four Aladdin science detectors, numbered # 1 to # 4 from left to right. The detectors are not science grade arrays and show bad cosmetics. Only the half–bottom part of each detector is used as indicated by the thick, black rectangle. The mosaic used for science observations therefore consists of $4 \times 1024 \times 512$ pixels.

2.3 Detectors

The spectrograph focal plane provides a useful optical field of $135 \times 21\,\mathrm{mm}$ which is well covered by a 4x1 mosaic of four Raytheon 1024x1024 pixel InSb Aladdin III detectors, with a pixel size of 27μm. The spacing between 2 successive detectors corresponds to approximately 280 pixels, and is slightly different from one gap to the other. Fig. 2 shows their relative orientation. In particular, it should be noted that only the 'bottom' half of the mosaic is used and that the reading-out is executed parallel to the mosaic for detectors 2 and 3 and perpendicular to it for detectors 1 and 4.

A fifth Aladdin III detector is used in the slit viewer. The arrays are read out using standard ESO IRACE controllers having 64 channels (4×16) for the science arrays and 32 channels for the slit viewer one.

3 Warm part: the adaptive optics system

The adaptive optics system of CRIRES is discussed by Paufiqué et al. (2004, SPIE 5490, 216). The multi-applications curvature adaptive optics system (MACAO) for CRIRES corrects a turbulent wavefront and provides diffraction limited images at the focal plane. The overall sensitivity is thereby improved by about a factor two for point-sources. To highlight the advantage of combining MACAO and CRIRES a PSF is shown in Fig.3 in AO open loop (uncorrected) and closed loop, where the PSF is reconstructed from wavefront measurements. The non–circular PSF in open loop is due to the very short integration time used.
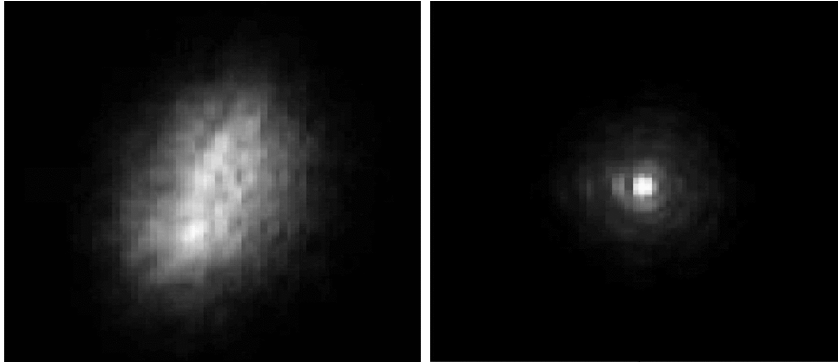
Figure 3: PSF without (left) and with (right) AO correction. Images have been taken in the lab using a turbulence generator.

3.1 Introduction

The following section provides an introduction to the field of adaptive optics and atmospheric turbulence, and essentially is taken from the NACO user manual. For further reading, see for example: "Adaptive optics in astronomy", Rodier 1999, Cambridge University Press, or "Introduction to adaptive optics", Tyson 2000, Bellingham/SPIE.

3.1.1 Atmospheric turbulence

The VLT theoretical diffraction limit is $1.22 \cdot \lambda/D = 0.07$ arcsec at $\lambda = 2.2 \mu$m. But the resolution is severely limited by atmospheric turbulence to $\lambda/r_0 \approx 1$ arcsec, where r_0 is the Fried parameter. r_0 is directly linked to the strength of the turbulence and depends on the wavelength as $\lambda^{6/5}$. For average observing conditions, r_0 is typically 60cm at $2.2\,\mu$m.

Temperature inhomogeneities in the atmosphere induce temporal and spatial fluctuations in the air refractive index and therefore cause fluctuations in the optical path. This leads to random phase delays that corrugate the wavefront (WF). The path differences are, to a good approximation, achromatic. Only the phase of the WF is chromatic. The coherence time of WF distortions is related to the average wind speed V in the atmosphere and is typically of the order of $r_0/V = 60$ ms at $2.2\,\mu$m for V = 10 m/s.

3.1.2 Adaptive Optics

A technique to overcome the degrading effects of atmospheric turbulence is real-time compensation of the deformation of the WF by adaptive optics (AO, Figure 4).

The wavefront sensor (WFS) measures WF distortions which are processed by a real-time computer (RTC). The RTC controls a deformable mirror (DM) to compensate the WF distortions. The DM is a continuous thin plate mirror mounted on a set of piezoelectric actuators that push and pull on the back of the mirror.

Because of the significant reduction in the WF distortions by continuous AO correction, it is possible to record near diffraction-limited images with exposure times that are significantly longer than the turbulence coherence time. The residual error from the WF compensation (WF error) directly determines the quality of the formed image. One of the main parameters characterizing this image quality is the Strehl ratio (SR), which corresponds to the amount of light contained in the diffraction-limited core relative to the total flux.
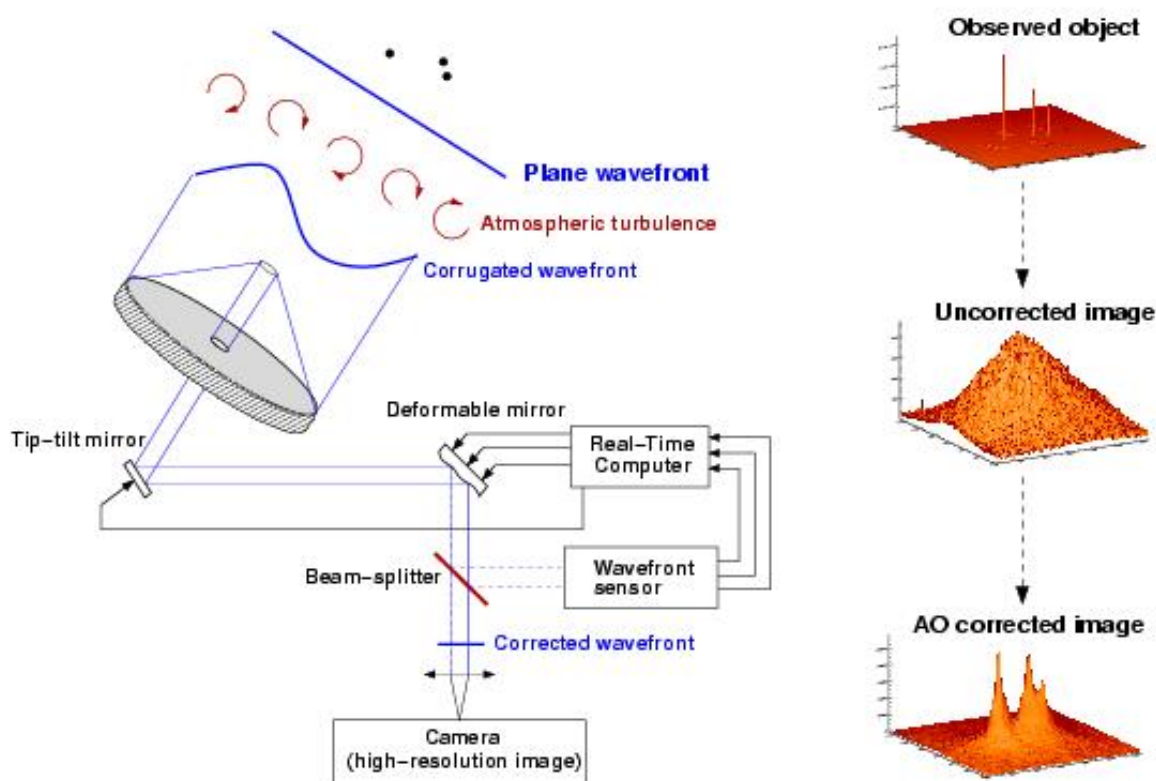
Figure 4: Principle of Adaptive Optics. Note that in practice, and contrary to this schematic design, CRIRES has no dedicated Tip-Tilt mirror, but performs low- and high-order corrections with a single deformable mirror mounted on a tip-tilt stage (see Figures 5 − 6).

An AO system is a servo-loop system working in closed loop. The DM flattens the incoming WF and the WFS measures the residual WF error.

A commonly used WFS is the Shack-Hartmann WFS, used for example in NACO. However, CRIRES, as well as the other ESO MACAO systems, relies on a curvature WFS: it is designed to measure the WF curvature as opposed to the WF slope. This is achieved by comparing the irradiance distributions of two planes placed behind and in front of the focal plane. In practice, a variable curvature mirror (membrane) is placed in the telescope focus. By vibrating, inside

and outside focus blurred pupil images can be imaged on a detector array: in the case of CRIRES, a lenslet array feeds avalanche photo-diodes (APDs). The modulation frequency of the membrane corresponds to the temporal sampling frequency of the WFS. The difference between the inside and outside pupil image measures the local WF curvature.

The performance of an AO system is related to the number of lenslets in the lenslet array, the number of actuators behind the DM, and the rate at which WF errors can be measured, processed and corrected (the server-loop bandwidth).

The performance of an AO system is also linked to the observing conditions. The most important parameters are the seeing, the brightness of the reference source used for WFS and the distance between the reference source and the object of interest.

In case of good conditions and a bright, nearby reference source, the correction is good and the resulting point spread function (PSF) is very close to the diffraction limit. A good correction in the K-band typically corresponds to a SR larger than 30%.

At shorter wavelengths (particularly in the J-band) or in the case of poor conditions or a faint, distant reference source, the correction is only partial - the Strehl ratio may only be a few percent.

3.2 Hardware description

The MACAO system for CRIRES is based on a 60-actuator deformable mirror, inserted in a so-called relay optics. These optics and the wavefront sensor optics are mounted on a breadboard located between the Nasmyth focus and the spectrometer. It is about 1.5m wide and a top view of the warm optics overlaid by the optical path is shown in Fig. 5, the assembly of the deformable mirror is displayed in Fig. 6.

3.2.1 The corrective optics

The wavefront correction is performed by a 60 electrode bi-morph mirror developed by CILAS, with a pupil diameter of 60 mm. The 60 electrodes are sandwiched between two thin piezoelectric PZT layers with opposite polarization. The outside surface of the PZT layers are grounded and covered with 0.1mm glass layers, the mirror side being silver coated. Applying a voltage to one electrode produces a constant curvature over its surface. The geometry of the electrodes in the 4 central rings (40 electrodes) matches that of the lenslet array sub-apertures, while the 20 remaining electrodes are located outside the pupil and constrain the edge of the pupil to correct 0-curvature aberrations: tip–tilt, astigmatism, etc. The deformable mirror (DM) provides a stroke to compensate atmospheric aberrations up to an optical seeing of $1''$. In order to relax the use of the outer electrodes of the mirror, the tip–tilt error is slowly offloaded to a tip–tilt mount designed and built by LESIA, which provides a $\pm 240''$ mechanical stroke, i.e. $\pm 3.6''$ on the sky, with a 100 Hz -3dB internal closed-loop bandwidth. The assembly of the DM and tip–tilt mount is shown in Fig.6.

3.2.2 The Wavefront Sensor

The following functions are sequentially implemented in the wavefront analyzer:

- Extraction of the reference star beam (field selector).
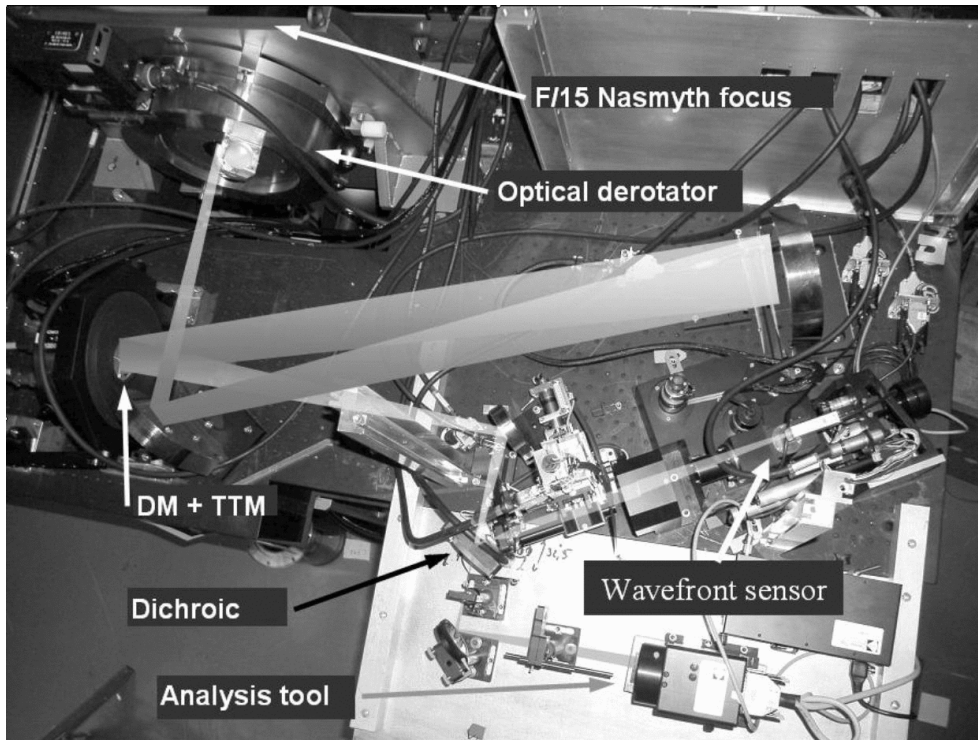
Figure 5: Top view of the warm optics of the MACAO – CRIRES system. From f/15 Nasmyth focus and after the optical derotator, one notices the deformable mirror and tip–tilt mount assembly. Light enters from the dichroic to the cold and warm part of the instrument. For the latter the wavefront sensor and some analysis tools are visible.

- Projection of the reference star image on the membrane mirror (imaging lens).

- Scan of the intra– and extra–pupil regions by modulation of the membrane mirror curvature.

- Creation of a pupil image centered on the lenslet array.

- Reduction of the flux to work within the linear range of the APDs by means of neutral density filters.

- Re-imaging of the 60 sub-pupils on the 60 fiber cores by the lenslet array unit.

- Injection of the collected beams onto the 60 APDs.

The scanning lens of the field selector is mounted on an XYZ table: the XY axes enable the star used for AO correction to be selected in the $50'' \times 50''$ field-of-view, while the Z stage compensates for the VLT field curvature. The position of the field selector defines the reference for the pointing. The imaging lens creates an image of the AO star on the membrane mirror, which is mounted on an acoustic cavity. A voice coil is mounted to the other end of the cavity, and driven at 2.1kHz by the APD counter module to force an oscillation of the focus mode of the membrane mirror. The incidence angle of the beam on the membrane mirror depends on the position of the guiding star in the field. In order to keep the pupil image (obtained when the membrane mirror is flat) centered on the lenslet array, the membrane mirror is mounted on a 2 axis gimbal mount, which is co-ordinated with the field selector. For each (x, y) positions
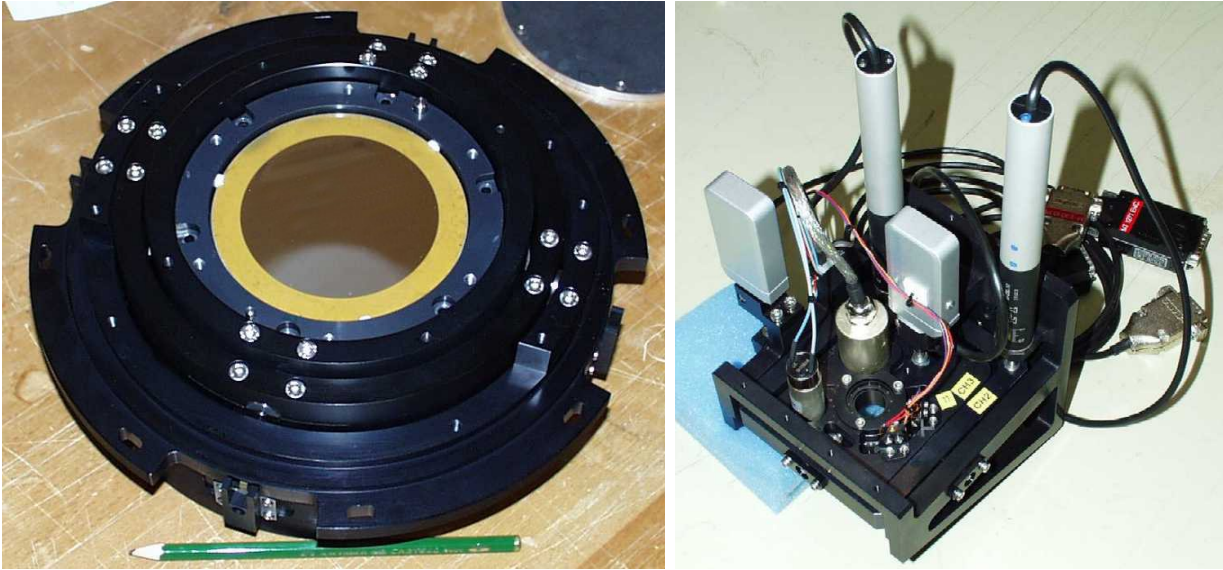
Figure 6: Assembly of the deformable mirror (DM) and tip–tilt mount (TTM) (left) and of the gimbal mount (right).

of the field selector the gimbal mount is moved so that the light is reflected to the same focus. A diaphragm in front of the membrane enables the field to be adjusted to the observing conditions (seeing and guiding reference size). The assembly of the gimbal mount is shown in Fig. 6.

The wavefront sensor box consists of 4 mirrors, which provide parallel beam to image the pupil on the lenslet array. First, the beam is collimated by a spherical mirror. It is then folded by a flat mirror and injected in the beam expander, which adapts its diameter to the lenslet array (14 mm). The optical path of the wavefront sensor box is shown in Fig. 7.

The lenslet array intercepts the beam and divides the flux in 60 sub-aperture. Each sub-pupil is imaged on a fiber, with a 100 μm core diameter. When the membrane mirror vibrates, the pupil image is projected on both sides of the lenslet array plane. The normalized difference between the intra– and extra–pupil flux collected by each sub–aperture is proportional to the local wavefront curvature, which provides the wavefront error. The fibers drive the signal from the fiber feed module to the APD cabinet, mounted on the instrument. The APD counts are recorded by the APD counter module, synchronously with the membrane signal. The front–end assembly of the fiber bundle is shown in Fig. 8.

3.2.3 Control loop

The oscillating membrane produces a signal modulated proportional to the local wavefront curvature. This signal, collected by APDs, is sent to the real time computer (RTC). The RTC computes this modulation, and retrieves the voltages to be applied to the mirror and tip-tilt mount to optimally compensate for the local curvature measured. For this, a precise calibration of the system is required, which includes synchronization of the membrane mirror, determination of the membrane curvature, pupil alignment and interaction matrices.
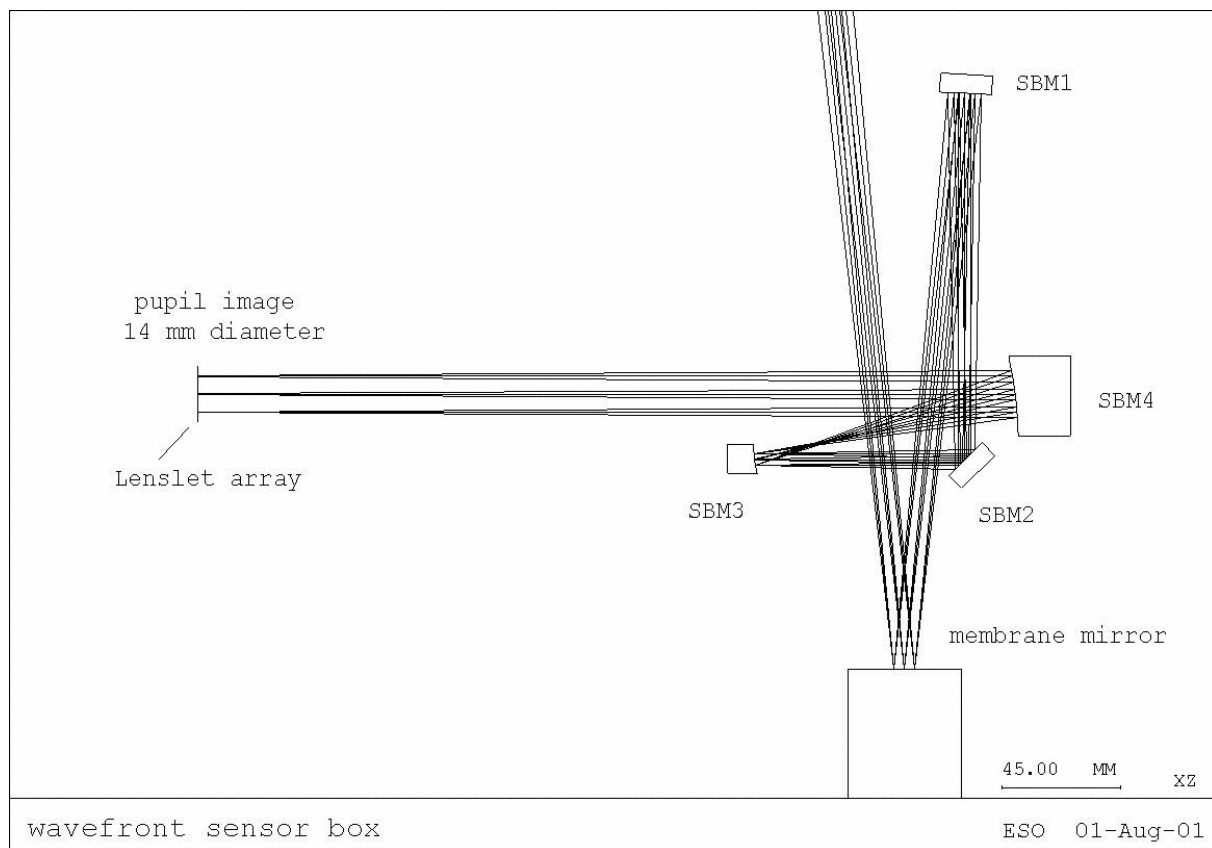
Figure 7: The optical path of the wavefront sensor box.
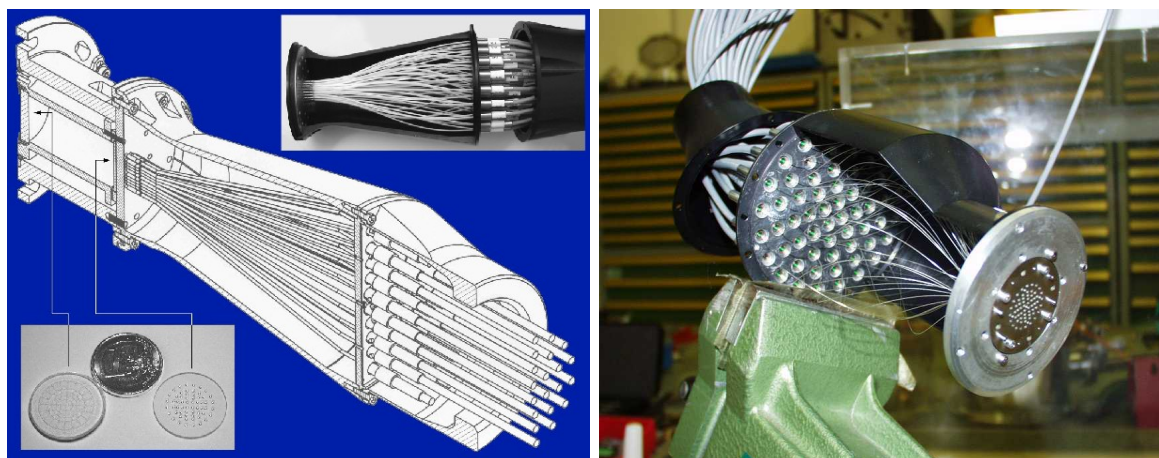
Figure 8: Front–end assembly of the 60 fiber bundle which guide the light to the sensors.

3.2.4   Membrane setting

The membrane mirror curvature represents an optical gain for the aberrations measurements. A way to increase the performance of the system is therefore to increase the curvature of this mirror. Increasing the curvature, however, requires increasing the field of view of the wavefront sensor optics as well. This and some other non-linear effects can degrade the estimate of the curvature. For the same reason, extended sources will affect the quality of curvature measurement, and lead to a different optimal gain. In some extreme cases, the system can be unable to close the loop (extended $6''$ planetary nebula with a faint blue white dwarf in the middle, or a faint star close to the Moon, for example). A trade-off is needed, and an optimal optical gain has to be determined. This optimal gain mainly depends on the seeing, and marginally on the star magnitude and other factors. It is tabulated in the configuration of the software and is transparent for the user.

Part II
Instrument Performance

4   Overview

The sensitivity of the instrument from K-band up to the L and M bands is limited by the thermal background, whereas it is limited by detector performance in J and H. In the thermal background observations benefit from the high resolving power of CRIRES as telluric features are better removed compared to spectrographs at lower resolution.

Possible sources of fringing (e.g interference filters) were avoided in the spectrograph design. The requirement on the grating reproducibility has been set to ~ 0.05 pixel. Currently, the absolute wavelength reproducibility is achieved by the optical model to ≈ 3 pixels.

The detectors are not science grade arrays: they show bad cosmetics and amplifier glow; their response to incident light is non-linear. Information loss caused by bad pixels can be removed by jittering; the amplifier glow in any given exposure can be subtracted out by a dark obtained with the same detector integration time (DIT, see below). However, amplifier glow as well as other systematic effects are best removed by telescope nodding. A method to correct for the non-linearity of the detector has been implemented in the pipeline.

A first light spectrum of the sky is shown in Fig 9. The OH doublet at 1708.6nm is resolved at the resolution of CRIRES. In the dispersion direction the FWHM is 2.8 pixels.

Figure 9:   First light spectrum of the sky. The OH doublet at 1708.6nm is resolved at the resolution of CRIRES.

5 AO performance

The performance achieved by the MACAO system of CRIRES has been evaluated by laboratory simulations by comparing two cases: (i) in closed loop with guide stars of various magnitudes and (ii) in open loop, thus without AO corrections. The optimization was done over the encircled energy on a 0.2 ″ slit, representative of the available energy for the spectrograph. Lab results are confirmed by on-sky measurements and demonstrate some gain in J (more than to 40% for an optical seeing of 0.6″) and a strong (factor ~ 2) increase of the fraction of the energy available for the spectrometer in the K and M band, respectively (Fig. 10).
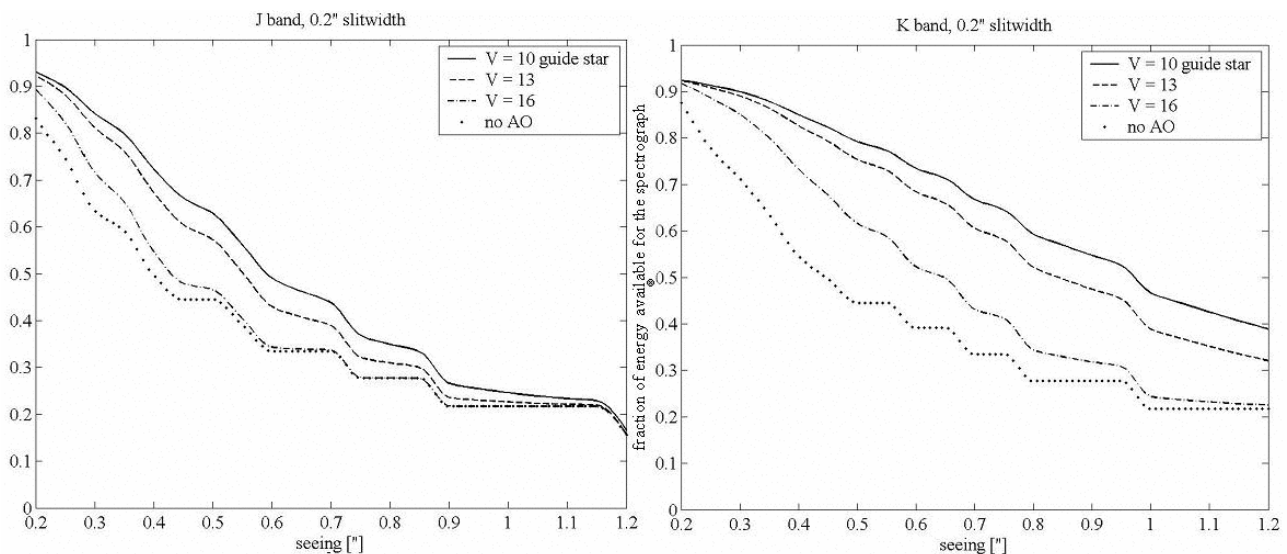
Figure 10: The fraction of energy available for the spectrograph in a 0.2 ″ slit, as a function of optical seeing is shown for the J (left) and K (right) band for AO stars of V=10, 12, 16 mag and without AO correction. For reference please consult the Exposure Time Calculator, (ETC).

Fig. 11 illustrates the increased throughput made possible thanks to the use of the adaptive optics. The graphs shows the spatial profile (summed over a few columns) at $\lambda = 2170$nm of the spectrum of a $m_{\mathrm{RTC}} = 5.3$, in open- and closed- loop. The DIMM seeing was 0.67 and 0.72 ″, respectively, and the coherence time was 3 ms. In both cases, the exposure time was 2 min. The gain in integrated flux is 1.63. In other words, the same flux level is reached in closed-loop in 61% of the time needed in open-loop.

5.1 AO guide stars

CRIRES wavefront sensing is done in the R band. The performance of the adaptive optics system depends on the distance to the science target and on the brightness of the selected guide star.
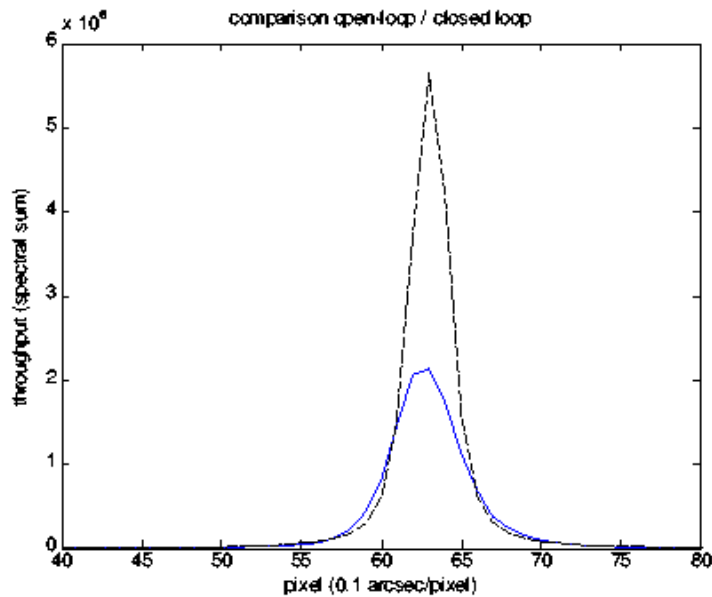
Figure 11: Improved throughput thanks to the use of the MACAO. Flux measured along the slit, measured in open-loop (blue, solid line) and in closed loop (black, dashed line), in the K band.

5.1.1 The distance of the AO star

Although the field selector allows the selection of the AO star within 30 $''$ from the nominal position of the science target, the AO star should be as close as possible to the scientific target, usually closer than 10 $''$: ideally, it is the science target itself. Depending on the atmospheric conditions, in particular, on the isoplanatic angle, θ_0, mild improvement on the amount of encircled energy can still be obtained if a bright ($R < 11$) AO star is used $20 - 30$ $''$ from the scientific target.

It is important to recall that the isoplanatic angle decreases with zenith distance z as $\theta_0 \propto (\sec z)^{-8/5}$ and increases with wavelength as $\theta_0 \propto \lambda^{6/5}$. On the other hand, the Strehl ratio decreases with the angular distance to the AO star θ as $SR \propto \exp\left(-(\theta/\theta_0)^{5/3}\right)$.

5.1.2 The brightness of the AO star

The intra– and extra–focal pupil of the AO star is imaged on a lenslet array. Each lenslet feeds an avalanche photo-diode (APD) that ultimately forwards its signal to the Real Time Computer (RTC) (Sect. 3).

The flux on an APD is limited to 1 million counts in order not to damage the devices. The optimal brightness of the AO star is R $\sim$ 11 mag. Brighter stars up to a bright magnitude limit of $R \sim 0.2$ mag can be dimmed using neutral density filters. Depending on the B-R color, some stars with slightly brighter R magnitude can be used.

Good correction is still obtained with stars as faint as R$\sim$14 mag under average seeing condi-

tions, while moderate image quality improvement is seen with stars as faint as $R \sim 16-17\,\mathrm{mag}$ under good seeing ($\leq 0.6''$) conditions. Stars fainter than R$\sim$17 mag will not result in any improvement.

5.1.3 The color of the AO star

The color is essential for precise atmospheric refraction compensation. The AO system takes into account the differential atmospheric refraction between the wavelength used for the AO and the central wavelength of the spectrograph set-up in the calculation of the tip-tilt mirror orientation.

5.2 Limiting magnitude of slit viewer

Target centering in the NIR is optimized by slit viewing. The slit viewer (SV) is sufficiently sensitive that any emitting point source for which one aims to obtain a spectrum should be seen on the SV image. In particular in AO mode, stars of $J \approx 14$ or $H \approx 14$ are easily detected in a 10 s exposure, a typical time scale for guiding.

In NoAO mode, J=16.5, H=16.0, or Ks=15.4 stars are barely detected (3σ) in a similar 10 s integration under 0.9 $''$ seeing when located away from the slit. For guiding on target in NoAO mode, the limiting magnitude is much brighter as only a small fraction of the light is reflected by the slit jaws to the slit viewer detector. Under 0.9 $''$ seeing and a slit of 0.4 $''$, reasonable guiding was possible with stars of J = 14.1, H = 13.8, Ks = 13.3.

Table 1: Summary of detector parameters.

Parameter	Detector			
	# 1	# 2	# 3	# 4
Dark current (e$^-$/s)	0.053	0.32	0.37	0.34
Gain (e$^-$/ADU)	6.97	6.89	6.92	7.27
Quantum efficiency (e$^-$/γ)	0.92	0.97	0.83	0.73
Read-out-noise (e$^-$ RMS)	9.9	9.7	9.6	10
Saturation level (e$^-$)	120000	120000	120000	120000
Operating Temperature (K)	27.5	27.5	27.5	27.5

6 Detector characteristics

The focal plane of CRIRES is equipped with four 1024 × 1024 pixel InSb Aladdin III, 27 μ pixel detector arrays. However, only the bottom half of each detector is actually illuminated by the slit, so that the useful mosaic actually consists of 4 × 1024 × 512 pixels (Fig. 2). The observer needs to specify only two detector parameters: the detector integration time (DIT) and the number of individual exposures (NDIT) to be averaged in a single exposure, whose total integration time is therefore NDIT×DIT. Both parameters should be adjusted with help of the ETC (Sect. 10.2). Bright objects or observations in the L or M bands require short DITs to avoid saturation; in particular, heavily saturated spectra lead to detector remanence that affects subsequent observations. On the other hand, faint targets in the J, H or even K bands may require DITs up to 900s to decrease the readout-noise contribution. Long DITs are strongly affected by the detector glows which can be corrected by nodding (Sect. 9.2).

All other detector settings such as bias, voltages, operating temperature, etc. are automatically set by the system. Currently, the only read-out mode used is *Fowler Sampling* (Fowler & Gatley 1990 ApJ 353, L33): the detector is first reset, then each pixel is non-destructively read NDSAMPLES/2 times at the start of the exposure, then again NDSAMPLES/2 at the end of the exposure of exposure time DIT. The slope of the relation provides the intensity of the given pixel. The value of NDSAMPLES is 2 for DITs strictly smaller than 10 s, 4 for DITs at least equal to 10 s but strictly smaller than 20 s, etc... up to a maximum of 128.

6.1 Dark and gain

In Fig. 12 dark current and conversion gain of detector # 2 are shown. The dark current is estimated from the slope of the signal (in ADU or e$^-$) as a function of integration time (s) for the linear region. Dark current, gain, read-out-noise, saturation of the four detectors # 1, # 2, # 3, and # 4 as well as the operating temperature are given in Table 1. Note that the raw gain values (cf. Fig 11) have been corrected by a factor of 0.9 to take into account the interpixel capacitance (see Finger et al. 2006, SPIE 6276, 62760F).
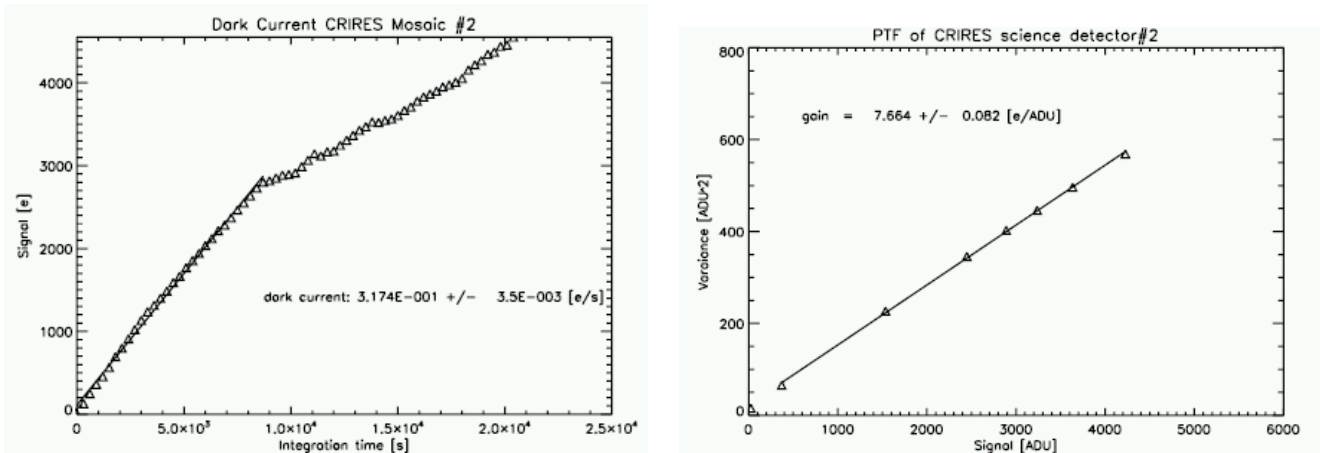
Figure 12: Dark current (left) and conversion gain (right) of detector # 2.

6.2 Glow

The detectors show glow over areas close to the amplifiers, as clearly visible in Fig.13. It is stable and can be subtracted by an exposure obtained with the same DIT. Therefore, in order to best remove it as well as other detector systematics, it is recommended that observations in any given wavelength setting should include at least one nodding cycle. Note however that areas affected by the glow suffers from increased Poisson noise.
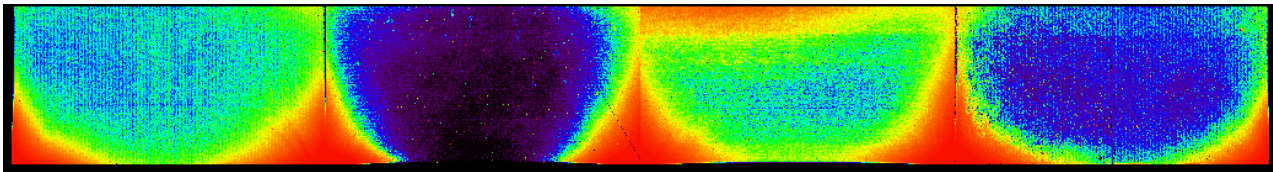
Figure 13: Example of the detector glow on a dark exposure. The detector glow (in red) is emerging from the bottom corners of each detector .

6.3 Fringes

No detector fringes are detected in the wavelength range useful for science observations. Fringes are only visible beyond 5μm, outside the atmospheric window.

6.4 Odd-even effect

Images obtained with the science detectors show a pattern aligned with the reading direction. In other words, the pattern is aligned with the rows of the detectors, parallel to the spectral dispersion, for detectors # 2 and # 3. For detectors # 1 and # 4, the pattern is instead aligned with the columns, i.e. perpendicular to the spectral dispersion. This pattern consists of alternating rows or columns of larger and smaller intensities than the mean value.
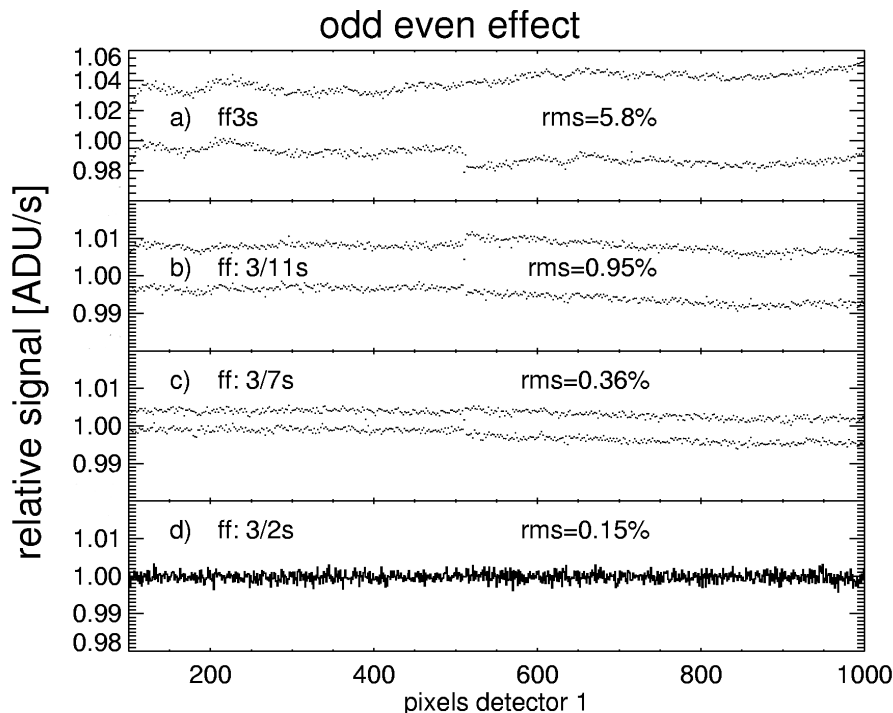
Figure 14: Flats obtained with the halogen lamp at different DITs, for detector 1. Each graph represents 1000 pixels of the image collapsed along the columns. A DIT=1s dark exposure has been subtracted from each image. From top to bottom: (a) a 3 s flat (ff3s) normalized to its median value shows a bimodal distribution of intensities, reflecting the odd–even effect. The measured RMS of the normalized flat is 5.8%. Panel (b) shows the ratio between two dark subtracted flats of 11s and 3s, respectively. The ratio shows an RMS of 0.95%. Panel (c) is similar to (b) but for flats with DITs of 3 and 7s, respectively. The RMS of the ratio is 0.36%. Panel (d) shows that the ratio for 2 flats obtained with DITs of 2s and 3s, respectively has an RMS of 0.15%. The decrease of the scatter in the ratio of flats when DITs tend to be similar demonstrates that the odd–even effect depends on the signal level.

This effect cannot be removed by simple flat fielding and is still visible after nodding. Figure 14 gives an example based on a sequence of flats obtained with different DIT settings. It shows that this "odd-even" effect depends on the signal level. A method to correct for the odd-even effect is described in the next paragraph.

6.5   Detector linearity

All common IR detectors suffer from non-linear effects. In the case of CRIRES, non-linearity effects are of the order of 3% at about 4,000 ADUs ($\approx 32,000e^-$) and increase with flux.

The CRIRES team has developed a method that appears to efficiently correct for the non-linear behavior of the detector, including the odd-even effect. Results obtained at the date of issue of this manual indicates that a total signal (dark + sky + object) smaller than about 10,000 ADUs ($\approx 70,000e^-$) can be corrected with good accuracy (residuals much smaller than 1%), providing *both* the science *and* the flat-fields are taken with DITs longer than 2 s. Data obtained with shorter DITs are affected by the finite reset time of the detector arrays.

The method is more detailed in the description of the CRIRES pipeline at `http://www.eso.org/observing/dfo/quality/CRIRES/pipeline/pipe_gen.html` and, in particular, in the section dealing with the science recipes. Static calibration files necessary to correct for the non-linearity are available at `http://www.eso.org/observing/dfo/quality/ALL/ref_frames/ref_crires.html`.

7 Characteristics of the spectrograph

7.1 Wavelength settings

Wavelength settings are defined by a *reference wavelength* that corresponds to the wavelength at the middle of detector 3. In a few cases (see 7), this reference wavelength is not sufficient, and an additional number, the *grating order* is needed.

Set-ups are done by using the instrument model to position the spectrum with an absolute accuracy to better than 30 pixels and a reproducibility $\approx$ 3 pixels.

Typically about 200 CRIRES settings are sufficient to cover the entire infrared spectrum in the range of $950 \leq \lambda \leq 5400$nm. Standard wavelength settings are detailed in Sect. 15. Wavelength can also be set using free wavelength settings: allowed ranges for the reference wavelength are listed in Tab. 6a. However, as the characterization of the instrument improves, the CRIRES team realized that the current set of standard wavelength settings does not guarantee a full coverage without some risk of vignetting by the intermediate slit or contamination by adjacent orders.

Tables 4a-4h (Tables 5a-5h) therefore now provide under the columns *Unvignetted range* the wavelength (wavenumber) ranges for which reproducibility of the illumination is estimated to be better than 1 % for a 0.2″ slit. Wavelength outside of these ranges but still covered by a detector are subject either to - sometimes severe - vignetting by the intermediate slit - or contamination from adjacent orders. The wavelength range for which the reproducibility of the illumination is better than 1% is smaller for a wider slit.

Because of the time needed to resolve the vignetting problem described in §1.5, the CRIRES team did not have time to prepare a new configuration table to palliate this deficiency, as earlier announced in the previous version of this manual. Critical features can therefore fall at a wavelength not covered by any unvignetted range. In case of doubt regarding the influence on some spectral features, the user should email the appropriate contact listed in § 1.4.

Vacuum wavelength are used throughout this manual..

7.2 Wavelength calibration

7.2.1 Standard means: ThAr lamp and N_2O and CO gas-cells

Wavelength calibration of CRIRES spectra is difficult. Depending on the wavelength and on the required accuracy, different methods can be used. For an accuracy corresponding to 3 pixels, the start and end wavelengths and the derived dispersion assumed to be linear for each detector is sufficient, in particular for the standard settings.

If present in raw data, either emission or absorption sky lines can be used in the data reduction to improve the absolute wavelength calibration. The CRIRES team has started to obtain data to quantify the absolute accuracy of such a method. However, the number of sky lines is insufficient to achieve a high precision absolute wavelength calibration for many settings, in particular those below 2500 nm.

The density of lines provided by arc lamps is usually small in the IR. However, the Thorium-Argon lamp can provide a large number of lines up to about 2500 nm. The ESO Calibration and Instrument Modelling group in Garching together with the US National Institute of Standards and Technology have collaborated to increase the number of identified Thorium and Argon lines in the NIR. This collaboration to support the wavelength calibration of CRIRES

lead to a paper available in the Tools section in the CRIRES web page. Users whose science has benefitted from the ThAr calibration should cite Kerber, F., Nave, G. & Sansonetti, C.J, 2008, accepted for publication in ApJ.

At the time of issuing this Manual, the catalogue available at the *CRIRES calibration data* page at http://www.eso.org/observing/dfo/quality/CRIRES/pipeline/pipe_calib.html and part of the CRIRES pipeline distribution catalogue only contain lines that were identified before this later work. Check these web pages for any update.

An additional high–precision method is provided by the use of a N_2O gas-cell in front of a halogen lamp, as the N_2O lines are recognized wavelength standards beyond 3500 nm. However, they are only present in a limited number of settings. The list of N_2O lines is also available at http://www.eso.org/observing/dfo/quality/CRIRES/pipeline/pipe_calib.html and is also part of the CRIRES pipeline distribution.

The following guidelines shall be considered in case high precision absolute wavelength calibration is required. Section 18 details the recommended method to carry–out an accurate wavelength calibration for each order.

1. *Sky lines*: A possible output of the ETC is the emission sky spectrum for the requested reference wavelength. Its examination should provide enough information as to decide if the required wavelength accuracy can be achieved.

2. *ThAr lamp*: For wavelengths below 2300 nm the Thorium–Argon lamp provides enough lines for a good wavelength calibration. Since April 2008, the ThAr spectra are obtained by means of a set of fibers. This method allows to avoid strong scattered light sometimes mimicking real lines and making the identification difficult. The several spectra obtained also provides a way to determine the distortion of the spectrograph.

3. *N_2O gas-cell*: For wavelength longer than 3500 nm, N_2O is a strict (National Institute of Standards and Technology, NIST) wavelength standard. For shorter wavelengths, the available line list originates from the HITRAN database, itself based on Toth et al. (see http://cfa-www.harvard.edu/hitran/). Unfortunately, N_2O has no lines below 1650 nm and only weak lines between 1650–2100 nm. Their distribution over the detectors for a given wavelength setting can be seen by using the ETC. A line list can be accessed from the Tools section in the CRIRES web page.

4. *CO gas-cell*: A CO gas-cell is now available since April 2008. The line list is also available at the NIST web site and will soon be available at the Tools section of the CRIRES web page.

It is also possible to use the N_2O *during the observations themselves*, that is to have the gas-cell on the light-path of the astronomical object. First results from science verification or commissioning data or regular science observations indicate that a radial velocity accuracy of the order of ~ 20 to 30 m s^{-1} can be reached. A monitoring programme has started to determine the long-term behavior

It is important to note that the atmosphere itself contains N_2O. Therefore, it is difficult to disentangle the origin of N_2O lines originating in the gas-cell from the ones originating in the atmosphere, at least in the L or M band. In the K band, N_2O lines originating from the atmosphere are weaker but still present. Similarly, the CO gas-cell can also be used for observations. Its use is particularly recommended in the K band (order 24).

The CRIRES team is actively working on alternative solutions for wavelength calibration, such as an accurate instrument model or the use of additional gas-cells. In particular, it is currently testing an OCS gas-cell in laboratory.

7.2.2   Radial velocity measurements

Huelamo et al. (2008, A&A 489, 9) and Seifahrt & Kaeufl (2008, A&A 491, 929) have demonstrated that accurate radial velocity measurements to better than ≈ 35 ms^{-1}, even possibly to 10 ms^{-1}, are feasible with CRIRES. The Seifahrt & Kaeufl (2008) study covered data over only $\approx$ 4h 30m, while the Huelamo et al. (2008) study extends over slightly less than 7 days. Although the long term accuracy of CRIRES radial velocity measurements has not yet been demonstrated, there is no *a priori* reason to expect that a similar accuracy cannot be reached over a time span of months or years.

Wavelength calibration is of course the critical aspect of all radial velocity measurements: a 10 ms^{-1} precision corresponds to a mean error on the solution of ≈ 0.007 science detector pixel. Some fundamental parameters regarding radial velocity measurements can be found in Bouchy, F., Pepe, F., & Queloz, D. (2001, A&A, 374, 733). However, this paper mainly deals with measurements in the optical regime though, and some results are not valid in the CRIRES accessible spectral range.

Regarding CRIRES observations, the following aspects require particular attention: (1) number of (absorption) lines of the star within the spectral range of interest; (2) number of lines used for wavelength calibration; (3) spectral resolution; (4) slit illumination and photocenter error; (5) flat-fielding error. There are briefly discussed in the following:

1. in general, the number of absorption lines should be as high as possible; however, blending or presence of broad lines should be avoided;

2. the number of lines used for wavelength calibration should also be as high as possible; here also, the presence of broad lines should be avoided. In the spectral range of CRIRES, telluric lines offer a natural choice of wavelength calibration lines. However, the following caveats regarding telluric lines have to be taken into account:

   (a) on the long term, a fundamental limitation is the overall motion of clouds giving rise to telluric lines. The fastest coherent cloud motion is caused by the jet-stream, which can reach velocities exceeding 55 ms^{-1} (during the Seifahrt & Kaeufl 2008 study, it reached ≈ 29 ms^{-1}); it can therefore possibly induce a shift of up $\cos$ (zenithal distance)$\times \cos$ (difference of azimuth between jet-stream direction and direction of observation) $\times$ jet-stream speed for lines that are only produced at the jet stream altitude, and some possible line shape changes for lines that are partially produced at this altitude. However, the largest contribution to most telluric absorption lines (except O_3) arise in the first scale height of the atmosphere above the telescope;

   (b) many settings of CRIRES cover spectral ranges that include water vapor lines: the column density of water vapor can change on a time scale of a few minutes. In addition, since water vapor is mainly located at low altitude, its column density dependence on airmass can be different from the one of other molecules. Presence of weak water vapor lines can subtly change the centroid of other telluric lines with which they are blended;

(c) ThAr spectra are now produced using a set of fibers that illuminate the entrance slit. Currently, ESO cannot guarantee that the photo-center of the light coming out of the fibers is reproducible to the level of accuracy required for reaching a precision better than 100 m/s;

3. for a discussion on spectral resolution see Bouchy, F., Pepe, F., & Queloz, D. (2001, id)). One should note that in the case of CRIRES, the choice of resolution is intimately related to the choice of slit width in the case that the PSF FWHM is larger than the slit width. If it is smaller, the resolution actually depends on the FWHM of the PSF and on the centering error caused by the secondary guiding algorithm;

4. the location of the star photocenter on a slit not uniformly illuminated is a crucial aspect. A mean precision of $10 \ \mathrm{ms^{-1}}$ requires a mean error on the centering of the target of ≈ 0.015 slit-viewer detector pixel, from one observation to the next. This precision must be reached in spite of various seeing and transparency conditions. In the case of AO observations, this precision must also be reached despite variations on the quality of the AO corrections, which depends on atmospheric turbulence, airmass,... There is no guarantee that the algorithm used for the secondary guiding on the slit viewer can reach such a level of accuracy on a constant basis with so many variable parameters. Two solutions can be adopted:

   • observations in NoAO mode with the narrowest slit in bad seeing conditions (FWHM *at the observing wavelength* larger than at least $\approx 4 - 5$ times the slit width). In this case, the slit illumination is likely to be uniform enough that the exact location of the photocenter is not a problem;

   • in case of AO observations, it is important that the light path includes one of the offered gas-cells so that the reference lines it offers are fixed relative to the spectrograph. Note that some problems listed in point (2) above are also valid here: (a) line blending of the gas-cell lines with the star absorption lines as the star radial velocity changes with the Earth motion around the Sun, or by the presence of planet around the star under study; (b) line blending with telluric lines of varying intensity depending on airmass or varying atmospheric conditions. However, in any case, the use of a gas-cell appears as the solution offering the highest radial velocity accuracy.

5. the shape of the absorption lines can be changed subtly if the flat-fielding was done with a slit width slightly different from the one obtained during the observations. It is therefore important to attach a flat-field in the corresponding OB.

7.2.3 Visitor gas-cells

For ultra precise radial velocity work users may wish to employ a special gas-cell in absorption during their scientific observations, similar to the Iodine Cell method employed in the optical. For the moment users have to supply their own gas-cell(s) at their own risk. In this context one should keep in mind the problem of pressure shift (c.f. Fig. 2b in Glenar et al. ADV. HELIO- AND ASTEROSEISMOLOGY: I.A.U. SYMP.123 P.481, 1988 which gives a practical example of the associated error). *The use of gas-cells not part of the observatory standard set* (which currently only includes N_2O and CO gas-cells) *is limited to runs executed in visitor mode,* as their use would interfere with regular service mode observations.
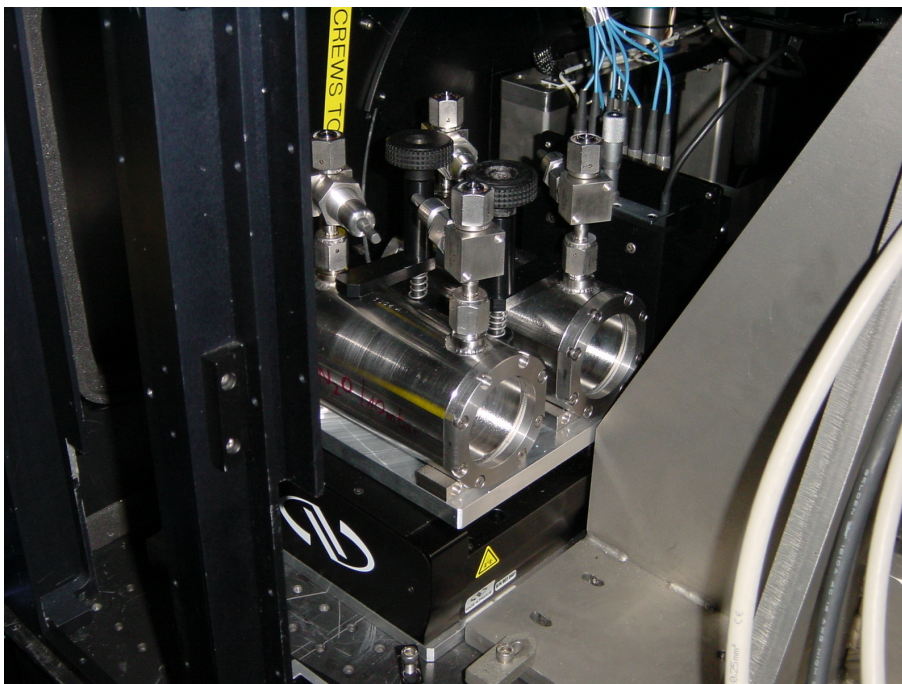
Figure 15: The N$_2$O and CO gas-cells mounted on the carriage

Mechanical lay-out Figure 15 shows the way the present ESO's gas-cells are mounted on the carriage. Figure 16 describes their mechanical lay-out. In principle the cells are held in place by a bar pressed down with a knurled nut. Any mechanical design which is compatible with the overall design space and this very generic fixation method is acceptable. The minimum optical clear diameter should be 22mm to have sufficient field for acquisition and nodding.

The optical quality of the entrance windows has to be sufficient to allow for diffraction limited imaging. Low order aberrations (e.g. spherical aberration or astigmatism) are acceptable, as the MACAO adaptive optics system would correct for them. The windows have to be transmitting and of good quality for both the AO-reference wavelength (600-1000nm) as well as for the spectral region of interest to be covered by CRIRES.

One of the windows is very close to the telescope focus, so it is important that at least one of the two windows is scratch free and clean! If relevant, the preferred orientation of the gas-cell needs to be indicated.

The gas-cell will operate in an f/15 beam so that fringing in the windows is not a big issue. Still if slightly wedged windows are used, they have to be aligned such that the net prismatic deflection is close to zero to avoid differential refraction effects.

Logistics As part of the proposal process all relevant information as to the properties of the visitor gas cell have to be submitted to ESO. In addition the fill-gas has to be described and if relevant handling and safety procedures have to be clarified. The cell(s) have to be sent to ESO Garching at least 4 weeks prior to the observing run properly packed for oversea shipment by airfreight. ESO takes the responsibility of shipping the cells to and from the observatory.

At this stage, only non-toxic gases are allowed in gas-cells.

Operations   At the beginning of the visitor run ESO will remove one of the two observatory gas cells and mount one of the user's gas cells to the instrument. A change of the cells during one observing night is not possible.

7.3   Flat fields

Dedicated flats are best taken with the Halogen lamp. DIT and NDIT are automatically determined by the template. In particular, DITs are always longer than 2 s for the reason given in §6.4.

There is *a priori* no need to take flat fields at night time, as the detector characteristics are sufficiently stable in time, and the spectrograph wavelength setting sufficiently accurate. However, flat-fields may be important for very accurate radial velocity measurements. They may also be important when the interesting lines appear at the blue or red edge of a spectral setting, where possible vignetting by the intermediate slit may affect the detector illumination (see §8.4).

Flat-fields that are part of the calibration plan (see Sect. 12) have a signal-to-noise ratio per pixel larger than 200 at the peak efficiency of a given setting. A systematic atlas of the S/N/pixel of the flat-fields for each standard wavelength setting has started and will be made available at http://www.eso.org/observing/dfo/quality/ALL/ref_frames/ref_crires.html Users requiring flat-fields with larger S/N should contact ESO through the email addresses listed in §1.4.

7.4   Spectrograph field-of-view, slit width and seeing

The field-of-view of the spectrograph is *slit width* × 31 ″. The appearance of a spectrum on the science detector is illustrated in Figure 17. Note in particular that the default centering position is not at the center of the slit.

A slit width of 0.4 ″ offers a close to maximal throughput in most AO observations. For non-AO observations, the optimal slit width would in principle be given by the external seeing at the wavelength of observations. *However, it is not recommended to use slit width larger than 0.4 ″, as the spectral range for which the illumination is reproducible to better than 1% shrinks considerably (see §7.1.* In addition, for faint targets, not enough light is reflected by the slit jaws for proper secondary guiding.

It is worth to recall that the seeing FWHM ϵ depends on the wavelength λ following

$$\epsilon(\lambda) = \epsilon(\lambda = 500\text{nm}) \ \left(\frac{\lambda(\text{nm})}{500\text{nm}}\right)^{-1/5}, \tag{1}$$

and on the zenith distance, z, following

$$\epsilon(z) = \epsilon(z = 0) \ (\sec z)^{0.6}. \tag{2}$$
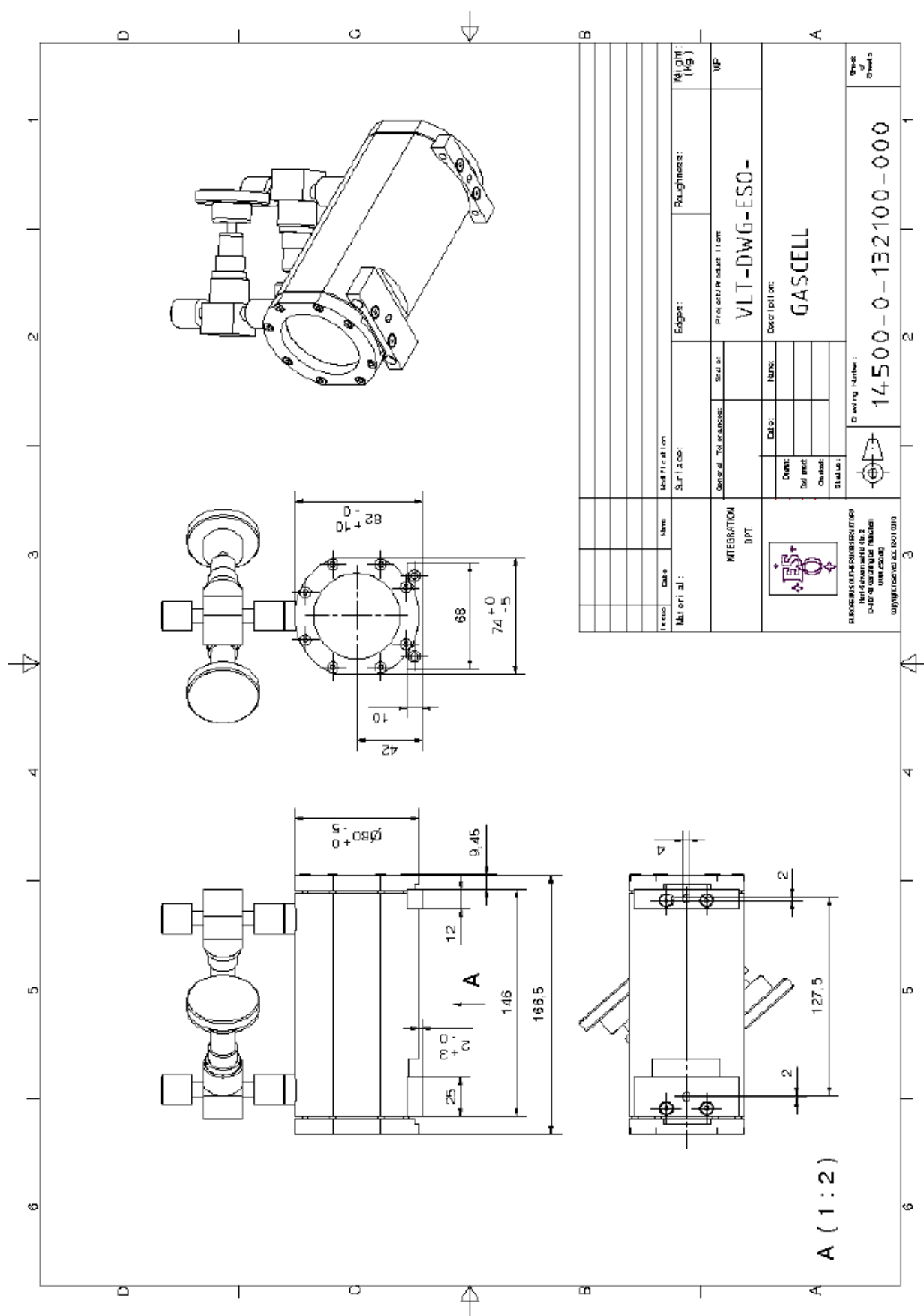
Figure 16: Mechanical lay-out of a gas-cell
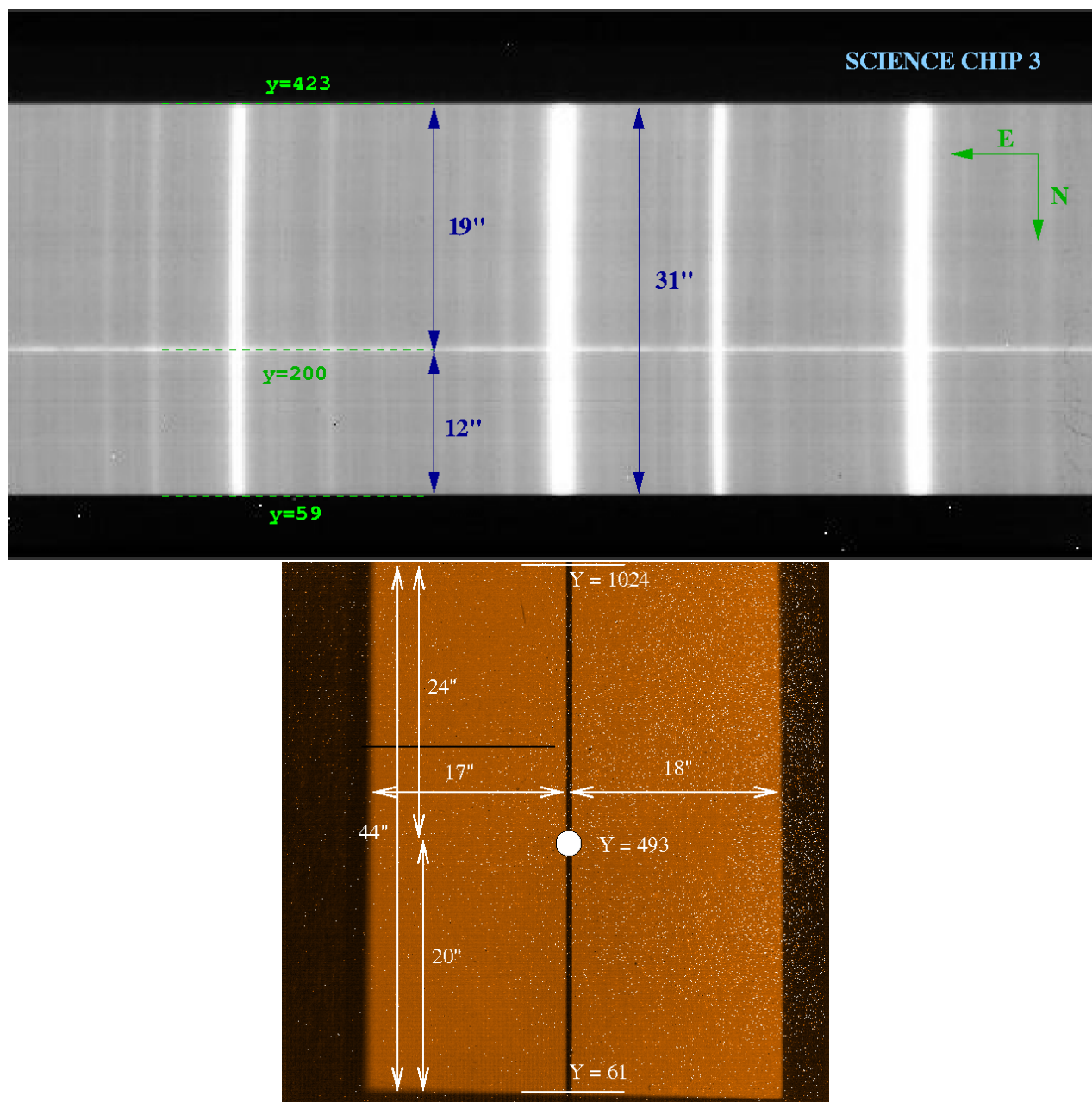
Figure 17: Illustration of the geometry of the science and slit viewer detectors for a position angle of 0 degree on sky. On the science detector, North is to the bottom and East to the left, while North is to the top and East to the left on the slit viewer detector. The centering position of the science target is the center of the slit in x and pixel $y = 493$ along the slit. This position corresponds to pixel $y \approx 200$ on the science mosaic; the exact value depends on the detector. With the templates CRIRES_spec_obs_AutoNodOnSlit and CRIRES_spec_obs_SpectroAstrometry, nodding is done symmetrically along the slit around the centering position. For nodding position A, the image of the target appears at larger y values on the slit-viewer and lower y value on the science detector, at half the nod throw from the centering position. In other words, for a position angle of 0 degree, the telescope position at nodding position A is South of the centering position. Conversely, for nodding position B, the image of the target appears at smaller y values on the slit-viewer and larger y value on the science detector. On the science detector, wavelengths increase from left to right.

7.5   Spectral resolving power

A spectral resolution of 96,000 has been measured with a slit width of 0.2 ″ at 2172 nm. Simi-
larly, a spectral resolution of 60,000 has been measured with a slit width of 0.3 ″. Currently, the
relation slit-width to spectral resolution R is such that $R \times$ slit width (in ")/$0.2'' \approx 100,000$,
which is valid for slit width between 0.2 and ≈ 0.8". However, *as of December 2008*, the
entrance slit width reproducibility can show peak-to-peak variation of up to $\approx 20\%$. In par-
ticular, observations made with slit width larger than 0.2" may be affected if they involve
change of wavelength settings: indeed, a change of wavelength setting triggers an algorithm
to check that the spectrum in well-centered on the intermediate slit (see §8.4); this algorithm
uses a slit width of 0.2". It is expected that the reproducibility of the entrance slit width will
improve after an intervention in January 2009.

Figure 18 shows the optical depth profile obtained from the combination of 5 ^{12}CO lines seen
in absorption toward the young star DG CrA, using a 0.2 ″ slit width. A Gaussian fit to this
profile, taking into account the finite pixel width, gives a FWHM of $3.18\,\mathrm{km\,s^{-1}}$, corresponding
to a resolution of 94,300. This value is therefore a lower limit to the spectral resolving power
of CRIRES.
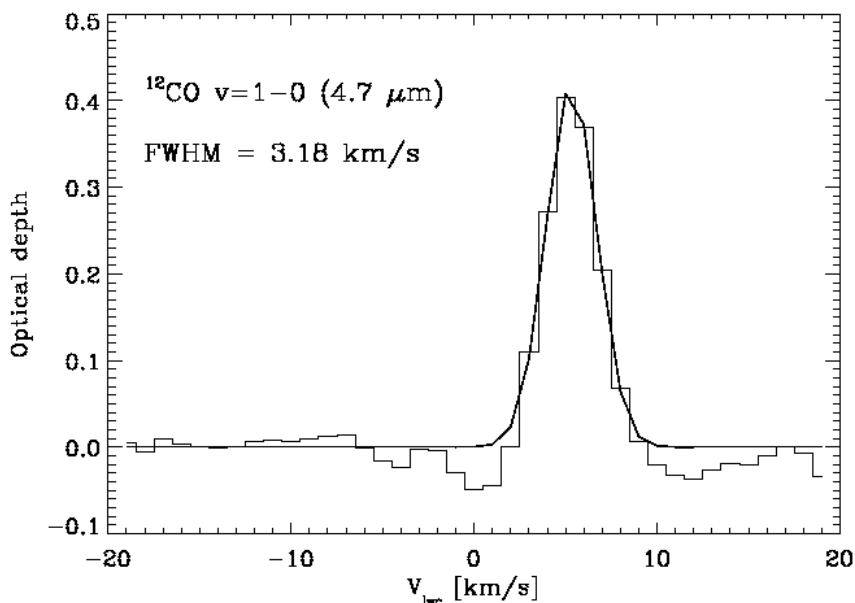
Figure 18: Optical depth profile obtained from the combination of 5 ^{12}CO lines seen in ab-
sorption toward the young star DG CrA. Courtesy Klaus Pontoppidan.

A slit width narrower than 0.2" is possible, in particular, in the case of observations of very
bright targets. However, there is no guarantee that the requrested slit width can be achieved
for slit narrower than 0.2", due to the limitations of the slit mechanism. Also, there is no
guarantee that the spectral resolution can be larger than 100,000.

8 System efficiency and throughput

The overall efficiency of CRIRES has been measured on spectrophotometric standard stars. The flux, F_ν, of such a star, expressed in Jy, is converted to the flux, N_γ, in photons/s/pixel by

$$N_\gamma = \frac{c}{\lambda^2} F_\nu \cdot \frac{A_{\text{Tel}}}{E_\gamma} \cdot \Delta\lambda \tag{3}$$

where $E_\gamma = hc/\lambda$ is the photon energy, A_{Tel}, the telescope collecting area. The dispersion $\Delta\lambda$ is output by the ETC.
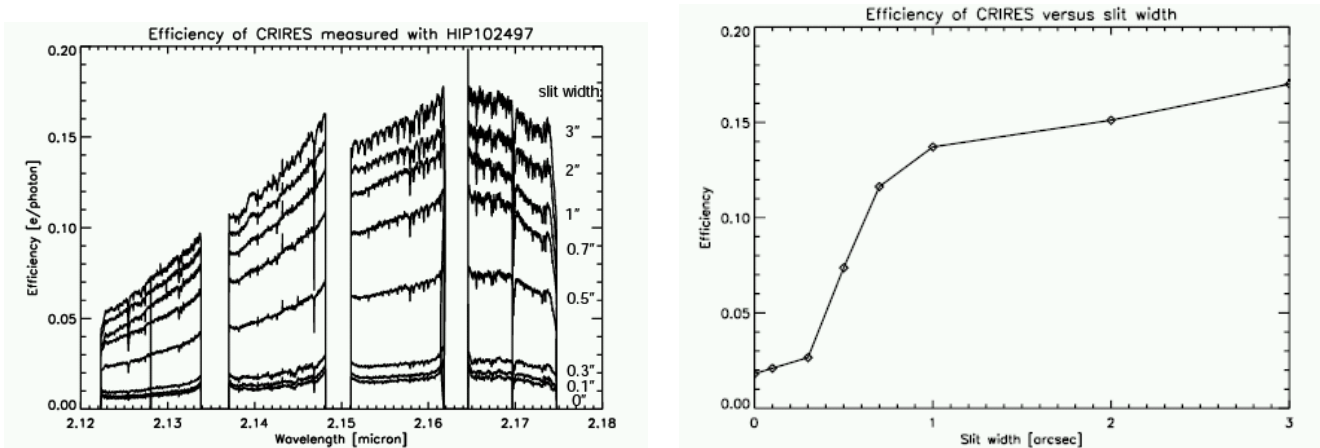
Figure 19: Overall system efficiency, also called throughput. The wavelength dependence of the efficiency for a particular wavelength setting is shown for different slit widths on the left. The peak efficiency as a function of slit width is shown on the right.

The overall efficiency or throughput τ, is defined as the ratio of e$^-$/s/pixel as measured on the detector divided by the theoretical expected photon flux (photons/s/pixel) arriving above the Earth's atmosphere (Eq. 3). In Fig. 19 the overall efficiency as a function of slit width for order 26 at 2150 nm is shown together with the peak efficiency versus slit width. During these observations, atmospheric conditions were rather bad (seeing of $\geq 1.6\,''$ and coherence time of 2 ms, see Sec. 3) so that the AO could not work effectively, leading to significant slit loss. Measurements have been repeated under better conditions and are currently under analysis.

8.1 Transmission of the entrance window

The transmission of the dichroic window which also serves as entrance window for the spectrograph has been measured in the laboratory in Garching for $\lambda > 1000$nm. It is shown as a function of wavelength in Fig. 20. For shorter wavelengths, only manufacturer measurements exist: they indicate that the blue wavelength cut-off (transmission smaller than 50%) occurs at ≈ 950nm.
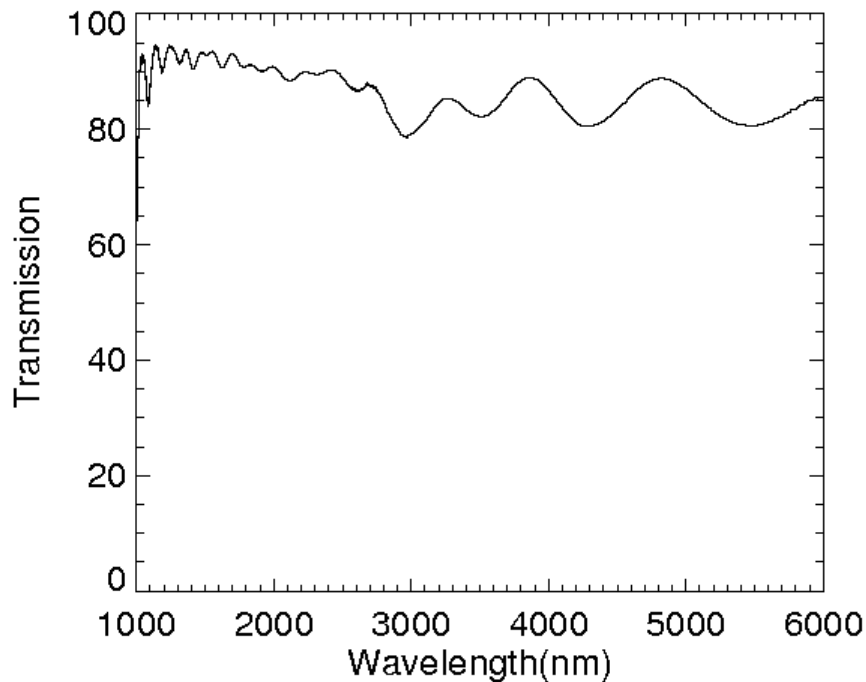
Figure 20: Transmission curve of the entrance window.

8.2 Sensitivity

Table 2 lists the instrument sensitivities. The table is intended as a quick reference only. Proposers should refer to the Exposure Time Calculator (Sect. 10.2) for more precise estimates. In particular, one should note that the grating blaze function introduces a large sensitivity variation within any given order.

Table 2: Point source sensitivities determined using a 0.4 ″slit, adaptive optics, optical seeing of 0.8 ″. The values listed correspond to a S/N of 10 for a 1h on–source integration in one spectral dispersion element. They are obtained by integrating the profile along the spatial direction.

Band	Sensitivity	Magnitude
	(mJy)	
J	1.1	15.4
H	1.1	15.1
K	1.1	14.6
L	9.5	11.2
M	26	9.4

Short-ward of 1100 nm, the spectral range accessible to CRIRES overlaps with the one accessible to UVES. For the observations of specific spectral features in this region, it is interesting to compare the efficiency of the two spectrographs. Figure 21 shows the S/N of two spectra of the J = 1.3 star β Col obtained nearly simultaneously with CRIRES and UVES on February 7, 2007, while the star was at an airmass < 1.07, with very similar seeing conditions.

In both cases, the slit was constantly aligned along the parallactic angle (ELEV mode). The first spectrum (in red) was obtained with UVES with a slit width of 0.3″, providing a resolution R ≈ 110,000. The other one (in blue) was obtained with CRIRES using AO and a slit width of 0.2″, providing a resolution R ≈ 100,000. For observations of specific lines accessible in one setup, CRIRES is clearly more efficient red-ward of ≈ 970nm.
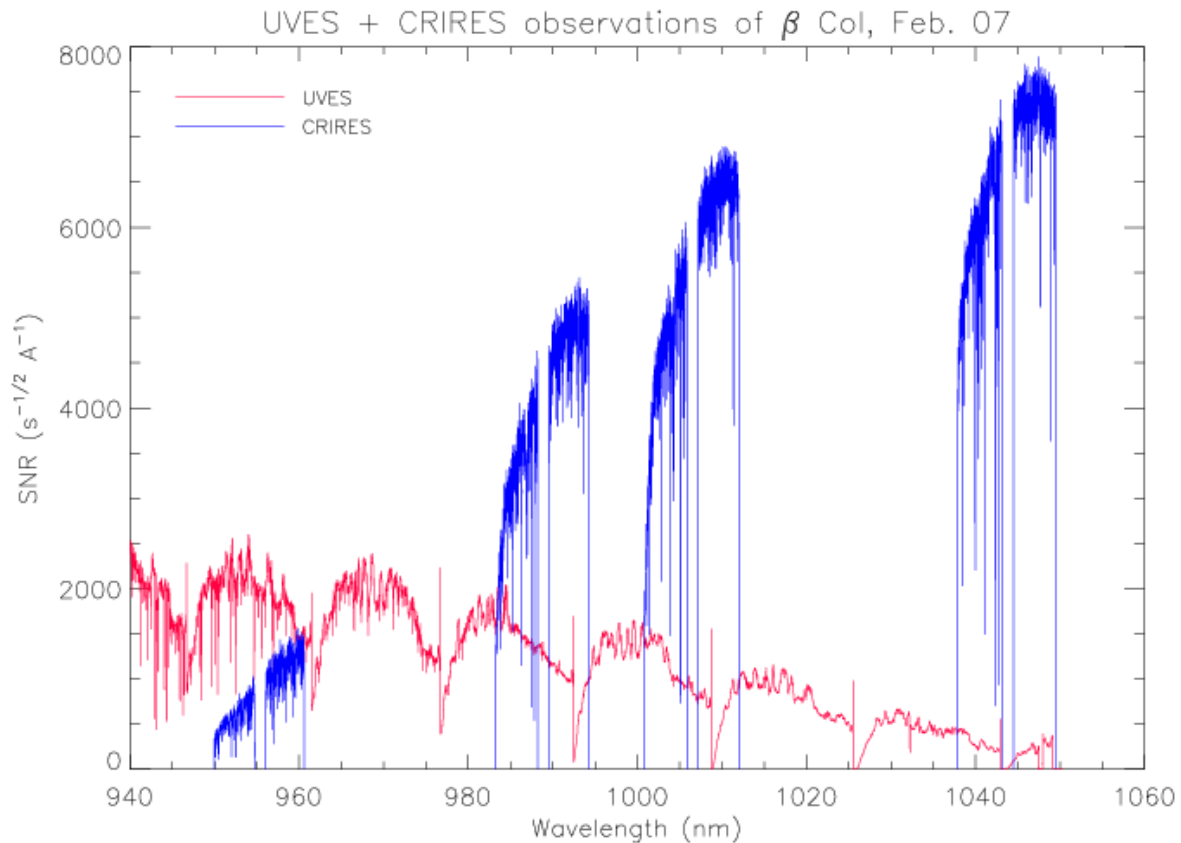
Figure 21: Comparison of S/N/Å per second$^{1/2}$ of integration time obtained during nearly simultaneous observations of β Col. Courtesy S. Uttenthaler.

8.3 Optical ghosts

Occasionally, especially when using the CRIRES Echelle grating in high order, a quasi white – light ghost is visible on the data. It results from a retro-reflection from the detector onto the grating, which is redirected onto the detector in a different order and with reduced dispersion. Ghosts cancel out by nodding, as sky emission lines do. One example of a ghost visible in a staring image is given in Fig. 22.

8.4 Stability and reproducibility

For wavelength calibration the stability and reproducibility of the different mechanical functions (grating, prism, slit) are important. The absolute setting of the prism and grating guarantees that a given standard wavelength setting is accurate to better than 30 pixels, even
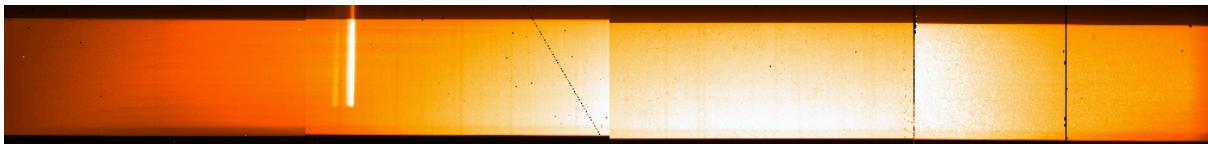
Figure 22:   Example of a quasi-white light ghost observed with a reference wavelength of 1153.8 nm. The ghost is visible in staring frames top left on the second detector. Also, a diagonal (middle) and a vertical (right) detector scratches are also visible.

possibly after a minor intervention. A model of the instrument currently achieves a wavelength calibration of ≈ 3 pixels without simultaneous wavelength calibration.

A measurement of the stability of the instrument has been obtained by measuring the location of an emission line in short exposures spread over a span of ≈ 10 minutes. A preliminary value is 1/20 pixel. Such tests need to be repeated for different wavelength settings.

A problem has recently been found with the intermediate slit[1]. The main function of this element is to avoid contamination of the spectrum by adjacent orders and to limit the background. Unfortunately, the whole unit appears to have moved and shows a lack of reproducibility, affecting in particular the settings shorter than $\lambda 2200$ nm. A software solution to insure that the spectral range seen by the detector is well centered in the intermediate slit has been implemented early July 2007. An additional software check to insure that the intermediate slit has the correct width is ready to be implemented. On the other hand, an encoder has been installed in April 2008 and its installation slightly modified in June 2008. Although the error on the reproducibility of the intermediate slit width is not yet available - being tested as this manual is being released -, it has largely improved.

---

[1]This element is not shown in Figure 1. It is located between the collimator (the concave mirror located after the prism) and the small flat mirror located before the TMA.

Part III
Observing with CRIRES at the VLT

9 Introduction

9.1 Atmospheric transmission

The transmission of the Earth's atmosphere in the J, H, K, L and M bands is shown in Fig. 23. The amount of telluric absorption varies non-linearly with zenith distance and precipitable water vapor. In order to facilitate the identification of sky regions affected by water vapor absorption lines, Fig. 24 shows the atmospheric transmission spectrum only including water vapor absorption lines..

The transmission spectrum of the sky for a particular setting is an optional output provided by the ETC. This tool allows one to select spectra based on different amount of precipitable water vapor.

9.2 Background removal

9.2.1 Sky emission spectrum

The sky background emission can be divided in two regimes depending on the wavelength. Below 2200 nm, the sky emission is dominated by OH lines, formed at an altitude of 80 km. Detailed sky spectra with OH line identifications are available on

http://www.eso.org/instruments/isaac/tools/.

Beyond 2200 nm, the thermal background dominates with contributions from both atmospheric and telescope emission.

The sky emission spectrum for a particular setting is an optional output provided by the ETC.

9.2.2 Nodding

The purpose of *nodding* is to correct or remove sky emission, detector dark current and glow (Fig. 13), and some ghosts. In a simple application of this technique a spectrum is taken at telescope position A, after which the telescope is moved along the direction of the slit to position B and another spectrum is taken. By subtracting the A and B images, dark and sky subtractions are performed. The number of nodding cycles and the nodding throw, if smaller than 20″, are free observing parameters. Because of the extended wings of the PSF a nodding throw greater than 5 ″ is recommended, preferably 10 ″.

9.2.3 Jittering

The purpose of *jittering* is to correct for bad pixels and decrease systematics due to the detector. This is particularly important for CRIRES observations. Indeed, the detectors suffer
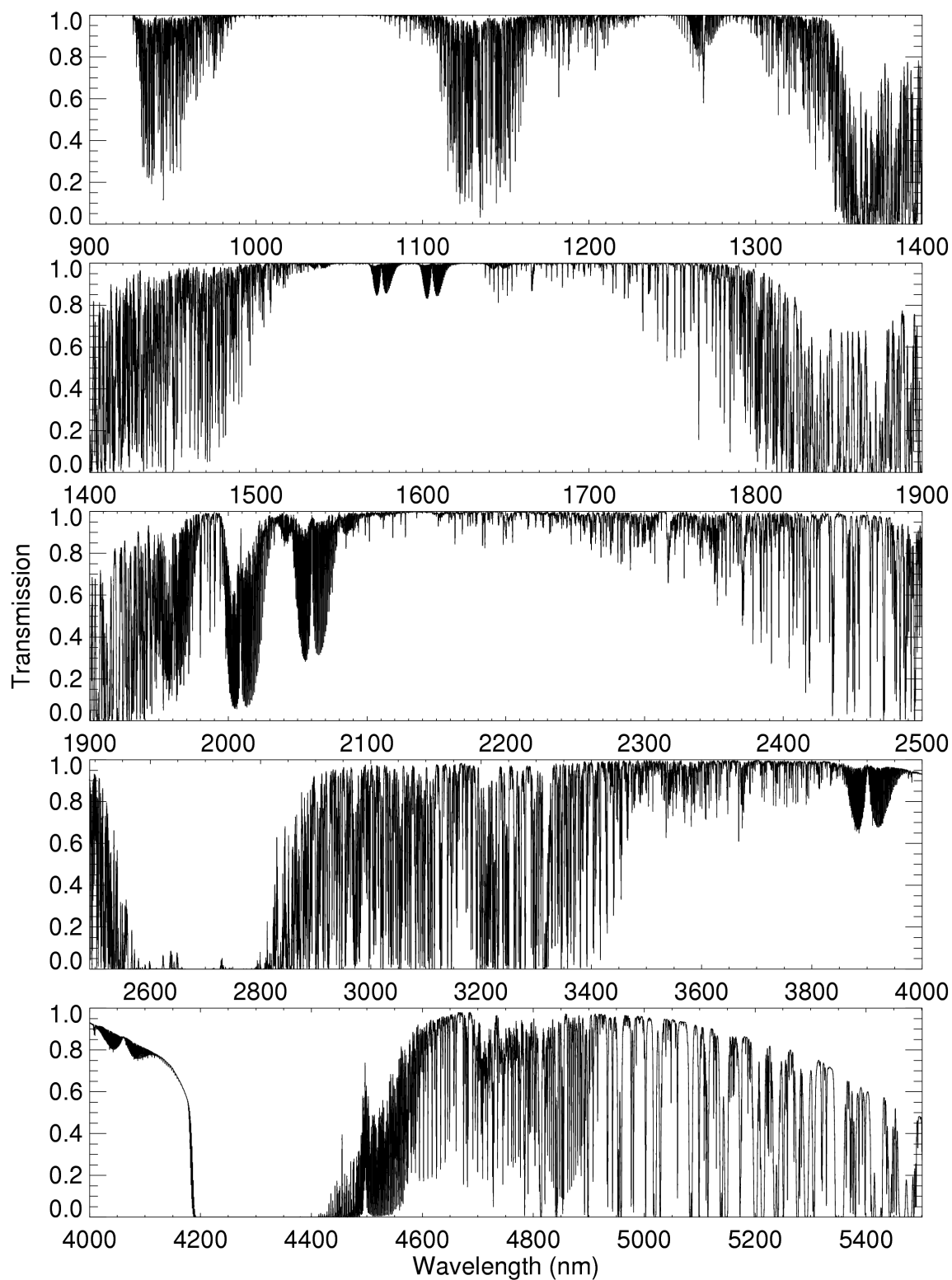
Figure 23: Atmospheric transmission from 900 – 5500nm computed with PCLnWin/HITRAN for a Paranal atmosphere, precipitable water vapor (PWV) of 2.5mm, at zenith and smoothed to a resolution of $\lambda/\Delta\lambda = 10^4$.
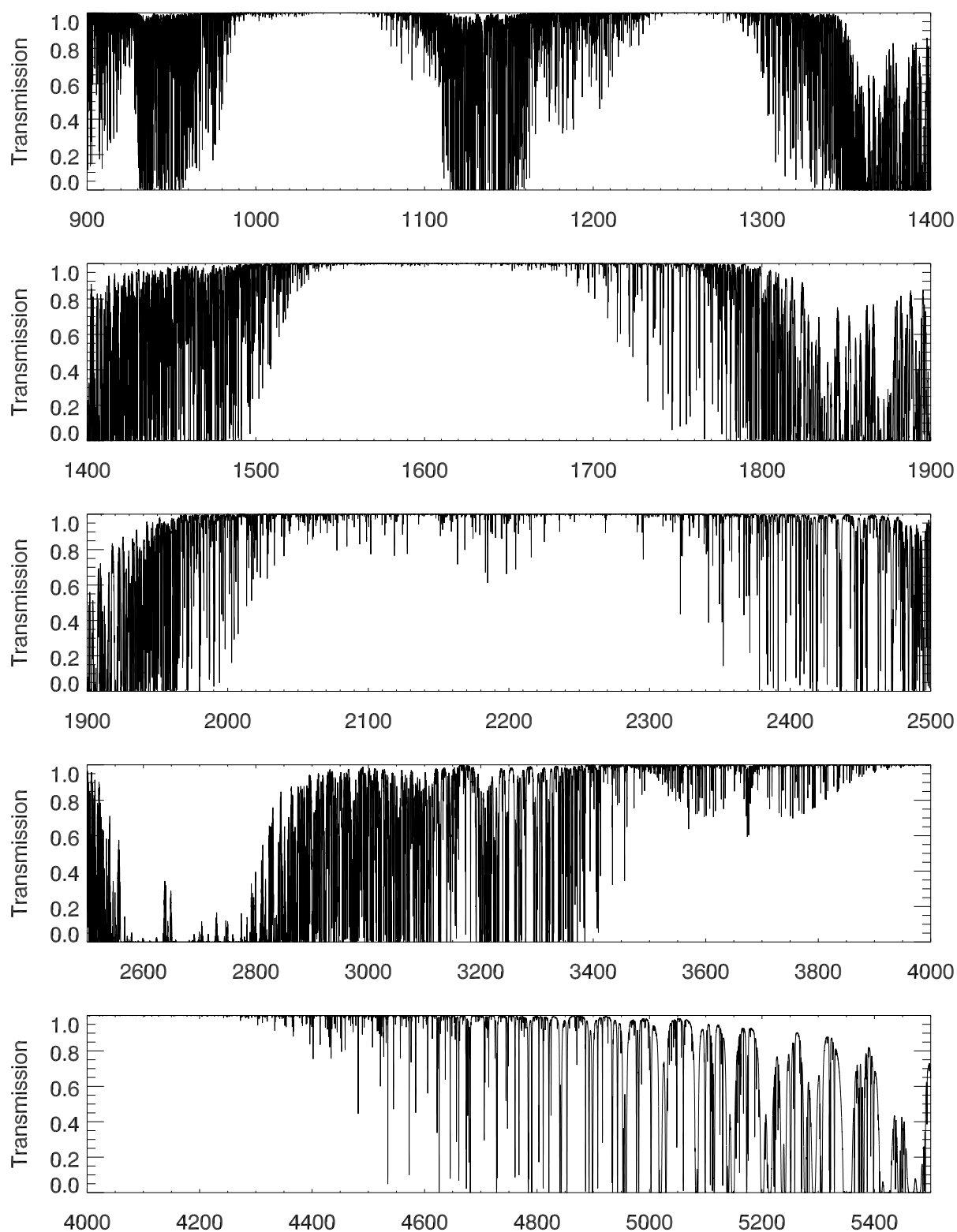
Figure 24: Water-vapor only atmospheric transmission from 900 − 5500nm computed with RFM/HITRAN for a Paranal atmosphere, precipitable water vapor (PWV) of 2.5mm, at zenith at a resolution of $\lambda/\Delta\Lambda = 100000$.

from a relatively large number of bad pixels. In addition, the spatial extent of a spectrum is at most a few pixels in nominal conditions. Jittering is obtained by adding a small, random offset to the telescope in addition to the nodding offset. The recommended maximum size of the jitter offset is a free parameter. It must be smaller than half the nodding offset but larger than the spatial extent of the minimum feature that one hopes to detect; for point sources, it should be larger than the width of the spatial profile.

9.3 Flux calibration and telluric correction

9.3.1 General procedure

Flux calibration and telluric correction are generally carried out in three steps. The first step removes telluric absorption features of the extracted, wavelength calibrated science spectrum by dividing it by the one of a telluric standard. The second step removes the intrinsic spectral features of the telluric standard that are imprinted onto the science spectrum because of the first step. The third step uses a spectro-photometric standard to set the absolute flux scale.

The spectro-photometric standard and the telluric standard can be the same star. Note that CRIRES, as spectrometers in general, is not meant to provide high absolute spectro–photometric accuracy.

The Observatory does not offer observations of telluric or spectro-photomeric standard stars. Observers who wish to correct for telluric features or flux calibrate their spectrum therefore need to supply a standard star OB. Observing time needed to execute telluric or spectro-photometric standard stars is charged to the observer and must be taken into account in the amount of time requested during Phase 1.

9.3.2 Telluric correction

The most prominent features in IR spectra are telluric lines created by the Earth's atmosphere. Unfortunately, many telluric absorption lines are saturated and do not scale linearly with airmass. Therefore, it is necessary to observe a telluric standard as close as possible in airmass and with the same instrument setup as that used for the science target. Furthermore, the strength of some telluric lines varies with time, so it is also necessary to observe the standard soon after or soon before the science target. Thereafter, the spectrum of the science target is directly divided by the one of the telluric standard.

Ideally, the spectrum of the telluric standard should be known, so that features belonging to it can be removed (step 2 above). However, this is usually not the case, so one has to use standards in which the spectrum is approximately known. At present no high precision IR atlas of standard stars with bona fide spectra exists. The CRIRES Team will compile such a list of spectro-photometric standard stars and, once it is available, will put it on the CRIRES home page http://www.eso.org/instruments/crires/.

9.3.3 Hot stars as telluric standards

Usually either hot stars or solar analogs should be used as telluric standards. Spectra of stars hotter than B4 are well fitted by a black-body, with the exception of a few lines (for example, neutral hydrogen Brackett lines). So, by knowing its spectral type, the continuum of a star

can be fitted by a Planck function with the appropriate temperature. On the other hand, the spectra of stars cooler than A0 show molecular features.

Some hot stars also have emission lines or are in dusty regions, and should therefore be avoided. A positive value of the V-I color of a star can be used as an indicator of reddening due to the presence of dust on its line–of–sight.

Hot stars tend to lie near the galactic plane. Correction of telluric features for objects close to the galactic pole may therefore require a different strategy.

9.3.4   Late–type stars or G stars as telluric standards

Unfortunately, spectra of hot stars do contain some features, usually lines of hydrogen and helium, that can be difficult to remove. If the region around the hydrogen and helium lines is of interest, then a late type star could instead be observed, as its spectrum only show weak hydrogen and helium lines.

Solar analogs, for the purpose of removing telluric features, are stars with spectral type G0V to G4V. These stars have many absorption lines in the IR, particularly in the J band. These features can be removed by dividing the solar analog spectrum by the solar spectrum at the resolution of the observations.

In addition to hot stars and solar analogs, IR astronomers have used other stellar types as telluric standards. For example, F dwarfs are commonly used.

9.3.5   Catalogs

The CRIRES tools web page http://www.eso.org/instruments/crires/tools provides a number of catalogs of stars that can be used as telluric standards.

9.4   The influence of the Moon

Moonlight does not noticeably increase the background in any of the CRIRES modes, so there is no need to request dark or gray time for this reason. However, it is recommended not to observe targets closer than 30º to the moon to avoid problems linked to the telescope guiding or active optics system.

On the other hand, the moon may affect the quality of the adaptive optics correction if the source used for wavefront sensing is fainter than R=15 mag. In these cases, reducing the lunar illumination constraint to approximately 0.7 and increasing the distance to the Moon to approximately 50 degrees is generally adequate.

Observers in visitor mode are encouraged to carefully check their target positions with respect to the Moon at the time of their scheduled observations. Backup targets are recommended whenever possible, and users are encouraged to contact ESO in case of severe conflict, i.e. when the distance to the Moon is closer to 30º. Visitors can use the tools that are available at

http://www.eso.org/observing/support.html

Select the link "airmass" which is under "User Support Tools" to help to determine the distance between targets and the moon for given dates.

10 Observing in Visitor and Service Mode

10.1 Overview

For CRIRES there are no deviations from standard VLT operational procedures. As for all ESO/VLT instruments, CRIRES users must prepare their observations with the P2PP tool, available at

http://www.eso.org/sci/observing/phase2/P2PP/P2PPTool.html.

Acquisitions, observations and calibrations are coded via templates. Two or more templates make up one observation block (OB), which then contains all information necessary for the execution of an observing sequence. CRIRES and the telescope are setup according to the content of the OB. There is one Real–Time Display (RTD) for the slit viewer and one RTD for the spectrometer. Daytime calibrations, as described in the calibration plan (see Sect. 12) are executed the following morning by the Observatory staff.

In particular for service mode observers, it is important to properly take into account the amount of time required for telluric corrections. The execution time of a science OB is typically 1 hour. Therefore, at the time of submitting a proposal, an observer has to already foresee that the observing time will be split in a number of OBs, each of which usually requires an associated OB of a telluric star.

Service mode observers should submit their OBs before the Phase 2 deadline whose date is announced in the web-letters.

The most important points for successful observations are listed in § 19 at the end of this manual.

10.2 The Exposure Time Calculator

The CRIRES exposure time calculator can be found at:

http://www.eso.org/observing/etc/

It returns an estimate of the on-source integration time necessary to achieve a given S/N as a function of different input parameters:

- The input magnitude can be specified for a point or an extended source. For the latter, the input parameter corresponds to the magnitude per square ″. Also input flux can be specified as surface brightness. If the 'single line' option is chosen, it corresponds either to the total line flux, for a point source, or to the surface brightness for an extended source.

- If the observing date is known it may be used together with the target coordinates to compute the radial velocity shift due to orbital and rotational movement of the Earth. Alternatively, this tool allows the user to select the best time of the year to observe an object so that the targeted feature avoids a specific telluric line.

- If an AO guide star is used, R mag and spectral type must be specified. They can be obtained from online catalogs available at Simbad/Vizier.

- Requested output can be either exposure time to achieve a given signal-to-noise ratio (SNR) or SNR achieved in a given exposure time. In both cases the DIT needs to be specified (see Sect. 11.3).

The following items should be remembered:

- ETC outputs the on-source integration time. Depending on observing technique and accounting for overheads, the total execution time will be longer (Sect.10.3).

- It is always useful to ask the ETC to show the SNR as a function of wavelength due to the presence of numerous telluric features: a small difference in the requested wavelength may lead to very different SNR for a given total integration time or, alternatively, very different integration time for a requested SNR. In addition, it helps to visualize the wavelength coverage of each detector.

- For a point source, the SNR corresponds to the one obtained by integration over the spatial diffraction profile and is given per spectral pixel and not per resolution element. To compute the SNR for a resolution element the right number of pixels needs to be combined; typically 2 pixels for the 0.2 ″ slit.

- For an extended source, the SNR corresponds to the one obtained by integrating the signal over 1″. It also corresponds to a SNR per step in wavelength..

- When the NGS (AO mode) is selected, the ETC also outputs the estimated Strehl ratio in the K band. This value is needed in the constraints set of an OB. For extended objects, only FWHM should be entered.

- Starting with period 82 (Phase 2) and ETC v3.2.6, the user can specify the vertical amount of precipitable water vapor (PWV) in the atmosphere: the ETC therefore uses the appropriate emission and transmission spectra for the PWV and airmass chosen. This functionality allows one to determine if the SNR will be or not affected by water vapor. One should note that the effect of water vapor lines also depend on the temperature at the time of observation, as well as the altitude of the layers where the water vapor is concentrated, therefore limiting the accuracy of the SNR determination to a few 10%. In period 82, when relevant, users are suggested to group wavelength settings in OBs requiring similar PWV values; USD will flag OBs requiring low PWV so that the night time astronomers observe them in appropriate conditions. ESO considers the possibility to add a constraint on the water vapor in the P2PP constraint set for future periods.

For more detailed information, see the online help provided on the ETC page.

10.3 Overheads

Estimated overheads are listed in Table 3. Actual values for the change of wavelength setting itself vary considerably, between 46 to 105 s, depending on the orientation of the prism and/or grating before the requested change. However, to the average value of 65 s for the wavelength setting change, additional overheads are added in order to insure that the intermediate slit does not vignette the spectrum (cf. §8.4).

Table 3: Telescope and instrument overheads. The overhead for change of derotator position angle applies to the CRIRES_spec_obs_SpectroAstrometry template.

	Action	Time (s)
Telescope	Preset	360
CRIRES	Acquisition without AO	180
CRIRES	Acquisition with AO	300
CRIRES	Read–out (DIT in s)	$2.3 + 0.9\ \mathrm{NDIT} + 0.1\ \mathrm{NDIT\ DIT}$
CRIRES	Nodding cycle	24
CRIRES	Change of wavelength setting	210
CRIRES	Attached wavelength calibration	150
CRIRES	Attached lamp flat	120
CRIRES	Change of derotator position angle	60

11 Preparation of Observation Blocks

This sections provides some guidelines on how to prepare CRIRES observation blocks. A CRIRES Tutorial with a more detailed description has been prepared and it is available at:

http://www.eso.org/sci/observing/phase2/CRIRES/P2PPTutorialCRIRES.html.

11.1 Information required

The following are important considerations for a successful creation of CRIRES observation blocks.

- CRIRES acquisition templates may involve 3 different stars observed in 3 different wavelengths:

    1. the adaptive optics guide star, usually referred to as NGS, for natural guide star, which is used to determine the shape of the wave front; only the R band magnitude and B-R color of this star matters;

    2. the slit viewer guide star (SVGS) which is used for fine guiding using the slit viewer in one of 3 bandpasses, J, H or K. This star is also used as a reference star, which can be acquired before a blind offset is made to center the target into the slit;

    3. the target object itself, with a relevant wavelength between 940 and 5400 nm.

    To be complete, the user can provide coordinates for a 4th star, which is the telescope guide star.

- Target coordinates should be as accurate as possible. VLT absolute pointing accuracy is better than 3 $''$ RMS;

- If any of the science target, the SVGS and NGS are different objects, it is important that their coordinates have been determined in the same coordinate system;

- In particular, if the SVGS is different from the target, it is *crucial* that their separation *at the time of observation* is known with high accuracy, ideally to better than 1/4 of the slit width. In this respect, proper motions of both the target and the SVGS must be taken into account.

- For observations without AO guide star, the acquisition template allows one to specify an offset between the SVGS and the target that is larger than half the width of the slit viewer (up to 40 $''$). In this case, guiding on the SVGS is therefore actually not possible. The SVGS is then only a reference star.

- Nodding in the case of extended objects larger than $\approx$ 30 $''$ may require observations of offset fields to obtain sky measurements. Their frequency depends on the band (more frequent in J, H, less in K) and on the accuracy with which one wants to subtract them. Significant sky variations occur on timescales of a few minutes. The CRIRES_spec_obs_GenericOffset is recommended in this case.

- For moving targets, ephemeris files must be attached to each OB. Slit Viewer guiding can only be done on the target.

11.2   Observation Blocks and Templates

An Observation Block is the smallest scheduling unit. It consists of different templates, which are described in more details below. `Science` OBs must contain one and only one acquisition template. It is followed by a number of science and possibly calibration templates used to obtain wavelength calibration exposures or flat–fields. `Calibration` OBs are intended for observations of telluric/spectro-photometric standard stars. They must contain one acquisition template, followed by the template used for telluric standard stars.

11.2.1   Acquisition

The objective of the acquisition template is to preset the telescope and to center the target in the slit. Point sources shall preferably be observed in ELEV mode where the slit is constantly aligned with the parallactic angle, in other words, along the atmospheric refraction direction. For specific needs to align the slit on the sky at some position angle, the SKY mode shall be used. CRIRES offers two types of acquisitions:

1. The target itself or a star angularly close to it (closer than 30 $''$) can be used to determine the shape of the wave front and therefore can be used to drive the adaptive optics system;

2. No adaptive optics is possible (or requested), because there is only an extended or a faint science target without a bright, compact object in the field.

Two acquisition templates allow to distinguish between the acquisition modes:
  AO :   `CRIRES_spec_acq_NGS`
  No AO :   `CRIRES_spec_acq_noAO`.
AO correction is always performed on an NGS [2].

In both acquisition methods, a sky frame can be taken in an offset field. The slit viewer detector control system subtracts this sky from each new image used for guiding in order to enhance the contrast in the SV image. It is crucial for faint targets.

Two acquisition images are usually delivered to the user in the final data package: the sky frame as well as the final centering of the target in the slit at the end of the execution of the acquisition template. However, for bright objects, a sky frame is not required for good guiding, and therefore, may not be taken.

In crowded fields, the choice of a good slit viewer guide star (SVGS) is important. It must not be too close to another star, in particular, to a brighter star; the latter should be chosen instead. No object should contribute significant flux within the area limited by the guiding box, whose width is optimally set by the instrument operator. The guiding box has a minimum width of $\approx 0.4''$. Note that if the SVGS is also the target – and therefore also partially hidden by the slit–, the width of the guiding box will typically be at least $0.2''$ wider than the slit width.

11.2.2   Acquisition sequences with AO

In this section, we briefly describe the sequence of events taking place during the execution of the acquisition templates.

---

[2]NGS is an AO natural guide star contrary to a LGS which is laser guide star using the LGS facility. This is not available for CRIRES.

General case: NGS ≠ SVGS ≠ Target The most general acquisition for observation with AO takes place when the science target, the SV guide star and the AO guide star (NGS) are all different. Its sequence is the following:

1. preset the telescope to the NGS, possibly recenter it;

2. acquire the NGS with MACAO and close the AO loop;

3. offset the telescope to the SVGS;

4. interactively re-center the SVGS;

5. start guiding;

6. offset the telescope to the target; if the target is bright enough, recenter it.

Case NGS = SVGS ≠ Target If the same star is used for slit viewing and for the AO, but is different from the target, this sequence becomes:

1. preset the telescope to the NGS, possibly recenter it;

2. acquire the NGS with MACAO and close the AO loop;

3. start guiding;

4. offset the telescope to the target; if the target is bright enough, recenter it.

Case Target = SVGS ≠ NGS If the target is used for guiding using the slit viewer, but another star is needed for the AO, the sequence becomes:

1. preset the telescope to the NGS, possibly recenter it;

2. acquire the NGS with MACAO and close the AO loop;

3. offset the telescope to the target;

4. interactively re-center the target;

5. start guiding.

Case Target = NGS ≠ SVGS If instead the target can be used for the AO but is too faint for guiding using the slit viewer so that another star is needed as a SVGS, the sequence becomes:

1. preset the telescope to the target, possibly recenter it;

2. acquire the target with MACAO and close the AO loop;

3. offset the telescope to the SV guide star;

4. interactively re-center the SVGS;

5. start guiding;

6. offset the telescope back to the target; if the target is bright enough, recenter it.

Case Target = NGS = SVGS   If the same star is the target, the AO star and the SVGS, the sequence simplifies to:

1. preset the telescope to the target, possibly recenter it;

2. acquire the target and close the AO loop;

3. start guiding.

Required information regarding the NGS   Acquisition with AO requires the following information:

- The coordinates of the AO guide star at equinox J2000 and at the epoch of the observations, unless the science target is also the AO Guide Star.

- The B-R color of the star used for AO (AO star or NGS). This is used to compute the guiding wavelength for the field selector holding the AO guide star, which in turn is used to correct for atmospheric refraction effects.

- The FWHM of the NGS in order to optimize a diaphragm in the AO system. This diaphragm is set as a function of the seeing such that it optimizes the amount of light received from the object with respect to the amount of background light from the sky. If the NGS is a point source, the FWHM is best left to zero (then only the seeing will be taken into account). Only if your AO guide star is significantly extended with respect to the seeing should this parameter be set to a value different from zero.

11.2.3   Acquisition sequences without AO

The most general acquisition sequence for observation without AO is the following:

1. preset the telescope to the slit viewer guide star (SVGS);

2. interactively re-center the SVGS in the slit;

3. start guiding;

4. offset to the target.

Of course, if the SVGS and the target are the same object, the sequence simplifies to:

1. preset the telescope to the target;

2. interactively re-center the target in the slit;

3. start guiding.

11.2.4 Science

Three templates are offered in P83. The `CRIRES_spec_obs_AutoNodOnSlit` is the preferred observing template for point-like sources. It allows staring or nodding observations with a fixed nodding throw along the slit, with optional jittering. The `CRIRES_spec_obs_SpectroAstrometry` essentially does the same as `CRIRES_spec_obs_AutoNodOnSlit`, but for each value of a list of slit position angles. This template is particularly suitable for applying the spectro-astrometry technique (Beckers, J., 1982, Opt. Acta, 29, 361; Bailey, J., 1998, MNRAS 301, 161 and references therein). First results using this technique with CRIRES are described in Pontoppidan et al. 2008. Note that this template can currently only be used with adaptive optics and if the target is also the slit viewer guide star (but the AO star can be different).

The `CRIRES_spec_obs_GenericOffset` allows generic offsets suitable for observations of very extended objects.

The observing templates are described in Sect. 14.

11.2.5 Calibration

Darks, flat fields and wavelength calibrations are taken during daytime as part of the calibration plan (see Sect. 12). A Halogen lamp is used for flat fields. Fiber-fed ThAr spectra or the N_2O or CO gas cell in front of the halogen lamp are used for wavelength calibration.

Observed sky lines which can be identified by HITRAN have the advantage that wavelength calibration is done from the science observations themselves. Unfortunately, sufficient sky lines are not necessarily available for all settings, sometimes because they are saturated. General recommendations on absolute wavelength calibration is given in Sect. 7.1. *However, observers are strongly advised to use the* ETC *with the output options* **Sky Emission Spectrum** *and* **Sky Absorption Spectrum** *and to check for themselves if enough unsaturated telluric lines are available for a proper wavelength calibration in the spectral range of interest.*

Dedicated OBs for wavelength calibration shall be attached immediately before or after the science template so that prism and grating are not moved in between. Most observers wish to correct for telluric features and therefore need to supply a standard star OB. Observing time needed to execute telluric or spectro-photometric standard stars is charged to the observer.

11.3 DIT setting

In principle there is a free choice to select a DIT between the minimum of 1s and the maximum of 900s. However, it is strongly recommend to choose the one of the DITs listed below. A first reason is that the dark which depends on a particular DIT is taken during day time calibration for all settings used during the previous night: if a too large set of different and long DITs is used, there is a risk that daytime calibrations cannot be performed entirely. In addition, the method to correct for non–linear detector effects (including the 'odd-even' effect; see Sect. 6.4) requires a large number of calibrations: at this stage, the CRIRES team can only aim at providing the necessary information to apply such a method for the following DIT values.

- Short exposures on objects brighter than J,H,K $\sim$ 8–10 mag, or in the L or M bands, should use DITs of 1 s, 1.5 s, 2 s, 3 s, 5 s, 7 s, 10 s, 15 s, 20 s, 30 s or 45 s.

- Long exposures on faint targets *must* select DITs of 60 s, 90 s, 120 s, 180 s, 300 s or 600 s. For DIT of 900 s a waiver is required.

Note however that optimal flat-fielding correction (in particular for the odd-even effect) requires that DIT be at least 2 s (§6.4).

NDIT is specified by the observer to reach the required SNR as computed with the ETC.

11.4 README and finding charts

General instructions on the README file and finding charts are given at:

<p align="center">http://www.eso.org/observing/p2pp</p>

while CRIRES-specific requirements can be found at:

<p align="center">http://www.eso.org/observing/p2pp/CRIRES/CRIRES-P2PP.html</p>

Appropriate and detailed finding charts are *crucial* for the success of observations, especially in crowded fields.

- The field of view of the finding chart should be 50 ″ by 50 ″ in size, with a clear indication of field orientation. The target should be clearly marked by an arrow. If observations are performed with the derotator in SKY mode, the slit orientation should be clearly drawn.

- For high proper motion stars (> 1"/year) the present day position should be indicated by an arrow pointing from the target in the chart to the present day position (especially if similar bright sources are around).

- The finding chart has to show the field in the NIR band closest to the observing wavelength, λ_{OBS}:

    - in J band, if 950 nm < λ_{OBS} ≤ 1300 nm,
    - in H band, if 1300 nm < λ_{OBS} ≤ 2000 nm, or for very bright targets;
    - in K band, if 2000 nm < λ_{OBS} ≤ 5400 nm.

    Note that the ESO infrared digitized sky II actually correspond to the I band and should not be used if other infrared images are available (e.g. 2MASS).

- In crowded fields, a second finding chart should be attached to the corresponding OB, with a zoom-in on the science target(s).

- In case of binary or multiple stars, the target must be clearly indicated, in particular, (a) in case of large proper motion, including relative proper motion; (b) in case the finding chart was obtained in a band-pass that does not include the observing wavelength.

- AO, SVGS and science target should be clearly marked. If the AO star or SVGS are less than 15″ from the edge of the finding chart (centered on the target), another 2 ′ by 2 ′ finding chart should be provided.

The magnitude of the AO and SV guide stars, of the science target, and of the standard stars should be explicitly given in the `Instrument Comments` field of each OB. Please check the CRIRES P2PP-related information at :

<p align="center">http://www.eso.org/observing/p2pp/CRIRES/CRIRES-P2PP.html</p>

for more details.

11.5 Constraints

11.5.1 Moon

As stated above (§9.4), an FLI of 1.00 is suitable for most observations. However, telescope guiding and active optics can be compromised for moon distance smaller than 30 deg. A smaller FLI value is recommended only in the case of AO observations with an AO star fainter than R = 15 mag. In this case, a value 0.7 and a moon distance larger than 50 deg is generally adequate.

11.5.2 Seeing and Strehl ratio for adaptive optics observations

For closed loop AO observations, the users must specify in the constraint set the desired on-axis Strehl ratio, i.e. the ratio of the maximal intensity of the PSF to the maximal intensity expected for the theoretical PSF with no turbulence. This is the main parameter regarding atmospheric turbulence. It should be set for the K band; this value is produced by the ETC.

In addition, all closed loop AO observations should enter also the FWHM of the seeing, although this constraint is less relevant. The constraint on the seeing refers to the seeing measured by the DIMM or by the guide probe, as they are the most relevant for the MACAO system. It is used as a guide, together with the coherence time, in order to estimate the achievable Strehl ratio.

If the AO star is not the science target, it is worth noting that the isoplanatic angle θ_0 depends on airmass$^{-8/5}$, and on the wavelength as $\lambda^{6/5}$. On the other hand, the Strehl ratio, SR, decreases with the angular distance to the AO star θ as $SR \propto \exp\left(-(\theta/\theta_0)^{5/3}\right)$.

11.5.3 Seeing for seeing limited observations, no adaptive optics

For NoAO observations, only the seeing at the wavelength of observations is relevant. The user should therefore specify the FWHM for the respective bands of the science observations. The constraints set and definitions are the same as for all other seeing limited VLT instruments. The input field for the Strehl ratio should remain unchanged (i.e., N/A).

The classification of each observation will be based either (a) on the measured spatial profile of the spectrum if the object is a point source, or (b) on FWHM of a star seen on the Slit Viewer if there are more stars available, or (c) on the seeing measured on the guide probe otherwise, using the Roddier formula to convert it to the seeing at the observed wavelength.

11.5.4 Transparency

Thin clouds (THN) usually do not hamper CRIRES observations for bright objects. Clear (CLR) conditions are justified for observations requiring stable Strehl ratios, for example to study the close environment of the target, as clouds could otherwise adversely affect the adaptive optics. For the same reason, CLR conditions should be requested for AO observations using AO stars fainter than R ≈ 14.

11.5.5 Airmass

In addition to the influence of airmass on the quality of the adaptive optics correction mentioned above, observations in SKY mode can be strongly affected by differential refraction

effects. Some guide lines are given in §8.2.

11.6 Water vapor

Observations in the NIR can be severely affected by the presence of water vapor in the atmosphere: large amount of water vapor can significantly decrease the sky transmission, and, in particular, in the L and M bands increase the sky emission background.

The ETC offers the possibility to select sky spectra calculated with a set of representative amounts of water vapor in the atmosphere. Service mode users with the help of USD can then indicate in the README file which observations can be adversely affected by large amount of water vapor. ESO considers the possibility to add a constraint on the water vapor in the P2PP constraint set for future periods.

11.7 Offset conventions and definitions

CRIRES follows the standard astronomical offset conventions and definitions.

Position angles (PAs) are measured from 0 to 360 degrees. North corresponds to a PA of 0 degree, East, to a PA of 90 degrees.

All offsets are given in arc seconds.

Proper motions must be given in $''$ per year.

For solar system objects, additional tracking velocities are given in arcsec per second.

For a position angle of 0 in SKY mode, the reconstructed slit viewer image shows North up and East left.

Part IV

Reference material

12   CRIRES calibration plan

The calibration plan defines the default calibrations obtained and archived for the user by the Paranal Science Operations. The CRIRES science calibration plan includes the following measurements:

- *daily:* darks obtained with the same DITs as the science, telluric or spectro-photometric standard star observations, as well as for any flat-fields or wavelength calibrations. Note that the frequency may change to *weekly* if darks are found to be stable enough;

- *daily:* flat-fields obtained with the same wavelength setting as the science and telluric or spectro-photometric standard star observations;

- *daily:* wavelength calibration obtained with the same wavelength setting as the science and telluric or spectro-photometric standard star observations, for reference wavelengths shorter than 2400 nm. Currently, the reproducibility of the wavelength setting between night–time observations and day–time calibrations is ≈ 3 pixels.

- *daily:* bad-pixel maps, derived from darks and flat-fields. Note that the frequency may change to *weekly* or *monthly* these quantities are found to be stable enough;

- approximately *monthly:* linearity.

- *yearly or after instrument warm-up:* distortion map and photon transfer function;

- typically once per night CRIRES is used: radial velocity standard.

Flats and wavelength calibration are only obtained with a slit width of 0.2 ″and DIT ≥ 2 s.

13 Data format and reduction

13.1 Format

The SV image and the spectra recorded on the four science detectors are saved in extended FITS files. Each of the 4 extensions for the science images have format of 1024×512 pixels (see Fig. 2).

13.2 Pipeline

A first version of the CRIRES pipeline has been released by ESO/SDD. It uses the ESO/CPL library. The main observation and calibration templates are supported by an automatic version of the pipeline for quick-look analysis at the telescope. Raw images are combined, spectra extracted and calibrated in wavelength. Photometric conversion factors based on standard star observations are provided.

More information can be found at:

> http://www.eso.org/sci/data-processing/software/pipelines/

and

> http://www.eso.org/observing/dfo/quality/index_crires.html

14   Template parameters

All scientific and calibration observations with ESO instruments are prepared as observation blocks (OBs) and with the phase 2 proposal preparation tool (P2PP).

Observation blocks consist of the target information, a small number of user selected templates, the constraints sets and the scheduling information. The input parameters of the templates described below are list of keywords that define the telescope pointing and instrument configuration. One OB contains only one acquisition template and is followed by one or more science or calibration templates.

User accessible input parameters of CRIRES templates for acquisition, science, dark, flat, wavelength calibration and or standard star observation are described in the following sections. The pipeline is triggered by DPR keywords which are described in the pipeline user manual. There are given here for completeness.

14.1   Acquisition templates

All science and standard star OBs *must* start with an acquisition template. Two acquisition templates are available:

- CRIRES_spec_acq_NGS,

- CRIRES_spec_acq_NoAO.

CRIRES_spec_acq_NGS acquires the AO star with MACAO, which allows the user to make the following science or standard star observations with the adaptive optics system. On the other hand, observations following the CRIRES_spec_acq_NoAO acquisition template will not be done with the adaptive optics system.

The acquisition templates contain the parameters required for the pointing and tracking of the telescope, centering of the target in the slit, setting of the derotator mode which includes the orientation of the slit on the sky. CRIRES_spec_acq_NGS also includes parameters used to acquire the natural guide star (NGS) and close the loop of the Adaptive Optics system.

Note that currently the observing template CRIRES_spec_obs_SpectroAstrometry can only be used if the acquisition template is CRIRES_spec_acq_NGS, with the additional restriction that the target is the SVGS.

14.1.1   Target and SVGS parameters

TEL.TARG.ALPHA, TEL.TARG.DELTA, TEL.TARG.EQUINOX   (P2PP: *RA, DEC, Equinox*) are the coordinates of the science target and the equinox for which these coordinates correspond to. In case of multiple objects in the slit or of extended objects, these coordinates correspond to the telescope pointing during the observations.

TEL.TARG.PMA, TEL.TARG.PMD   (P2PP: *Proper Motion Alpha, Delta*) are proper motion values in RA and DEC and specified in units of ″/year. If they are different from 0, the epoch, TEL.TARG.EPOCH (P2PP: *Epoch*) , at which the coordinates were valid should be given.

TEL.TARG.ADDVELALPHA, TEL.TARG.ADDVELDELTA (P2PP: *Diff. in RA, DEC*) are additional velocities in α, δ and in units of $''$/second. For solar system objects, the coordinates should be the J2000 ICRF, astrometric coordinates. In particular, the user should *not* provide the apparent coordinates!

Note: Starting with P2PP 2.12, the differential velocities for moving targets are to be specified directly in the target package, and not in the acquisition template as in previous versions (i.e., the fields *Telescope: Alpha/Delta additional tracking velocity* should be left blank). Please check Section 5.5.3 of the P2PP User Manual for more details.

TEL.TARG.OFFSETALPHA and TEL.TARG.OFFSETDELTA: (P2PP: *RA/DEC offset between target and SV guide star*). In some cases, such as:

- relatively faint targets observed through a relatively wide slit, for which not enough light is reflected from the slit jaws to the slit viewer detector; this situation may occur e.g. for $H \simeq 14$ targets and slit wider than 0.3 $''$, in good seeing conditions,

- diffuse objects on which guiding is difficult or impossible,

the use of a brighter object in the field of the slit viewer is recommended. This object will be used as a reference object for initial centering and as a guide star for secondary guiding. It is referred to as slit viewer guide star (SVGS).

In this case, TEL.TARG.OFFSETALPHA and TEL.TARG.OFFSETDELTA correspond to the offsets in $''$ between the SVGS and the target.

If α(SVGS) and δ(SVGS) are the coordinates of the slit viewer guide star, the sign conventions are as follow:

TEL.TARG.ALPHA + TEL.TARG.OFFSETALPHA = α(SVGS)

TEL.TARG.DELTA + TEL.TARG.OFFSETDELTA = δ(SVGS)

In other words, TEL.TARG.OFFSETALPHA and TEL.TARG.OFFSETDELTA are positive if the SVGS is located to the East and North of the target.

Example: one wishes to observe the target at
α_{2000}(Target) = 04h53m50.678s, δ_{2000}(Target) = -25°25'56.017". To center it in the slit, the nearby star at α_{2000}(SVGS) = 04h53m49.690s, δ_{2000}(SVGS) = -25°25'45.078" is used as a reference star as well as the slit viewer guide star. Both these objects have negligible proper motions. Then,

$$\text{TEL.TARG.OFFSETALPHA} = \Delta\alpha = \alpha_{2000}(\text{SVGS}) - \alpha_{2000}(\text{Target}), \qquad (4)$$
$$\text{TEL.TARG.OFFSETDELTA} = \Delta\delta = \delta_{2000}(\text{SVGS}) - \delta_{2000}(\text{Target}). \qquad (5)$$

Therefore, the relevant P2PP parameters are

$$
\begin{aligned}
\text{RA} &= \quad 04:53:50.678 \\
\text{DEC} &= -25:25:56.017 \\
\text{RA offset between target and SV guide star} &= \quad -13.38, \\
\text{DEC offset between target and SV guide star} &= \quad +10.94.
\end{aligned}
$$

Notes:

1. the use of a SVGS different from target is only possible if the derotator is set to SKY mode;

2. the use of the CRIRES_spec_obs_SpectroAstrometry template is only possible if the SVGS is also the target.

14.1.2 NGS parameters

The following parameters are only required by the template CRIRES_spec_acq_NGS.

SEQ.NGS.ISTARGET (P2PP: *Target = AO guide star*) is a flag. If set to 'T' (default) the natural guide star (NGS) used for the adaptive optics is also the science target of the observations. If this flag is set to 'F' then the user needs to provide the NGS coordinates SEQ.NGS.ALPHA and SEQ.NGS.DELTA. However, see also the note 3 below (§14.1.7) for a special case.

SEQ.NGS.COLOR (P2PP: *AO guide star: B-R color value*) gives the B-R color of the NGS. This parameter is needed for accurate correction of the differential refraction between the wavelength used for the observations and the effective wavelength of the wavefront sensor.

SEQ.NGS.FWHM (P2PP: *AO guide star: FWHM (arcsec)*) gives the FWHM (in ″) of the object used as natural guide star. For a point source, a value of 0 is appropriate

SEQ.NGS.SNR (P2PP: *AO guide star: Minimum S/N*) gives the required signal-to-noise ratio that MACAO needs on the wavefront sensor to be able to close the loop. The default value is fine for most cases, except for the faintest objects that the MACAO can acquire, in which case a smaller value is to be given.

SEQ.NGS.USELASTSKY (P2PP: *Use the last sky measurement for the WFS*) is a flag. If set to 'T', the MACAO will not repeat the sky measurement for the wavefront sensor. The sky measurement is used to determine the signal-to-noise ratio of the wavefront sensor flux. The default value ('T') is adequate for bright AO stars ($R < 10$). For fainter targets, it should be set to 'F'. In this case, the following parameters (SEQ.NGS.SKYALPHA and SEQ.NGS.SKYDELTA) should be determined with care if observations take place in crowded fields.

SEQ.NGS.SKYALPHA and SEQ.NGS.SKYDELTA (P2PP: *WFS Alpha/Delta sky offset (arcsec)*) gives the offsets of the location relative to the NGS where MACAO measures the sky.

If SEQ.NGS.SKYALPHA > 0, the sky is measured to the East of the NGS.

If SEQ.NGS.SKYDELTA > 0, the sky is measured to the North of the NGS.

Default values are usually fine, except in crowded fields.

SEQ.NGS.ISSVGS (P2PP: *SV Guide Star = AO Guide Star*) is a flag. If set to 'T' (default) the natural guide star (NGS) used for the adaptive optics is also the slit viewer guide star (SVGS). If this flag is 'F' then the user needs to provide the offsets TEL.TARG.OFFSETALPHA and TEL.TARG.OFFSETDELTA. However, see also the note 3 below (§14.1.7) for a special case.

14.1.3   Parameters related to the slit viewer

SEQ.SV.USELASTSKY (P2PP: *Use the last sky measurement for the SV*). Generally one can use the last sky measurement and therefore leaves SEQ.SV.USELASTSKY = 'T' untouched from its default value. However, if one observes a faint target, a new sky should be obtained for the slit viewer. In this case set SEQ.SV.USELASTSKY = 'F'.

TEL.SKY.OFFSETALPHA, TEL.SKY.OFFSETDELTA. (P2PP: *RA/DEC offset to sky*) are only relevant if SEQ.SV.USELASTSKY = 'F'. By default sky exposures are taken 30 ″ in RA and DEC from the science target position. In crowded fields however, one has a high chance that the sky exposures is contaminated by some other source(s). Therefore these parameters offer freedom to specify RA and DEC offset positions. These offsets are usually executed early in the procedure, at the time of the acquisition of the NGS. The convention for these RA, DEC offsets are:

$$\text{TEL.SKY.OFFSETALPHA} = \alpha_{\text{SKY}} - \alpha(NGS),$$
$$\text{TEL.SKY.OFFSETDELTA} = \delta_{\text{SKY}} - \delta(NGS).$$

14.1.4   Telescope guide star parameters

Sometimes, the telescope operator may have difficulties to find an appropriate telescope guide star, which is also used to set-up the M1 active optics. This often happens in the Orion nebula, in other nebulae that appear as saturated in the Digital Sky Survey, or in extended dark nebulae. In these cases, it is useful to provide a telescope guide star.

TEL.AG.GUIDESTAR (P2PP: *Telescope guide star selection*): if set to 'CATALOGUE', the Telescope Control System semi–automatically searches for a telescope guide star. If the user wishes to provide the coordinates of the telescope guide star, then TEL.AG.GUIDESTAR should be set to 'SETUPFILE'.

TEL.GS1.ALPHA, TEL.GS1.DELTA (P2PP: *RA/DEC of telescope guide star*) are only relevant if TEL.AG.GUIDESTAR = 'SETUPFILE'. These parameters correspond to the J2000 coordinates, epoch of the observations, of the telescope guide star. Otherwise, both parameters should be kept to default 0.

14.1.5   Derotator parameters

INS.DROT.MODE (P2PP label: *Derotator: Mode*) determines the derotator mode: SKY or ELEV. In ELEV mode, the slit is constantly aligned with the parallactic angle in order to reduce slit loss introduced by differential refraction. This is particularly important if slit viewer

guiding has to be made in one band (e.g., in K) and the observations in another one (e.g., M). *However, in ELEV mode, guiding with a SVGS different from target is not implemented.*

The use of the CRIRES_spec_obs_SpectroAstrometry and CRIRES_spec_obs_GenericOffset templates is only possible if the derotator mode is set to SKY.

INS.DROT.POSANG (P2PP label: *Position angle*) determines the position angle (PA) of the slit if INS.DROT.MODE = SKY. The values must be set such that INS.DROT.POSANG = PA.

14.1.6 Spectrograph parameters

INS.SLIT.WID (P2PP: *Entrance slit width*) determines the slit width in ″. Recommended value is 0.2 – 0.4 ″ with AO. Without AO, the optimal S/N is obtained with a slit width equal to the seeing, however, a value larger than 0.4″is not recommended, as a large fraction of the spectral range can be affected by vignetting or lack of reproducibility (see §8.4). A value of 0.2 ″ gives the highest resolution.

INS.WLEN.REF (P2PP: *Reference wavelength*) is the reference wavelength. This wavelength corresponds to pixel 512 of detector # 3. Tables 4a to 4f provide the reference wavelengths of the standard settings. Tables 6a and 6b lists the allowed minimum and maximum ranges for a given order. For visual inspection of the start and end wavelengths of each detector, unvignetted spectral range, detector gaps (Fig. 2) or the appearance of sky lines, the ETC should be used.

INS.GRAT.ORDER (P2PP: *Grating order*) is the grating order. For most wavelength settings there is a unique relation between the reference wavelength and the grating order. In this case INS.GRAT.ORDER can be kept as its default value of 0. However, for some reference wavelengths in order 39–43 and 21–22 there is no unique relation and the grating order has to be specified by the user. Table 6a lists the orders and wavelength ranges for which this parameter must be given.

14.1.7 Notes

1. If both SEQ.NGS.ISTARGET and SEQ.NGS.ISSVGS are set to 'T', then the target is the AO guide star and the slit viewer guide star. Therefore, only the target coordinates TEL.TARG.ALPHA and TEL.TARG.DELTA must be provided.

2. If SEQ.NGS.ISTARGET is 'T' and SEQ.NGS.ISSVGS is 'F', then the target is the AO guide star but it is not used for guiding with the slit viewer. In this case, in addition to TEL.TARG.ALPHA and TEL.TARG.DELTA, TEL.TARG.OFFSETALPHA and TEL.TARG.OFFSETDELTA should be provided (see above for the convention).

3. If SEQ.NGS.ISTARGET is 'F' and SEQ.NGS.ISSVGS is 'T', then the slit viewer guide star is the AO guide star but not the target. In this case, of course, TEL.TARG.ALPHA and TEL.TARG.DELTA should be provided. On the other hand, the user can either enter the coordinates of the AO guide star (SEQ.NGS.ALPHA and SEQ.NGS.DELTA)

or the offsets TEL.TARG.OFFSETALPHA and TEL.TARG.OFFSETDELTA (following the convention above).

14.2 Observation template

This section describes the three observation templates offered in P83:

- CRIRES_spec_obs_AutoNodOnSlit,

- CRIRES_spec_obs_GenericOffset,

- CRIRES_spec_obs_SpectroAstrometry.

An observation template sets up the instrument, if different from the acquisition, as well as the detector integration time (DIT) and number of individual integrations averaged to create an exposure (NDIT). It defines the number of exposures taken at each nodding position as well as the nodding and, if needed, jittering offsets.

The following paragraphs describe only the parameters that are not defined in the previous sections.

14.2.1 Detector

DET1.DIT (P2PP: *DIT*) defines the exposure time of an individual integration, in seconds. For bright objects, saturation of the detector (120,000 e$^-$) must be avoided. On the other hand, correction of the non–linearity of the detectors (incl. the odd-even effects; see Sect. 6.4) has so far been achieved to a reasonable accuracy only for a signal (dark + sky + object) smaller than about 10,000 ADUs ($\approx 80,000$e$^-$). DIT settings leading to stronger count rate should therefore be avoided. The ETC outputs a 'Max. intensity at central pixel per DIT (object+sky)' and therefore allows one to check if the chosen DIT is adequate. It is important to check that the ETC input parameter 'requested wavelength' does not correspond to a deep absorption line (either in the target spectrum or caused by the Earth's atmosphere). For faint objects in the J, H, and K bands, long DITs are recommended in order to decrease the contribution of the RON to the overall noise. See Sect. 11.3 for recommended and offered values.

DET1.NDIT (P2PP: *NDIT*) determines the number of individual integration averaged into one exposure. Therefore DET1.NDIT $\times$ DET1.DIT sets the total integration time of one exposure.

SEQ.NEXPO (P2PP: *Number of exposures per nodding position*) is the number of exposures in any nodding or offset position. Therefore the integration time spend in one nodding position is given by:

DET1.NDIT $\times$ DET1.DIT $\times$ SEQ.NEXPO

14.2.2 Gas cell

INS.OPTI1.NAME (P2PP: *Gas cell*) sets the gas cell to be used. The default value (FREE) should be set for observations without gas cell, while GAS_N2O or GAS_CO should be set for observations with the N$_2$O or CO gas cell, respectively. 1.4.

14.2.3 CRIRES_spec_obs_AutoNodOnSlit and CRIRES_spec_obs_SpectroAstrometry: nodding and jittering

SEQ.NABCYCLES (P2PP: *Number of nodding cycles*) sets the number of AB or BA nodding cycles. Although the value of 0 is allowed (staring), it is not recommended because of detector glow and other systematic effects (Sect. 6.2). If set to a value ≥ 1, the total integration time of the template, in seconds, is:

$\quad$ DET1.NDIT $\times$ DET1.DIT $\times$ SEQ.NEXPO $\times$ SEQ.NABCYCLES $\times$2.

However, one should not confuse integration time with the total execution time of one OB caused by the various overheads which need to be added as described in Sec. 10.3.

Examples:

If SEQ.NABCYCLES = 1, the telescope first points to the A position: it is located to the South (if INS.DROT.POSANG = 0) at a distance equal to SEQ.NODTHROW/2 (see below) (and assuming SEQ.JITTER.WITDH = 0) from the centering position. After SEQ.NEXPO exposures, the telescope nods to the B position: it moves to the north by SEQ.NODTHROW, and takes SEQ.NEXPO additional exposures. Then the telescope moves back to its original position. The telescope has then executed one AB nodding cycle.

If SEQ.NABCYCLES = 3, the telescope first points to the A position, as defined in the previous paragraph, and takes SEQ.NEXPO exposures. It then moves to the B position, takes twice SEQ.NEXPO additional exposures. It then moves back to the A position, when it takes twice SEQ.NEXPO exposures. Then, it moves a last time to the B position for a last sequence of SEQ.NEXPO exposures before returning to the original position. The telescope had therefore executed 3 nodding cycles: AB BA AB.

SEQ.NODTHROW (P2PP: *Nod throw along the slit*) is the nodding throw, or telescope offset between two nodding positions (Sect. 9). It should be large enough so that the spatial profiles of the target in the two nodding positions do not overlap. The nodding positions are located symmetrically (at SEQ.NODTHROW/2) around the centering location.

SEQ.JITTER.WIDTH (P2PP: *Jitter width*) A jitter is a small offset added to each nodding offset. It helps correcting for bad detector pixels (Sect. 9). SEQ.JITTER.WIDTH gives the width of the jitter box: the maximum offset from the nodding position is therefore given by half of this value. The successive values of the jitter offset in a given template are drawn from a set of 100 numbers determined from a Poisson random number generator. Jittering is currently not possible if SEQ.NABCYCLES = 0 (staring mode).

14.2.4 CRIRES_spec_obs_GenericOffset only: list of offsets

The CRIRES_spec_obs_GenericOffset allows the user to define a list of offsets, offering more flexibility for sky subtraction in case of extended objects. It only makes sense to use this template if INS.DROT.MODE (Derotator mode) is set to SKY in the acquisition template.

SEQ.OFFSET.COORDS (P2PP: *Offset coordinate type selection*) determines if the list of offsets given in SEQ.OFFSET1.LIST and SEQ.OFFSET2.LIST are given in SKY or DE-TECTOR coordinates.

SEQ.OFFSET1.LIST, SEQ.OFFSET2.LIST   (P2PP: *Lists of offsets in RA or X, Lists of offsets in DEC or Y*)

In all cases, the list of offsets are in arcseconds.

If SEQ.OFFSET.COORDS is set to 'SKY', a positive value in SEQ.OFFSET1.LIST means that the new pointing of the telescope is to the east relative to the previous location; similarly, a positive value in SEQ.OFFSET2.LIST means that the new pointing of the telescope is to the north relative to its previous location. During the first exposure, the telescope points to the location given by (TEL.TARG.ALPHA, TEL.TARG.DELTA) + the first value given in (SEQ.OFFSET1.LIST, SEQ.OFFSET2.LIST). In other words, in this case, the offsets correspond to telescope offsets.
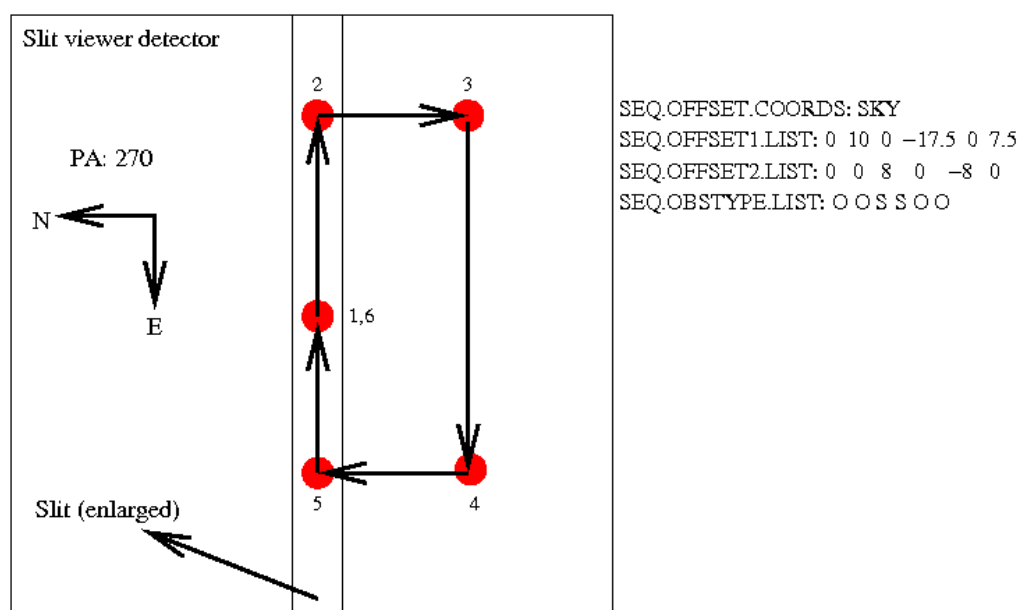
Figure 25: Illustration showing the apparent locations of a target as seen on the slit viewer detector for the given parameters, in the case of 'SKY' coordinate offsets.

If SEQ.OFFSET.COORDS is set to 'DETECTOR', the offsets correspond to the apparent motion of the target on the slit viewer detector, with X increasing from left to right (from E to W if the position angle is 0 deg) and Y increasing from bottom to top (from S to N if the position angle is 0 deg, see Fig. 17). In other words, in this case, a positive offset in both X and Y would bring the target to larger X and larger Y values as seen on the slit viewer. If the position angle is 0, this corresponds to a motion of the telescope to the East and South. Subsequent offsets are similarly made relative to the last telescope offset.

SEQ.OBSTYPE.LIST   (P2PP: *List of observation types (O or S)*) is a list that determines if the exposure taken once the corresponding offset has been completed is an 'OBJECT' ('O') or a 'SKY' ('S') measurement. Therefore, the total integration time of one exposure in an 'OBJECT' location is DET1.NDIT.OBJECT $\times$ DET1.DIT. Similarly, the total integration time of one exposure in 'SKY' location is DET1.NDIT.SKY $\times$ DET1.DIT. Note that SEQ.NEXPO exposures can be obtained at each location.
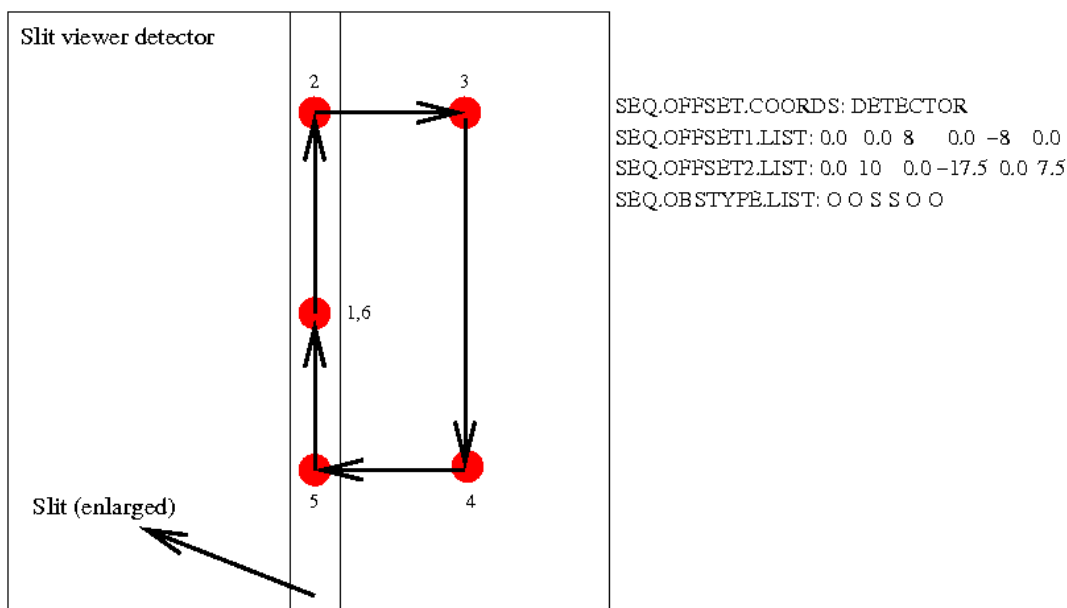
Figure 26: Illustration showing the apparent locations of a target as seen on the slit viewer detector for the given parameters, in the case of 'DETECTOR' coordinate offsets. Although the derotator mode must be set to 'SKY, the position angle is irrelevant since all the motions are made in detector coordinates.

SEQ.NOFF (P2PP: *Number of offset positions*) gives the total number of telescope positions that the telescope will have during the execution of the template. Minimum value is 1. If this value is larger than the number of values listed in SEQ.OFFSET1.LIST, or SEQ.OFFSET2.LIST then the list is started again.

For example, if SEQ.NOFF = 5, SEQ.OFFSET1.LIST = '0 0 0' and SEQ.OFFSET2.LIST = '0 10 -10', SEQ.OFFSET.COORDS = 'DETECTOR', the list of offsets will be '0 0 0 0 0' along the X direction, '0 10 -10 0 10' along the Y direction.

14.2.5 CRIRES_spec_obs_SpectroAstrometry only: list of derotator angles, jitter reset

The CRIRES_spec_obs_SpectroAstrometry template is allows one to apply the spectro-astrometry technique without having to re-acquire the target for each position angle. It only makes sense to use this template if INS.DROT.MODE (Derotator mode) is set to SKY in the acquisition template. Currently, this template is only implemented in AO mode.

INS.DROT.POSANG.LIST (P2PP: *List of position angles*) is the list of position angles: the CRIRES_spec_obs_SpectroAstrometry template allows one to repeat the same sequence of observations as the ones done for the CRIRES_spec_obs_AutoNodOnSlit template but for each value of the list of slit position angles given by this parameter.

Best results are obtained by giving a list of pairs of position angles differing by 180 degrees.

SEQ.JITTER.RESET (P2PP: *Reset jitter for each DROT posang*). Only relevant if SEQ.JITTER.WIDTH (Jitter width) is larger than 0. If this parameter is set to T the list of

jitter positions calculated by the observation software is repeated identically, in detector coordinates, for each value of the slit position angle. In other words, the location of the different spectra for each nodding position will be identically repeated for each position angle.

If set to F, each nodding position in the execution of the whole template will be given a different jitter value.

If the number of nodding cycles is small, it is probably better to set this parameter to T. For a large number of nodding cycles, any residual detector systematic effects may be further decreased by setting the parameter to F.

14.3 Calibration templates

14.3.1 Standard star or telluric observations

The calibration template CRIRES_spec_cal_AutoNodOnSlit is used to measure a telluric or spectro-photometric standard star (Sect. 9). Its functionality is similar to the observing template CRIRES_spec_obs_AutoNodOnSlit described above. The files produced here will be automatically recognized by the pipeline as standard star observations.

14.3.2 Flat field

Flat-fields can be obtained with the template CRIRES_spec_cal_LampFlats. However, there is no *a priori* necessity to obtain flat–fields during the night.
Only INS.WLEN.REF and INS.GRAT.ORDER must be defined in this template.

14.3.3 Wavelength calibration

High precision absolute wavelength calibration can be either obtained with sky emission lines or through the use of an arc lamp spectrum (see Sect. 7.1): currently, the reproducibility of the wavelength setting between night–time observations and day–time calibrations is ≈ 3 pixels. If required for your science experiment than insert the CRIRES_spec_cal_Wave template either before or after any new wavelength setting in order to perform a wavelength calibration.

The parameters required by this template are INS.LAMP, INS.WLEN.REF and possibly INS.GRAT.ORDER.

INS.LAMP (P2PP: *Wavelength calibration source*) determines the source used for the wavelength calibration. The values allowed are THAR for the Thorium–Argon lamp, HALOGEN+N2O_CELL for the Halogen + the N_2O gas-cell and HALOGEN+CO_CELL for the Halogen + the CO gas-cell. See Sect. 18.

14.3.4 Darks

Darks are obtained during daytime calibration by the VLT observatory. There is no need to execute dark exposures during the night.
The parameters required by this template are DIT, NDIT and NEXPO.

14.3.5 Template signatures

CRIRES_spec_acq_NGS		
To be specified:		
Parameter	Range *(Default)*	Label
SEQ.NGS.ISTARGET	T F *(T)*	Target = AO Guide Star
SEQ.NGS.ALPHA	*(0)*	RA of AO guide star
SEQ.NGS.DELTA	*(0)*	DEC of AO guide star
SEQ.NGS.COLOR	-1..5 *(0)*	AO guide star: B-R color value
SEQ.NGS.FWHM	0..10 *(0.0)*	AO guide star: FWHM (arcsec)
SEQ.NGS.SNR	0.0..10000.0 *(1000)*	AO guide star: Minimum S/N
SEQ.NGS.USELASTSKY	T F *(F)*	Use the last sky measurement for the WFS
SEQ.NGS.SKYALPHA	-30..+30 *(4.0)*	WFS Alpha sky offset (arcsec)
SEQ.NGS.SKYDELTA	-30..+30 *(4.0)*	WFS Delta sky offset (arcsec)
SEQ.NGS.ISSVGS	T F *(T)*	SV Guide Star = AO Guide Star
SEQ.SV.USELASTSKY	T F *(T)*	Use the last sky measurement for the SV
TEL.SKY.OFFSETALPHA	-120..120 *(30.0)*	RA offset to sky
TEL.SKY.OFFSETDELTA	-120..120 *(30.0)*	DEC offset to sky
TEL.AG.GUIDESTAR	NONE SETUPFILE CATALOGUE *(CATALOGUE)*	Telescope guide star selection
TEL.GS1.ALPHA	*(0.0)*	RA of telescope guide star
TEL.GS1.DELTA	*(0.0)*	DEC of telescope guide star
TEL.TARG.OFFSETALPHA	-22.5..22.5 *(0.0)*	RA offset between target and SV guidestar
TEL.TARG.OFFSETDELTA	-22.5..22.5 *(0.0)*	DEC offset between target and SV guidestar
INS.DROT.MODE	SKY ELEV *(NODEFAULT)*	Derotator: Mode
INS.DROT.POSANG	0.0..360.0 *(0.0)*	Position angle
INS.SLIT.WID	0.05..3.0 *(0.2)*	Entrance slit width
INS.WLEN.REF	958.3..5361.9 *(NODEFAULT)*	Reference wavelength
INS.GRAT.ORDER	0..59 *(0)*	Grating order
TEL.TARG.ALPHA	*(NODEFAULT)*	Right Ascension
TEL.TARG.DELTA	*(NODEFAULT)*	Declination
TEL.TARG.EQUINOX	-2000..3000 *(2000)*	Equinox
TEL.TARG.EPOCH	-2000..3000 *(2000)*	Epoch
TEL.TARG.PMA	-10..10 *(0)*	Proper Motion RA
TEL.TARG.PMD	-10..10 *(0)*	Proper Motion DEC
TEL.TARG.ADDVELALPHA	-15..15 *(0.0)*	Diff RA
TEL.TARG.ADDVELDELTA	-15..15 *(0.0)*	Diff DEC
Fixed values:		
Parameter	Value	Label
DPR.CATG	ACQUISITION	Data product category
DPR.TECH	IMAGE	Data product technique
DPR.TYPE	OBJECT	Data product type

CRIRES_spec_acq_NoAO		
To be specified:		
Parameter	Range *(Default)*	Label
SEQ.SV.USELASTSKY	T F *(T)*	Use the last sky measurement for the SV
TEL.SKY.OFFSETALPHA	-120..120 *(30.0)*	RA offset to sky
TEL.SKY.OFFSETDELTA	-120..120 *(30.0)*	DEC offset to sky
TEL.AG.GUIDESTAR	NONE SETUPFILE CATALOGUE *(CATALOGUE)*	Telescope guide star selection
TEL.GS1.ALPHA	*(0.0)*	RA of telescope guide star
TEL.GS1.DELTA	*(0.0)*	DEC of telescope guide star
TEL.TARG.OFFSETALPHA	-40..40 *(0.0)*	RA offset between target and SV guidestar
TEL.TARG.OFFSETDELTA	-40..40 *(0.0)*	DEC offset between target and SV guidestar
INS.DROT.MODE	SKY ELEV *(NODEFAULT)*	Derotator: Mode
INS.DROT.POSANG	0.0..360.0 *(0.0)*	Position angle
INS.SLIT.WID	0.05..3.0 *(0.2)*	Entrance slit width
INS.WLEN.REF	958.3..5361.9 *(NODEFAULT)*	Reference wavelength
INS.GRAT.ORDER	0..59 *(0)*	Grating order
TEL.TARG.ALPHA	*(NODEFAULT)*	Right Ascension
TEL.TARG.DELTA	*(NODEFAULT)*	Declination
TEL.TARG.EQUINOX	-2000..3000 *(2000)*	Equinox
TEL.TARG.EPOCH	-2000..3000 *(2000)*	Epoch
TEL.TARG.PMA	-10..10 *(0)*	Proper Motion RA
TEL.TARG.PMD	-10..10 *(0)*	Proper Motion DEC
TEL.TARG.ADDVELALPHA	-15..15 *(0.0)*	Diff RA
TEL.TARG.ADDVELDELTA	-15..15 *(0.0)*	Diff DEC
Fixed values:		
Parameter	Value	Label
DPR.CATG	ACQUISITION	Data product category
DPR.TECH	IMAGE	Data product technique
DPR.TYPE	OBJECT	Data product type

CRIRES_spec_obs_AutoNodOnSlit		
To be specified:		
Parameter	Range *(Default)*	Label
DET1.DIT	0..900 *(NODEFAULT)*	DIT
DET1.NDIT	1..1000 *(1)*	NDIT
SEQ.NEXPO	1..100 *(1)*	Number of exposures per nodding position
SEQ.NABCYCLES	0..100 *(1)*	Number of nodding cycles
SEQ.NODTHROW	0..22.5 *(10)*	Nod throw along the slit
SEQ.JITTER.WIDTH	0..8 *(0)*	Jitter width
INS.OPTI1.NAME	FREE GAS_N2O GAS_CO *(FREE)*	Gas cell
INS.WLEN.REF	958.3..5361.9 *(NODEFAULT)*	Reference wavelength
INS.GRAT.ORDER	0..59 *(0)*	Grating order
Fixed values:		
Parameter	Value	Label
DPR.CATG	SCIENCE	Data product category
DPR.TECH	SPECTRUM,NODDING/DIRECT, [JITTER/OTHER]	Data product technique
DPR.TYPE	OBJECT	Data product type

CRIRES_spec_obs_SpectroAstrometry		
To be specified:		
Parameter	Range *(Default)*	Label
DET1.DIT	0..900 *(NODEFAULT)*	DIT
DET1.NDIT	1..1000 *(1)*	NDIT
INS.DROT.POSANG.LIST	0.0..360.0 *()*	List of position angles
INS.GRAT.ORDER	0..59 *(0)*	Grating order
INS.OPTI1.NAME	FREE GAS_N2O GAS_CO *(FREE)*	Gas cell
INS.WLEN.REF	958.3..5361.9 *(NODEFAULT)*	Reference wavelength
SEQ.JITTER.RESET	F T *(T)*	Reset jitter for each DROT posang
SEQ.JITTER.WIDTH	0..8 *(0)*	Jitter width
SEQ.NABCYCLES	0..100 *(1)*	Number of nodding cycles
SEQ.NEXPO	1..100 *(1)*	Number of exposures per nodding position
SEQ.NODTHROW	0..22.5 *(10)*	Nod throw along the slit
Fixed values:		
Parameter	Value	Label
DPR.CATG	SCIENCE	Data product category
DPR.TECH	SPECTRUM,NODDING,JITTER, ASTROMETRY	Data product technique
DPR.TYPE	OBJECT	Data product type

CRIRES_spec_obs_GenericOffset		
To be specified:		
Parameter	Range *(Default)*	Label
DET1.DIT	0..900 *(NODEFAULT)*	DIT
DET1.NDIT.OBJECT	1..100 *(1)*	NDIT for the OBJECT positions
DET1.NDIT.SKY	1..100 *(1)*	NDIT for the SKY positions
INS.GRAT.ORDER	0..59 *(0)*	Grating order
INS.OPTI1.NAME	FREE GAS_N2O GAS_CO *(FREE)*	Gas cell
INS.WLEN.REF	958.3..5361.9 *(NODEFAULT)*	Reference wavelength
SEQ.NEXPO	1..100 *(1)*	Number of exposures on each position
SEQ.NOFF	1..100 *(NODEFAULT)*	Number of offset positions
SEQ.OBSTYPE.LIST	O S *(NODEFAULT)*	List of observation types (O or S)
SEQ.OFFSET.COORDS	SKY DETECTOR *(SKY)*	Offset coordinate type selection
SEQ.OFFSET1.LIST	*(NODEFAULT)*	List of offsets in RA or X
SEQ.OFFSET2.LIST	*(NODEFAULT)*	List of offsets in DEC or Y
Fixed values:		
Parameter	Value	Label
DPR.CATG	SCIENCE	Data product category
DPR.TECH	SPECTRUM	Data product technique
DPR.TYPE	OBJECT or SKY	Data product type

CRIRES_spec_cal_AutoNodOnSlit		
To be specified:		
Parameter	Range *(Default)*	Label
DET1.DIT	0..900 *(NODEFAULT)*	DIT
DET1.NDIT	1..1000 *(1)*	NDIT
SEQ.NEXPO	1..100 *(1)*	Number of exposures per nodding position
SEQ.NABCYCLES	0..100 *(1)*	Number of nodding cycles
SEQ.NODTHROW	0..22.5 *(10)*	Nod throw along the slit
SEQ.JITTER.WIDTH	0..8 *(0)*	Jitter width
INS.OPTI1.NAME	FREE GAS_N2O GAS_CO *(FREE)*	Gas cell
INS.WLEN.REF	958.3..5361.9 *(NODEFAULT)*	Reference wavelength
INS.GRAT.ORDER	0..59 *(0)*	Grating order
Fixed values:		
Parameter	Value	Label
DPR.CATG	CALIB	Data product category
DPR.TECH	SPECTRUM,NODDING/DIRECT, [JITTER/OTHER]	Data product technique
DPR.TYPE	STD	Data product type

CRIRES_spec_cal_LampFlats		
To be specified:		
Parameter	Range *(Default)*	Label
INS.WLEN.REF	958.3..5361.9 *(NODEFAULT)*	Reference wavelength
INS.GRAT.ORDER	0..59 *(0)*	Grating order
Fixed values:		
Parameter	Value	Label
DPR.CATG	CALIB	Data product category
DPR.TECH	SPECTRUM	Data product technique
DPR.TYPE	FLAT	Data product type

CRIRES_spec_cal_Wave		
To be specified:		
Parameter	Range *(Default)*	Label
INS.LAMP	THAR HALOGEN+N2O_CELL HALOGEN+CO_CELL *(THAR)*	Wavelength calibration source
INS.WLEN.REF	958.3..5361.9 *(NODEFAULT)*	Reference wavelength
INS.GRAT.ORDER	0..59 *(0)*	Grating order
Fixed values:		
Parameter	Value	Label
DPR.CATG	CALIB	Data product category
DPR.TECH	SPECTRUM	Data product technique
DPR.TYPE	WAVE,LAMP/ABSORPTION-CELL	Data product type

CRIRES_spec_cal_Darks		
To be specified:		
Parameter	Range *(Default)*	Label
DET1.DIT	0..900 *(60.)*	DIT
DET1.NDIT	1..1000 *(1)*	NDIT
SEQ.NEXPO	1..100 *(3)*	Number of exposures
Fixed values:		
Parameter	Value	Label
DPR.CATG	CALIB	Data product category
DPR.TECH	IMAGE	Data product technique
DPR.TYPE	DARK	Data product type

15 CRIRES standard wavelength settings

15.1 Wavelength ranges

Table 4a: Reference wavelengths, λ_{ref}, for the standard settings, defined as the wavelength at pixel 512 of the 3rd detector. Order number ($\mathcal{O}$), internal wavelength identification (ID), unvignetted spectral range and coverage for each of the four detectors are also given. The last column lists the mean dispersion, $\delta\lambda$, in 10^{-3} nm/pixel, for detector 3. A ^{c} indicates that the order number *must* also be specified as a parameter. Illumination outside of the unvignetted spectral range is affected by lack of reproducibility at more than 1% level, for a 0.2 arcsec slit: wavelength values given in italic fall outside the unvignetted range. *Wavelengths are vacuum expressed in nm. The accuracy on the positioning of the reference wavelength is ≈ 30 pixels. See Table 5a-5h for spectral ranges in wavenumber.*

λ_{ref}	$\mathcal{O}$	ID	Unvign. range $\lambda_{\min}$	$\lambda_{\max}$	Det. 1 $\lambda_{\min}$	$\lambda_{\max}$	Det. 2 $\lambda_{\min}$	$\lambda_{\max}$	Det. 3 $\lambda_{\min}$	$\lambda_{\max}$	Det. 4 $\lambda_{\min}$	$\lambda_{\max}$	$\delta\lambda$
958.3	59	59/0/n	949.1	961.6	*943.6*	*948.6*	949.9	954.7	956.0	960.6	*961.8*	*966.2*	4.5
961.0	59	59/0/i	951.8	964.3	*946.4*	*951.4*	952.7	957.5	958.7	963.3	*964.5*	*968.8*	4.4
974.8	58	58/0/n	965.3	978.2	*959.8*	*964.9*	966.3	971.2	972.5	977.1	*978.4*	*982.8*	4.6
977.6	58	58/0/i	968.2	981.1	*962.8*	*967.8*	969.2	974.0	975.3	979.9	*981.1*	*985.5*	4.5
991.9	57	57/0/n	982.2	995.5	*976.6*	*981.8*	983.3	988.2	989.5	994.3	*995.5*	*1000.0*	4.6
994.8	57	57/0/i	985.1	998.4	*979.7*	*984.8*	986.2	991.2	992.5	997.2	*998.4*	*1002.9*	4.6
1009.6	56	56/0/n	999.7	1013.3	*994.1*	*999.3*	1000.8	1005.8	1007.2	1012.0	*1013.3*	*1017.9*	4.7
1012.5	56	56/0/i	1002.6	1016.2	*997.1*	*1002.4*	1003.8	1008.8	1010.1	1014.9	*1016.1*	*1020.7*	4.7
1028.0	55	55/0/n	1017.8	1031.8	*1012.2*	*1017.6*	1019.0	1024.2	1025.5	1030.5	*1031.8*	*1036.4*	4.8
1030.9	55	55/0/i	1020.7	1034.8	*1015.3*	*1020.6*	1022.0	1027.1	1028.5	1033.3	*1034.6*	*1039.2*	4.7
1047.0	54	54/0/n	1036.5	1051.0	*1030.9*	*1036.4*	1037.9	1043.1	1044.5	1049.5	*1050.8*	*1055.6*	4.9
1050.0	54	54/0/i	1039.6	1054.0	*1034.1*	*1039.5*	1041.0	1046.2	1047.5	1052.5	*1053.8*	*1058.5*	4.8
1066.8	53	53/0/n	1056.1	1070.9	*1050.4*	*1056.0*	1057.5	1062.8	1064.3	1069.4	*1070.7*	*1075.6*	5.0
1069.8	53	53/0/i	1059.1	1074.0	*1053.6*	*1059.1*	1060.6	1065.9	1067.3	1072.3	*1073.6*	*1078.4*	4.9
1087.3	52	52/0/n	1076.3	1091.6	*1070.6*	*1076.3*	1077.8	1083.3	1084.7	1089.9	*1091.3*	*1096.2*	5.1
1090.4	52	52/0/i	1079.4	1094.7	*1073.9*	*1079.5*	1081.0	1086.4	1087.8	1093.0	*1094.3*	*1099.2*	5.0
1108.6	51	51/0/n	1097.3	1113.1	*1091.6*	*1097.4*	1099.0	1104.5	1106.0	1111.3	*1112.6*	*1117.7*	5.2
1111.8	51	51/0/i	1100.5	1116.3	*1095.0*	*1100.7*	1102.3	1107.7	1109.2	1114.4	*1115.8*	*1120.8*	5.1
1130.8	50	50/0/n	1119.2	1135.4	*1113.5*	*1119.3*	1121.0	1126.6	1128.1	1133.5	*1134.9*	*1140.1*	5.3
1134.0	50	50/0/i	1122.4	1138.7	*1116.8*	*1122.7*	1124.3	1129.9	1131.3	1136.7	*1138.1*	*1143.2*	5.2
1153.9	49	49/0/n	1142.0	1158.7	*1136.2*	*1142.2*	1143.9	1149.6	1151.2	1156.7	*1158.1*	*1163.4*	5.4
1157.2	49	49/0/i	1145.3	1162.1	*1139.7*	*1145.6*	1147.3	1153.0	1154.5	1159.9	*1161.4*	*1166.5*	5.3
1177.9	48	48/0/n	1165.6	1182.9	*1159.8*	*1166.0*	1167.7	1173.5	1175.1	1180.7	*1182.2*	*1187.5*	5.5
1181.3	48	48/0/i	1169.1	1186.4	*1163.4*	*1169.5*	1171.2	1177.0	1178.5	1184.1	*1185.5*	*1190.8*	5.4
1203.0	47	47/0/n	1190.4	1208.2	*1184.6*	*1190.8*	1192.5	1198.5	1200.1	1205.9	*1207.4*	*1212.8*	5.6
1206.4	47	47/0/i	1193.8	1211.7	*1188.2*	*1194.3*	1196.1	1202.0	1203.6	1209.2	*1210.7*	*1216.1*	5.5

Table 4b: Reference wavelengths, λ_{ref}, for the standard settings, defined as the wavelength at pixel 512 of the 3rd detector. Order number ($\mathcal{O}$), internal wavelength identification (ID), unvignetted spectral range and coverage for each of the four detectors are also given. The last column lists the mean dispersion, $\delta\lambda$, in 10^{-3} nm/pixel, for detector 3. A ^{c} indicates that the order number *must* also be specified as a parameter. Illumination outside of the unvignetted spectral range is affected by lack of reproducibility at more than 1% level, for a 0.2 arcsec slit: wavelength values given in italic fall outside the unvignetted range. *Wavelengths are vacuum expressed in nm. The accuracy on the positioning of the reference wavelength is $\approx$ 30 pixels. See Table 5a-5h for spectral ranges in wavenumber.*

λ_{ref}	$\mathcal{O}$	ID	Unvign. range $\lambda_{\min}$	$\lambda_{\max}$	Det. 1 $\lambda_{\min}$	$\lambda_{\max}$	Det. 2 $\lambda_{\min}$	$\lambda_{\max}$	Det. 3 $\lambda_{\min}$	$\lambda_{\max}$	Det. 4 $\lambda_{\min}$	$\lambda_{\max}$	$\delta\lambda$
1229.1	46	46/0/n	1216.1	1234.5	*1210.3*	1216.7	1218.4	1224.5	1226.2	1232.0	1233.6	*1239.2*	5.7
1232.6	46	46/0/i	1219.6	1238.1	*1214.0*	1220.3	1222.0	1228.1	1229.7	1235.5	1237.0	*1242.5*	5.7
1256.4	45	45/0/n	1243.0	1262.0	*1237.2*	1243.7	1245.5	1251.7	1253.4	1259.4	1261.0	*1266.7*	5.8
1260.0	45	45/0/i	1246.7	1265.7	*1241.0*	1247.4	1249.2	1255.4	1257.0	1263.0	1264.5	*1270.2*	5.8
1285.0	44	44/0/n	1271.2	1290.9	*1265.3*	1272.0	1273.8	1280.2	1281.9	1288.1	1289.7	*1295.5*	6.0
1288.7	44	44/0/i	1275.0	1294.6	*1269.2*	1275.8	1277.7	1284.0	1285.7	1291.7	1293.3	*1299.1*	5.9
1299.8	43	43/-1/n	1285.4	1305.7	*1278.8*	1285.9	1287.9	1294.7	1296.5	1303.1	1304.8	*1311.0*	6.4
1303.8	43	43/-1/i	1289.4	1309.8	*1283.1*	1290.1	1292.0	1298.8	1300.6	1307.0	1308.7	*1314.9*	6.3
1329.9	43	43/1/n	1315.9	1336.2	*1310.7*	1317.2	1319.0	1325.3	1326.9	1332.9	1334.5	*1340.1*	5.8
1333.5^c	43	43/1/i	1319.5	1339.8	*1314.5*	1320.9	1322.7	1328.9	1330.6	1336.5	1338.0	*1343.6*	5.8
1330.8^c	42	42/-1/n	1315.9	1337.0	*1309.4*	1316.6	1318.6	1325.6	1327.5	1334.2	1335.9	*1342.3*	6.5
1334.8	42	42/-1/i	1320.0	1341.0	*1313.6*	1320.8	1322.8	1329.7	1331.5	1338.1	1339.9	*1346.2*	6.5
1361.6	42	42/1/n	1347.1	1368.1	*1341.9*	1348.6	1350.4	1356.9	1358.5	1364.7	1366.3	*1372.1*	6.0
1365.2^c	42	42/1/i	1350.8	1371.8	*1345.7*	1352.3	1354.2	1360.5	1362.2	1368.2	1369.8	*1375.5*	5.9
1363.3^c	41	41/-1/n	1348.0	1369.8	*1341.3*	1348.8	1350.8	1358.0	1359.9	1366.7	1368.5	*1375.1*	6.7
1367.4	41	41/-1/i	1352.1	1373.9	*1345.7*	1353.0	1355.1	1362.1	1364.0	1370.8	1372.6	*1379.1*	6.6
1394.8	41	41/1/n	1379.9	1401.6	*1374.6*	1381.5	1383.4	1389.9	1391.7	1397.9	1399.6	*1405.5*	6.1
1398.5^c	41	41/1/i	1383.6	1405.4	*1378.5*	1385.3	1387.2	1393.7	1395.4	1401.6	1403.2	*1409.1*	6.0
1397.3^c	40	40/-1/n	1381.5	1404.0	*1374.8*	1382.4	1384.5	1391.8	1393.8	1400.8	1402.7	*1409.4*	6.9
1401.6	40	40/-1/i	1385.8	1408.4	*1379.3*	1386.9	1389.0	1396.2	1398.1	1405.1	1406.9	*1413.5*	6.8
1429.6	40	40/1/n	1414.2	1436.7	*1408.9*	1415.9	1417.9	1424.6	1426.4	1432.8	1434.5	*1440.6*	6.3
1433.5^c	40	40/1/i	1418.2	1440.6	*1413.1*	1420.0	1421.9	1428.6	1430.3	1436.7	1438.3	*1444.4*	6.2
1433.2^c	39	39/-1/n	1416.9	1440.2	*1410.1*	1417.9	1420.1	1427.6	1429.6	1436.8	1438.7	*1445.6*	7.0
1437.5	39	39/-1/i	1421.2	1444.6	*1414.7*	1422.4	1424.5	1432.0	1433.9	1441.1	1442.9	*1449.7*	7.0
1466.3	39	39/1/n	1450.4	1473.7	*1445.1*	1452.3	1454.3	1461.2	1463.0	1469.6	1471.3	*1477.6*	6.4
1470.2	39	39/1/i	1454.4	1477.6	*1449.2*	1456.4	1458.3	1465.1	1467.0	1473.5	1475.2	*1481.3*	6.4

Table 4c: Reference wavelengths, λ_{ref}, for the standard settings, defined as the wavelength at pixel 512 of the 3rd detector. Order number ($\mathcal{O}$), internal wavelength identification (ID), unvignetted spectral range and coverage for each of the four detectors are also given. The last column lists the mean dispersion, $\delta\lambda$, in 10^{-3} nm/pixel, for detector 3. A ^{c} indicates that the order number *must* also be specified as a parameter. Illumination outside of the unvignetted spectral range is affected by lack of reproducibility at more than 1% level, for a 0.2 arcsec slit: wavelength values given in italic fall outside the unvignetted range. *Wavelengths are vacuum expressed in nm. The accuracy on the positioning of the reference wavelength is ≈ 30 pixels. See Table 5a-5h for spectral ranges in wavenumber.*

λ_{ref}	$\mathcal{O}$	ID	Unvign. range $\lambda_{\min}$	$\lambda_{\max}$	Det. 1 $\lambda_{\min}$	$\lambda_{\max}$	Det. 2 $\lambda_{\min}$	$\lambda_{\max}$	Det. 3 $\lambda_{\min}$	$\lambda_{\max}$	Det. 4 $\lambda_{\min}$	$\lambda_{\max}$	$\delta\lambda$
1470.9	38	38/-1/n	1454.0	1478.2	*1447.2*	1455.2	1457.5	1465.2	1467.2	1474.6	1476.5	*1483.6*	7.2
1475.3	38	38/-1/i	1458.5	1482.7	*1451.9*	1459.8	1462.0	1469.6	1471.7	1479.0	1480.9	*1487.9*	7.1
1504.9	38	38/1/n	1488.5	1512.6	*1483.1*	1490.5	1492.6	1499.7	1501.5	1508.3	1510.1	*1516.5*	6.6
1508.9	38	38/1/i	1492.5	1516.6	*1487.4*	1494.7	1496.7	1503.7	1505.6	1512.2	1514.0	*1520.3*	6.5
1510.7	37	37/-1/n	1493.2	1518.4	*1486.4*	1494.6	1496.9	1504.8	1506.9	1514.5	1516.5	*1523.7*	7.4
1515.2	37	37/-1/i	1497.8	1522.9	*1491.1*	1499.3	1501.5	1509.4	1511.5	1519.0	1520.9	*1528.1*	7.3
1545.5	37	37/1/n	1528.5	1553.5	*1523.2*	1530.7	1532.8	1540.1	1542.0	1549.0	1550.8	*1557.4*	6.8
1549.7	37	37/1/i	1532.8	1557.7	*1527.6*	1535.1	1537.2	1544.4	1546.3	1553.1	1554.9	*1561.4*	6.7
1552.6	36	36/-1/n	1534.5	1560.6	*1527.6*	1536.1	1538.4	1546.5	1548.7	1556.5	1558.5	*1566.0*	7.6
1557.3	36	36/-1/i	1539.3	1565.3	*1532.6*	1540.9	1543.3	1551.3	1553.4	1561.2	1563.2	*1570.6*	7.5
1588.4	36	36/1/n	1570.8	1596.7	*1565.4*	1573.2	1575.4	1582.9	1584.8	1592.0	1593.8	*1600.6*	7.0
1592.7	36	36/1/i	1575.2	1601.1	*1570.0*	1577.7	1579.8	1587.2	1589.2	1596.2	1598.1	*1604.8*	6.9
1597.0	35	35/-1/n	1578.3	1605.4	*1571.3*	1580.0	1582.4	1590.8	1593.0	1601.0	1603.1	*1610.8*	7.8
1601.8	35	35/-1/i	1583.1	1610.2	*1576.4*	1585.0	1587.4	1595.6	1597.8	1605.8	1607.9	*1615.4*	7.7
1633.8	35	35/1/n	1615.6	1642.5	*1610.2*	1618.2	1620.4	1628.1	1630.1	1637.5	1639.4	*1646.4*	7.2
1638.2	35	35/1/i	1620.1	1646.9	*1614.9*	1622.8	1625.0	1632.6	1634.6	1641.8	1643.7	*1650.6*	7.1
1644.0	34	34/-1/n	1624.6	1652.7	*1617.6*	1626.5	1629.0	1637.6	1639.9	1648.1	1650.3	*1658.2*	8.1
1649.0	34	34/-1/i	1629.7	1657.8	*1622.8*	1631.7	1634.1	1642.7	1644.9	1653.1	1655.2	*1663.0*	8.0
1681.8	34	34/1/n	1663.0	1690.9	*1657.5*	1665.7	1668.0	1675.9	1678.0	1685.6	1687.6	*1694.7*	7.4
1686.4	34	34/1/i	1667.7	1695.5	*1662.4*	1670.5	1672.8	1680.6	1682.7	1690.1	1692.1	*1699.2*	7.3
1693.8	33	33/-1/n	1673.7	1702.9	*1666.6*	1675.8	1678.3	1687.2	1689.6	1698.1	1700.3	*1708.4*	8.3
1698.9	33	33/-1/i	1678.8	1708.1	*1671.9*	1681.1	1683.6	1692.4	1694.7	1703.1	1705.3	*1713.4*	8.2
1732.8	33	33/1/n	1713.3	1742.2	*1707.8*	1716.3	1718.6	1726.8	1728.9	1736.7	1738.7	*1746.1*	7.6
1737.4	33	33/1/i	1718.0	1746.9	*1712.6*	1721.1	1723.4	1731.4	1733.6	1741.3	1743.3	*1750.6*	7.5
1746.8	32	32/-1/n	1725.9	1756.4	*1718.7*	1728.2	1730.9	1740.0	1742.4	1751.2	1753.5	*1761.9*	8.6
1752.1	32	32/-1/i	1731.3	1761.7	*1724.3*	1733.7	1736.3	1745.4	1747.8	1756.4	1758.7	*1767.0*	8.5

Table 4d: Reference wavelengths, λ_{ref}, for the standard settings, defined as the wavelength at pixel 512 of the 3rd detector. Order number ($\mathcal{O}$), internal wavelength identification (ID), unvignetted spectral range and coverage for each of the four detectors are also given. The last column lists the mean dispersion, $\delta\lambda$, in 10^{-3} nm/pixel, for detector 3. A ^{c} indicates that the order number *must* also be specified as a parameter. Illumination outside of the unvignetted spectral range is affected by lack of reproducibility at more than 1% level, for a 0.2 arcsec slit: wavelength values given in italic fall outside the unvignetted range. *Wavelengths are vacuum expressed in nm. The accuracy on the positioning of the reference wavelength is ≈ 30 pixels. See Table 5a-5h for spectral ranges in wavenumber.*

λ_{ref}	$\mathcal{O}$	ID	Unvign. range $\lambda_{\min}$	$\lambda_{\max}$	Det. 1 $\lambda_{\min}$	$\lambda_{\max}$	Det. 2 $\lambda_{\min}$	$\lambda_{\max}$	Det. 3 $\lambda_{\min}$	$\lambda_{\max}$	Det. 4 $\lambda_{\min}$	$\lambda_{\max}$	$\delta\lambda$
1786.9	32	32/1/n	1766.7	1796.8	*1761.1*	1769.8	1772.3	1780.7	1782.9	1790.9	1793.0	*1800.6*	7.8
1791.7	32	32/1/i	1771.6	1801.6	*1766.2*	1774.8	1777.2	1785.6	1787.8	1795.7	1797.7	*1805.3*	7.7
1803.1	31	31/-1/n	1781.4	1813.1	*1774.1*	1783.9	1786.6	1796.1	1798.6	1807.6	1810.0	*1818.7*	8.8
1808.6	31	31/-1/i	1787.0	1818.6	*1779.9*	1789.6	1792.3	1801.7	1804.1	1813.1	1815.4	*1824.0*	8.7
1844.6	31	31/1/n	1823.6	1854.9	*1818.0*	1827.0	1829.5	1838.2	1840.5	1848.7	1850.9	*1858.8*	8.1
1849.5	31	31/1/i	1828.6	1859.8	*1823.2*	1832.1	1834.6	1843.2	1845.4	1853.6	1855.7	*1863.5*	8.0
1863.3	30	30/-1/n	1840.7	1873.8	*1833.4*	1843.5	1846.3	1856.0	1858.6	1868.0	1870.4	*1879.4*	9.1
1868.9	30	30/-1/i	1846.4	1879.4	*1839.3*	1849.3	1852.1	1861.7	1864.3	1873.5	1876.0	*1884.8*	9.0
1906.0	30	30/1/n	1884.2	1916.7	*1878.5*	1887.8	1890.4	1899.4	1901.7	1910.3	1912.5	*1920.6*	8.3
1911.1	30	30/1/i	1889.4	1921.9	*1883.9*	1893.1	1895.7	1904.5	1906.9	1915.3	1917.5	*1925.6*	8.2
1927.5	29	29/-1/n	1904.0	1938.5	*1896.5*	1907.0	1909.9	1920.0	1922.7	1932.3	1934.9	*1944.1*	9.4
1933.4	29	29/-1/i	1910.0	1944.4	*1902.7*	1913.1	1916.0	1926.0	1928.6	1938.2	1940.7	*1949.8*	9.3
1971.7	29	29/1/n	1949.0	1982.9	*1943.2*	1952.9	1955.6	1964.8	1967.3	1976.1	1978.4	*1986.9*	8.6
1977.0	29	29/1/i	1954.4	1988.3	*1948.8*	1958.4	1961.1	1970.2	1972.6	1981.4	1983.7	*1992.0*	8.5
1996.4	28	28/-1/n	1971.9	2007.9	*1964.3*	1975.2	1978.2	1988.6	1991.4	2001.4	2004.0	*2013.6*	9.8
2002.4	28	28/-1/i	1978.0	2014.0	*1970.7*	1981.4	1984.4	1994.7	1997.5	2007.4	2010.0	*2019.4*	9.7
2042.1	28	28/1/n	2018.5	2053.9	*2012.6*	2022.6	2025.4	2035.0	2037.5	2046.7	2049.1	*2057.8*	8.9
2047.6	28	28/1/i	2024.1	2059.4	*2018.4*	2028.3	2031.1	2040.6	2043.1	2052.1	2054.5	*2063.1*	8.8
2070.4	27	27/-1/n	2044.8	2082.5	*2037.2*	2048.4	2051.5	2062.3	2065.2	2075.6	2078.3	*2088.2*	10.1
2076.6	27	27/-1/i	2051.1	2088.8	*2043.7*	2054.8	2057.9	2068.6	2071.5	2081.7	2084.4	*2094.2*	10.0
2117.7	27	27/1/n	2093.1	2130.1	*2087.1*	2097.5	2100.4	2110.3	2113.0	2122.5	2124.9	*2134.0*	9.3
2123.4	27	27/1/i	2098.9	2135.8	*2093.2*	2103.4	2106.3	2116.1	2118.7	2128.1	2130.6	*2139.5*	9.2
2150.0	26	26/-1/n	2123.2	2162.8	*2115.5*	2127.2	2130.4	2141.6	2144.6	2155.4	2158.2	*2168.5*	10.5
2156.5	26	26/-1/i	2129.9	2169.3	*2122.3*	2133.9	2137.1	2148.2	2151.2	2161.8	2164.6	*2174.8*	10.4
2199.1	26	26/1/n	2173.3	2212.1	*2167.3*	2178.1	2181.1	2191.4	2194.2	2204.0	2206.6	*2216.0*	9.6
2205.0	26	26/1/i	2179.4	2218.1	*2173.6*	2184.3	2187.2	2197.4	2200.1	2209.9	2212.4	*2221.7*	9.5

Table 4e: Reference wavelengths, λ_{ref}, for the standard settings, defined as the wavelength at pixel 512 of the 3rd detector. Order number ($\mathcal{O}$), internal wavelength identification (ID), unvignetted spectral range and coverage for each of the four detectors are also given. The last column lists the mean dispersion, $\delta\lambda$, in 10^{-3} nm/pixel, for detector 3. A ^{c} indicates that the order number *must* also be specified as a parameter. Illumination outside of the unvignetted spectral range is affected by lack of reproducibility at more than 1% level, for a 0.2 arcsec slit: wavelength values given in italic fall outside the unvignetted range. *Wavelengths are vacuum expressed in nm. The accuracy on the positioning of the reference wavelength is ≈ 30 pixels. See Table 5a-5h for spectral ranges in wavenumber.*

λ_{ref}	$\mathcal{O}$	ID	Unvign. range		Det. 1		Det. 2		Det. 3		Det. 4		$\delta\lambda$
			$\lambda_{\min}$	$\lambda_{\max}$	$\lambda_{\min}$	$\lambda_{\max}$	$\lambda_{\min}$	$\lambda_{\max}$	$\lambda_{\min}$	$\lambda_{\max}$	$\lambda_{\min}$	$\lambda_{\max}$	
2236.1	25	25/-1/n	2208.0	2249.7	*2200.2*	2212.3	2215.7	2227.4	2230.5	2241.7	2244.6	*2255.4*	10.9
2242.8	25	25/-1/i	2214.9	2256.4	*2207.3*	2219.3	2222.6	2234.2	2237.3	2248.4	2251.3	*2261.8*	10.8
2287.1	25	25/1/n	2260.1	2300.9	*2254.1*	2265.3	2268.4	2279.1	2282.0	2292.2	2294.9	*2304.7*	10.0
2293.2	25	25/1/i	2266.3	2307.0	*2260.5*	2271.6	2274.7	2285.3	2288.1	2298.3	2300.9	*2310.6*	9.9
2329.3	24	24/-1/n	2299.8	2343.7	*2291.9*	2304.6	2308.1	2320.2	2323.5	2335.1	2338.2	*2349.4*	11.4
2336.3	24	24/-1/i	2306.9	2350.8	*2299.3*	2311.8	2315.3	2327.3	2330.5	2342.1	2345.1	*2356.1*	11.3
2382.3	24	24/1/n	2353.8	2397.0	*2347.9*	2359.6	2362.8	2374.0	2377.0	2387.7	2390.4	*2400.6*	10.4
2388.7	24	24/1/i	2360.4	2403.4	*2354.7*	2366.2	2369.4	2380.5	2383.4	2394.0	2396.7	*2406.8*	10.3
2430.6	23	23/-1/n	2399.4	2446.1	*2391.6*	2404.8	2408.5	2421.2	2424.5	2436.7	2439.9	*2451.5*	11.9
2437.9	23	23/-1/i	2406.8	2453.4	*2399.3*	2412.4	2416.0	2428.6	2431.9	2443.9	2447.1	*2458.6*	11.8
2485.8	23	23/1/n	2455.7	2501.5	*2449.9*	2462.1	2465.5	2477.1	2480.2	2491.4	2494.3	*2504.9*	10.9
2492.5	23	23/1/i	2462.5	2508.2	*2457.0*	2469.1	2472.4	2483.9	2487.0	2498.0	2500.9	*2511.4*	10.8
2512.4	22	22/-1/n	2478.7	2529.0	*2470.2*	2484.4	2488.4	2502.1	2505.8	2519.0	2522.5	*2535.1*	12.9
2520.3	22	22/-1/i	2486.7	2537.0	*2478.5*	2492.6	2496.5	2510.1	2513.8	2526.9	2530.3	*2542.8*	12.8
2570.0	22	22/0/n	2537.4	2586.9	*2530.8*	2544.1	2547.8	2560.5	2563.9	2576.1	2579.3	*2590.9*	11.9
2577.3	22	22/0/i	2544.8	2594.2	*2538.5*	2551.7	2555.3	2567.9	2571.3	2583.3	2586.5	*2598.0*	11.8
2627.6	22	22/1/n	2596.1	2644.8	*2591.8*	2604.0	2607.4	2619.0	2622.1	2633.1	2636.0	*2646.5*	10.8
2634.2^c	22	22/1/i	2602.9	2651.4	*2598.9*	2610.9	2614.2	2625.7	2628.8	2639.7	2642.5	*2652.9*	10.7
2632.1^c	21	21/-1/n	2596.0	2650.3	*2587.9*	2602.8	2607.0	2621.4	2625.2	2639.0	2642.7	*2655.9*	13.5
2640.5	21	21/-1/i	2604.5	2658.7	*2596.7*	2611.5	2615.6	2629.9	2633.7	2647.4	2651.0	*2664.1*	13.4
2692.4	21	21/0/n	2657.4	2710.9	*2651.3*	2665.3	2669.1	2682.5	2686.0	2698.8	2702.2	*2714.3*	12.5
2700.0	21	21/0/i	2665.1	2718.5	*2659.4*	2673.1	2677.0	2690.2	2693.7	2706.3	2709.6	*2721.7*	12.3
2752.6	21	21/1/n	2718.7	2771.5	*2715.1*	2727.9	2731.4	2743.6	2746.8	2758.4	2761.4	*2772.4*	11.3
2759.5	21	21/1/i	2725.8	2778.4	*2722.5*	2735.1	2738.6	2750.6	2753.8	2765.2	2768.2	*2779.1*	11.2
2763.9	20	20/-1/n	2724.9	2784.1	*2717.5*	2733.1	2737.5	2752.6	2756.6	2771.2	2775.0	*2788.9*	14.2
2772.7	20	20/-1/i	2733.8	2793.0	*2726.7*	2742.2	2746.6	2761.5	2765.5	2779.9	2783.7	*2797.4*	14.0

Table 4f: Reference wavelengths, λ_{ref}, for the standard settings, defined as the wavelength at pixel 512 of the 3rd detector. Order number ($\mathcal{O}$), internal wavelength identification (ID), unvignetted spectral range and coverage for each of the four detectors are also given. The last column lists the mean dispersion, $\delta\lambda$, in 10^{-3} nm/pixel, for detector 3. A ^{c} indicates that the order number *must* also be specified as a parameter. Illumination outside of the unvignetted spectral range is affected by lack of reproducibility at more than 1% level, for a 0.2 arcsec slit: wavelength values given in italic fall outside the unvignetted range. *Wavelengths are vacuum expressed in nm. The accuracy on the positioning of the reference wavelength is ≈ 30 pixels. See Table 5a–5h for spectral ranges in wavenumber.*

λ_{ref}	$\mathcal{O}$	ID	Unvign. range $\lambda_{\min}$	$\lambda_{\max}$	Det. 1 $\lambda_{\min}$	$\lambda_{\max}$	Det. 2 $\lambda_{\min}$	$\lambda_{\max}$	Det. 3 $\lambda_{\min}$	$\lambda_{\max}$	Det. 4 $\lambda_{\min}$	$\lambda_{\max}$	$\delta\lambda$
2827.0	20	20/0/n	2789.0	2847.6	*2783.9*	2798.5	2802.6	2816.6	2820.3	2833.7	2837.2	*2850.0*	13.1
2835.0	20	20/0/i	2797.2	2855.7	*2792.3*	2806.8	2810.8	2824.7	2828.4	2841.7	2845.1	*2857.8*	13.0
2890.0	20	20/1/n	2853.1	2911.1	*2850.6*	2864.0	2867.8	2880.5	2883.9	2896.1	2899.3	2910.8	11.9
2897.3	20	20/1/i	2860.6	2918.5	*2858.4*	2871.7	2875.3	2888.0	2891.3	2903.3	2906.5	2917.9	11.7
2909.6	19	19/-1/n	2867.0	2932.5	*2860.7*	2877.2	2881.8	2897.7	2902.0	2917.3	2921.3	*2935.9*	14.9
2918.8	19	19/-1/i	2876.3	2941.7	*2870.4*	2886.7	2891.3	2907.1	2911.2	2926.4	2930.3	*2944.8*	14.8
2975.8	19	19/0/n	2934.1	2999.3	*2930.4*	2945.8	2950.1	2964.8	2968.8	2982.9	2986.6	*3000.0*	13.8
2984.2	19	19/0/i	2942.6	3007.7	*2939.3*	2954.5	2958.8	2973.4	2977.2	2991.2	2994.9	*3008.2*	13.6
3041.9	19	19/1/n	3001.2	3066.1	*3000.5*	3014.6	3018.5	3031.9	3035.5	3048.3	3051.7	3063.8	12.5
3049.5	19	19/1/i	3008.9	3073.8	*3008.6*	3022.5	3026.4	3039.7	3043.2	3055.8	3059.2	3071.1	12.4
3071.5	18	18/-1/n	3024.2	3098.0	*3019.9*	3037.3	3042.2	3059.0	3063.4	3079.6	3083.8	*3099.3*	15.8
3081.3	18	18/-1/i	3034.1	3107.9	*3030.2*	3047.5	3052.3	3068.9	3073.3	3089.3	3093.5	*3108.8*	15.6
3141.1	18	18/0/n	3094.5	3168.4	*3093.2*	3109.4	3113.9	3129.5	3133.7	3148.6	3152.5	3166.7	14.6
3150.0	18	18/0/i	3103.5	3177.4	*3102.6*	3118.7	3123.1	3138.6	3142.6	3157.4	3161.2	3175.3	14.4
3210.6	18	18/1/n	3164.8	3238.9	3166.8	3181.7	3185.9	3200.1	3203.9	3217.4	3220.9	3233.8	13.2
3218.7	18	18/1/i	3173.0	3247.1	3175.5	3190.2	3194.3	3208.3	3212.0	3225.4	3228.9	3241.6	13.1
3252.6	17	17/-1/n	3199.1	3284.0	*3198.0*	3216.4	3221.6	3239.3	3244.1	3261.2	3265.6	3282.0	16.7
3262.9	17	17/-1/i	3209.5	3294.5	*3208.8*	3227.1	3232.2	3249.8	3254.5	3271.4	3275.8	3292.0	16.5
3325.8	17	17/0/n	3272.8	3358.4	3275.1	3292.3	3297.0	3313.5	3317.9	3333.7	3337.8	3352.9	15.4
3335.3	17	17/0/i	3282.4	3368.1	3285.1	3302.1	3306.9	3323.2	3327.5	3343.1	3347.2	3362.1	15.2
3399.1	17	17/1/n	3346.6	3433.1	3352.8	3368.5	3372.9	3388.0	3392.0	3406.3	3410.0	3423.6	14.0
3407.7	17	17/1/i	3355.2	3441.9	3361.9	3377.5	3381.8	3396.7	3400.6	3414.8	3418.5	3431.9	13.8
3456.3	16	16/-1/n	3394.6	3494.6	3398.3	3417.9	3423.4	3442.2	3447.2	3465.4	3470.1	3487.5	17.7
3467.2	16	16/-1/i	3405.5	3505.7	3409.8	3429.2	3434.6	3453.3	3458.2	3476.2	3480.9	3498.1	17.5
3533.7	16	16/0/n	3472.1	3573.6	3479.8	3498.1	3503.2	3520.7	3525.3	3542.1	3546.5	3562.5	16.4
3543.8	16	16/0/i	3482.2	3584.0	3490.5	3508.6	3513.6	3530.9	3535.5	3552.1	3556.4	3572.3	16.2

Table 4g: Reference wavelengths, λ_{ref}, for the standard settings, defined as the wavelength at pixel 512 of the 3rd detector. Order number ($\mathcal{O}$), internal wavelength identification (ID), unvignetted spectral range and coverage for each of the four detectors are also given. The last column lists the mean dispersion, $\delta\lambda$, in 10^{-3} nm/pixel, for detector 3. A ^{c} indicates that the order number *must* also be specified as a parameter. Illumination outside of the unvignetted spectral range is affected by lack of reproducibility at more than 1% level, for a 0.2 arcsec slit: wavelength values given in italic fall outside the unvignetted range. *Wavelengths are vacuum expressed in nm. The accuracy on the positioning of the reference wavelength is $\approx$ 30 pixels. See Table 5a-5h for spectral ranges in wavenumber.*

λ_{ref}	$\mathcal{O}$	ID	Unvign. range		Det. 1		Det. 2		Det. 3		Det. 4		$\delta\lambda$
			$\lambda_{\min}$	$\lambda_{\max}$	$\lambda_{\min}$	$\lambda_{\max}$	$\lambda_{\min}$	$\lambda_{\max}$	$\lambda_{\min}$	$\lambda_{\max}$	$\lambda_{\min}$	$\lambda_{\max}$	
3611.1	16	16/1/n	3549.5	3652.9	3561.8	3578.6	3583.2	3599.3	3603.5	3618.7	3622.7	3637.2	14.9
3620.2	16	16/1/i	3558.6	3662.3	3571.5	3588.1	3592.7	3608.5	3612.7	3627.7	3631.7	3645.9	14.7
3646.3	15	15/-2/n	3573.7	3693.1	3582.5	3604.0	3610.0	3630.8	3636.3	3656.3	3661.6	3680.8	19.5
3658.4	15	15/-2/i	3585.7	3705.5	3595.2	3616.5	3622.4	3643.0	3648.5	3668.3	3673.5	3692.5	19.3
3728.3	15	15/-1/n	3655.2	3777.3	3668.6	3688.8	3694.4	3713.8	3719.0	3737.6	3742.5	3760.3	18.2
3739.5	15	15/-1/i	3666.4	3788.8	3680.4	3700.4	3706.0	3725.2	3730.3	3748.7	3753.6	3771.2	18.0
3810.3	15	15/1/n	3736.8	3861.7	3755.2	3773.9	3779.1	3797.0	3801.8	3818.9	3823.3	3839.6	16.7
3820.5	15	15/1/i	3746.9	3872.2	3766.0	3784.5	3789.7	3807.4	3812.1	3829.0	3833.4	3849.5	16.5
3892.2	15	15/2/n	3818.2	3946.3	3842.3	3859.3	3864.0	3880.2	3884.5	3899.9	3903.9	3918.5	15.0
3901.4	15	15/2/i	3827.4	3955.8	3852.1	3868.9	3873.6	3889.6	3893.8	3909.0	3913.0	3927.3	14.8
3908.0	14	14/-2/n	3820.6	3967.7	3839.7	3862.7	3869.1	3891.4	3897.3	3918.7	3924.3	3944.9	20.9
3920.9	14	14/-2/i	3833.3	3981.1	3853.2	3876.0	3882.4	3904.4	3910.3	3931.5	3937.1	3957.4	20.7
3995.0	14	14/-1/n	3906.5	4057.7	3931.1	3952.7	3958.7	3979.5	3985.0	4005.0	4010.2	4029.3	19.5
4007.0	14	14/-1/i	3918.3	4070.1	3943.7	3965.1	3971.1	3991.7	3997.1	4016.9	4022.1	4040.9	19.3
4082.0	14	14/1/n	3992.3	4147.9	4022.9	4043.0	4048.6	4067.8	4072.9	4091.2	4096.0	4113.4	17.9
4093.0	14	14/1/i	4003.2	4159.4	4034.6	4054.4	4059.9	4078.9	4084.0	4102.1	4106.8	4124.0	17.7
4169.1	14	14/2/n	4078.3	4238.5	4115.6	4133.8	4138.9	4156.3	4160.9	4177.4	4181.7	4197.3	16.1
4178.9	14	14/2/i	4088.0	4248.8	4126.0	4144.1	4149.1	4166.2	4170.8	4187.1	4191.3	4206.7	15.9
4210.3	13	13/-2/n	4102.7	4288.1	4136.8	4161.6	4168.5	4192.4	4198.8	4221.8	4227.9	4250.0	22.5
4224.2	13	13/-2/i	4116.3	4302.6	4151.4	4175.9	4182.8	4206.5	4212.8	4235.6	4241.6	4263.5	22.3
4302.9	13	13/-1/n	4193.4	4384.6	4234.1	4257.4	4263.8	4286.2	4292.2	4313.7	4319.3	4339.8	21.0
4315.8	13	13/-1/i	4206.0	4398.1	4247.7	4270.7	4277.1	4299.3	4305.2	4326.4	4332.0	4352.3	20.8
4395.5	13	13/1/n	4284.0	4481.4	4331.9	4353.5	4359.5	4380.2	4385.6	4405.4	4410.6	4429.4	19.3
4407.3	13	13/1/i	4295.6	4493.8	4344.4	4365.7	4371.7	4392.1	4397.6	4417.1	4422.2	4440.8	19.1
4488.1	13	13/2/n	4374.7	4578.4	4430.3	4450.0	4455.5	4474.3	4479.2	4497.0	4501.7	4518.5	17.4
4498.7	13	13/2/i	4385.1	4589.6	4441.6	4461.1	4466.5	4485.0	4489.9	4507.5	4512.1	4528.7	17.2

Table 4h: Reference wavelengths, λ_{ref}, for the standard settings, defined as the wavelength at pixel 512 of the 3rd detector. Order number ($\mathcal{O}$), internal wavelength identification (ID), unvignetted spectral range and coverage for each of the four detectors are also given. The last column lists the mean dispersion, $\delta\lambda$, in 10^{-3} nm/pixel, for detector 3. A ^{c} indicates that the order number *must* also be specified as a parameter. Illumination outside of the unvignetted spectral range is affected by lack of reproducibility at more than 1% level, for a 0.2 arcsec slit: wavelength values given in italic fall outside the unvignetted range. *Wavelengths are vacuum expressed in nm.* The accuracy on the positioning of the reference wavelength is ≈ 30 pixels. *See Table 5a-5h for spectral ranges in wavenumber.*

λ_{ref}	$\mathcal{O}$	ID	Unvign. range λ_{min}	λ_{max}	Det. 1 λ_{min}	λ_{max}	Det. 2 λ_{min}	λ_{max}	Det. 3 λ_{min}	λ_{max}	Det. 4 λ_{min}	λ_{max}	$\delta\lambda$
4563.6	12	12/-2/n	4428.5	4666.5	4484.1	4510.9	4518.4	4544.3	4551.2	4576.1	4582.6	4606.5	24.3
4578.6	12	12/-2/i	4443.1	4682.2	4499.8	4526.4	4533.8	4559.4	4566.3	4591.0	4597.4	4621.1	24.1
4662.3	12	12/-1/n	4524.3	4770.2	4587.8	4613.0	4620.0	4644.2	4650.7	4674.0	4680.0	4702.3	22.7
4676.2	12	12/-1/i	4537.8	4784.8	4602.4	4627.4	4634.3	4658.3	4664.7	4687.7	4693.8	4715.7	22.5
4761.0	12	12/1/n	4620.2	4874.1	4692.0	4715.4	4721.9	4744.4	4750.3	4771.7	4777.3	4797.7	20.9
4773.8	12	12/1/i	4632.6	4887.6	4705.6	4728.7	4735.2	4757.4	4763.2	4784.4	4789.9	4810.1	20.7
4859.6	12	12/2/n	4716.0	4978.2	4796.8	4818.2	4824.2	4844.6	4850.0	4869.3	4874.4	4892.7	18.9
4871.1	12	12/2/i	4727.1	4990.4	4809.1	4830.3	4836.1	4856.3	4861.6	4880.7	4885.7	4903.7	18.7
4929.6	11	11/-2/n	4758.9	5064.1	4840.5	4870.5	4878.9	4907.9	4915.6	4943.6	4950.9	4977.8	27.3
4946.5	11	11/-2/i	4775.2	5082.0	4858.2	4888.0	4896.3	4925.0	4932.7	4960.4	4967.6	4994.2	27.0
5034.8	11	11/-1/n	4860.3	5175.4	4950.8	4979.2	4987.1	5014.4	5021.7	5048.0	5054.8	5080.0	25.6
5050.6	11	11/-1/i	4875.5	5192.1	4967.4	4995.5	5003.4	5030.4	5037.6	5063.6	5070.4	5095.3	25.4
5139.9	11	11/0/n	4961.5	5286.8	5061.5	5088.1	5095.5	5121.0	5127.7	5152.1	5158.5	5181.8	23.8
5154.6	11	11/0/i	4975.6	5302.4	5077.0	5103.3	5110.6	5135.9	5142.6	5166.7	5173.0	5196.0	23.6
5245.1	11	11/1/n	5064.7	5396.6	5172.9	5197.5	5204.3	5227.7	5234.0	5256.3	5262.1	5283.3	21.8
5258.4	11	11/1/i	5078.2	5410.1	5187.1	5211.4	5218.1	5241.3	5247.4	5269.5	5275.2	5296.1	21.5
5350.2	11	11/2/n	5171.9	5502.7	5285.1	5307.4	5313.5	5334.7	5340.2	5360.2	5365.4	5384.3	19.5
5362.1	11	11/2/i	5184.0	5514.7	5297.9	5319.9	5325.9	5346.8	5352.3	5372.0	5377.1	5395.7	19.2

15.2   Wavenumber ranges

Table 5a: Reference wavelengths, $\lambda_{\rm ref}$, in nm for the standard wavelength settings, defined as the wavelength at pixel 512 of the 3rd detector. Order number ($\mathcal{O}$), internal wavelength identification (ID), unvignetted spectral range and coverage in vacuum wavenumber (ν, expressed in cm^{-1}) for each of the four detectors are also given. The last column lists the mean dispersion, $\delta\nu$ in 10^{-3} cm^{-1} /pixel, for detector 3. A ^{c} indicates that the order number must also be specified as a parameter. Illumination outside of the unvignetted spectral range is affected by lack of reproducibility at more than 1% level, for a 0.2 arcsec slit: wavenumber values given in italic fall outside the unvignetted range. The accuracy on the positioning of the reference wavelength is ≈ 30 pixels. See Table 4a-4h for spectral ranges in wavelength.

$\lambda_{\rm ref}$	$\mathcal{O}$	ID	Unvign. range		Det. 1		Det. 2		Det. 3		Det. 4		$\delta\nu$
			$\nu_{\rm min}$	$\nu_{\rm max}$	$\nu_{\rm min}$	$\nu_{\rm max}$	$\nu_{\rm min}$	$\nu_{\rm max}$	$\nu_{\rm min}$	$\nu_{\rm max}$	$\nu_{\rm min}$	$\nu_{\rm max}$	
958.3	59	59/0/n	10536.3	10399.3	10597.7	10541.9	10527.4	10474.5	10460.3	10410.2	10397.2	10349.8	4.5
961.0	59	59/0/i	10506.4	10370.2	10566.4	10510.8	10496.5	10443.9	10430.8	10381.0	10368.1	10322.0	4.4
974.8	58	58/0/n	10359.5	10222.9	10418.8	10363.8	10348.8	10296.5	10282.8	10234.4	10220.8	10175.0	4.6
977.6	58	58/0/i	10328.4	10192.6	10386.4	10332.7	10317.8	10266.9	10253.3	10205.1	10192.6	10147.1	4.5
991.9	57	57/0/n	10181.2	10045.2	10239.6	10185.4	10169.8	10119.4	10106.1	10057.3	10045.2	10000.0	4.6
994.8	57	57/0/i	10151.3	10016.0	10207.2	10154.3	10139.9	10088.8	10075.6	10028.1	10016.0	9971.1	4.6
1009.6	56	56/0/n	10003.0	9868.7	10059.4	10007.0	9992.0	9942.3	9928.5	9881.4	9868.7	9824.1	4.7
1012.5	56	56/0/i	9974.1	9840.6	10029.1	9976.1	9962.1	9912.8	9900.0	9853.2	9841.6	9797.2	4.7
1028.0	55	55/0/n	9825.1	9691.8	9879.5	9827.0	9813.5	9763.7	9751.3	9704.0	9691.8	9648.8	4.8
1030.9	55	55/0/i	9797.2	9663.7	9849.3	9798.2	9784.7	9736.2	9722.9	9677.7	9665.6	9622.8	4.7
1047.0	54	54/0/n	9647.9	9514.7	9700.3	9648.8	9634.8	9586.8	9574.0	9528.3	9516.6	9473.3	4.9
1050.0	54	54/0/i	9619.1	9487.7	9670.2	9620.0	9606.1	9558.4	9546.5	9501.2	9489.5	9447.3	4.8
1066.8	53	53/0/n	9468.8	9337.9	9520.2	9469.7	9456.3	9409.1	9395.8	9351.0	9339.7	9297.1	5.0
1069.8	53	53/0/i	9442.0	9311.0	9491.3	9442.0	9428.6	9381.7	9369.4	9325.7	9314.5	9273.0	4.9
1087.3	52	52/0/n	9291.1	9160.9	9340.6	9291.1	9278.2	9231.1	9219.1	9175.2	9163.4	9122.4	5.1
1090.4	52	52/0/i	9264.4	9134.9	9311.9	9263.5	9250.7	9204.7	9192.9	9149.1	9138.3	9097.5	5.0
1108.6	51	51/0/n	9113.3	8983.9	9160.9	9112.4	9099.2	9053.9	9041.6	8998.5	8988.0	8946.9	5.2
1111.8	51	51/0/i	9086.8	8958.2	9132.4	9085.1	9071.9	9027.7	9015.5	8973.4	8962.2	8922.2	5.1
1130.8	50	50/0/n	8935.0	8807.5	8980.7	8934.2	8920.6	8876.3	8864.5	8822.2	8811.3	8771.2	5.3
1134.0	50	50/0/i	8909.5	8781.9	8954.2	8907.1	8894.4	8850.3	8839.4	8797.4	8786.6	8747.4	5.2
1153.9	49	49/0/n	8756.6	8630.4	8801.3	8755.0	8742.0	8698.7	8686.6	8645.3	8634.8	8595.5	5.4
1157.2	49	49/0/i	8731.3	8605.1	8774.2	8729.1	8716.1	8673.0	8661.8	8621.4	8610.3	8572.7	5.3
1177.9	48	48/0/n	8579.3	8453.8	8622.2	8576.3	8563.8	8521.5	8509.9	8469.6	8458.8	8421.1	5.5
1181.3	48	48/0/i	8553.6	8428.9	8595.5	8550.7	8538.3	8496.2	8485.4	8445.2	8435.3	8397.7	5.4
1203.0	47	47/0/n	8400.5	8276.8	8441.7	8397.7	8385.7	8343.8	8332.6	8292.6	8282.3	8245.4	5.6
1206.4	47	47/0/i	8376.6	8252.9	8416.1	8373.1	8360.5	8319.5	8308.4	8269.9	8259.7	8223.0	5.5

Table 5b: Reference wavelengths, λ_{ref}, in nm for the standard wavelength settings, defined as the wavelength at pixel 512 of the 3rd detector. Order number ($\mathcal{O}$), internal wavelength identification (ID), unvignetted spectral range and coverage in vacuum wavenumber (ν, expressed in cm^{-1}) for each of the four detectors are also given. The last column lists the mean dispersion, $\delta\nu$ in 10^{-3} cm^{-1}/pixel, for detector 3. A ^{c} indicates that the order number must also be specified as a parameter. Illumination outside of the unvignetted spectral range is affected by lack of reproducibility at more than 1% level, for a 0.2 arcsec slit: wavenumber values given in italic fall outside the unvignetted range. The accuracy on the positioning of the reference wavelength is $\approx$ 30 pixels. See Table 4a-4h for spectral ranges in wavelength.

λ_{ref}	$\mathcal{O}$	ID	Unvign. range $\nu_{\min}$	$\nu_{\max}$	Det. 1 $\nu_{\min}$	$\nu_{\max}$	Det. 2 $\nu_{\min}$	$\nu_{\max}$	Det. 3 $\nu_{\min}$	$\nu_{\max}$	Det. 4 $\nu_{\min}$	$\nu_{\max}$	$\delta\nu$
1229.1	46	46/0/n	8223.0	8100.4	*8262.4*	8219.0	8207.5	8166.6	8155.3	8116.9	8106.4	*8069.7*	5.7
1232.6	46	46/0/i	8199.4	8076.9	*8237.2*	8194.7	8183.3	8142.7	8132.1	8093.9	8084.1	*8048.3*	5.7
1256.4	45	45/0/n	8045.1	7923.9	*8082.8*	8040.5	8028.9	7989.1	7978.3	7940.3	7930.2	*7894.5*	5.8
1260.0	45	45/0/i	8021.2	7900.8	*8058.0*	8016.7	8005.1	7965.6	7955.4	7917.7	7908.3	*7872.8*	5.8
1285.0	44	44/0/n	7866.6	7746.5	*7903.3*	7861.6	7850.5	7811.3	7800.9	7763.4	7753.7	*7719.0*	6.0
1288.7	44	44/0/i	7843.1	7724.4	*7879.0*	7838.2	7826.6	7788.2	7777.9	7741.7	7732.2	*7697.6*	5.9
1299.8	43	43/-1/n	7779.7	7658.7	*7819.8*	7776.7	7764.6	7723.8	7713.1	7674.0	7664.0	*7627.8*	6.4
1303.8	43	43/-1/i	7755.5	7634.8	*7793.6*	7751.3	7739.9	7699.4	7688.8	7651.1	7641.2	*7605.1*	6.3
1329.9	43	43/1/n	7599.4	7483.9	*7629.5*	7591.9	7581.5	7545.5	7536.4	7502.4	7493.4	*7462.1*	5.8
1333.5^c	43	43/1/i	7578.6	7463.8	*7607.5*	7570.6	7560.3	7525.0	7515.4	7482.2	7473.8	*7442.7*	5.8
1330.8^c	42	42/-1/n	7599.4	7479.4	*7637.1*	7595.3	7583.8	7543.8	7533.0	7495.1	7485.6	*7449.9*	6.5
1334.8	42	42/-1/i	7575.8	7457.1	*7612.7*	7571.2	7559.7	7520.5	7510.3	7473.3	7463.2	*7428.3*	6.5
1361.6	42	42/1/n	7423.4	7309.4	*7452.1*	7415.1	7405.2	7369.7	7361.1	7327.6	7319.0	*7288.1*	6.0
1365.2^c	42	42/1/i	7403.0	7289.7	*7431.1*	7394.8	7384.4	7350.2	7341.1	7308.9	7300.3	*7270.1*	5.9
1363.3^c	41	41/-1/n	7418.4	7300.3	*7455.5*	7414.0	7403.0	7363.8	7353.5	7316.9	7307.3	*7272.2*	6.7
1367.4	41	41/-1/i	7395.9	7278.5	*7431.1*	7391.0	7379.5	7341.6	7331.4	7295.0	7285.4	*7251.1*	6.6
1394.8	41	41/1/n	7246.9	7134.7	*7274.8*	7238.5	7228.6	7194.8	7185.5	7153.6	7144.9	*7114.9*	6.1
1398.5^c	41	41/1/i	7227.5	7115.4	*7254.3*	7218.7	7208.8	7175.1	7166.4	7134.7	7126.6	*7096.7*	6.0
1397.3^c	40	40/-1/n	7238.5	7122.5	*7273.8*	7233.8	7222.8	7184.9	7174.6	7138.8	7129.1	*7095.2*	6.9
1401.6	40	40/-1/i	7216.0	7100.3	*7250.1*	7210.3	7199.4	7162.3	7152.6	7116.9	7107.8	*7074.6*	6.8
1429.6	40	40/1/n	7071.1	6960.4	*7097.7*	7062.6	7052.7	7019.5	7010.7	6979.3	6971.1	*6941.6*	6.3
1433.5^c	40	40/1/i	7051.2	6941.6	*7076.6*	7042.3	7032.8	6999.9	6991.5	6960.4	6952.7	*6923.3*	6.2
1433.2^c	39	39/-1/n	7057.7	6943.5	*7091.7*	7052.7	7041.8	7004.8	6995.0	6959.9	6950.7	*6917.5*	7.0
1437.5	39	39/-1/i	7036.3	6922.3	*7068.6*	7030.4	7020.0	6983.2	6974.0	6939.1	6930.5	*6898.0*	7.0
1466.3	39	39/1/n	6894.6	6785.6	*6919.9*	6885.6	6876.2	6843.7	6835.3	6804.6	6796.7	*6767.7*	6.4
1470.2	39	39/1/i	6875.7	6767.7	*6900.4*	6866.2	6857.3	6825.5	6816.6	6786.6	6778.7	*6750.8*	6.4

Table 5c: Reference wavelengths, λ_{ref}, in nm for the standard wavelength settings, defined as the wavelength at pixel 512 of the 3rd detector. Order number ($\mathcal{O}$), internal wavelength identification (ID), unvignetted spectral range and coverage in vacuum wavenumber (ν, expressed in cm^{-1}) for each of the four detectors are also given. The last column lists the mean dispersion, $\delta\nu$ in 10^{-3} cm^{-1}/pixel, for detector 3. A ^{c} indicates that the order number must also be specified as a parameter. Illumination outside of the unvignetted spectral range is affected by lack of reproducibility at more than 1% level, for a 0.2 arcsec slit: wavenumber values given in italic fall outside the unvignetted range. The accuracy on the positioning of the reference wavelength is ≈ 30 pixels. See Table 4a-4h for spectral ranges in wavelength.

λ_{ref}	$\mathcal{O}$	ID	Unvign. range $\nu_{\min}$	$\nu_{\max}$	Det. 1 $\nu_{\min}$	$\nu_{\max}$	Det. 2 $\nu_{\min}$	$\nu_{\max}$	Det. 3 $\nu_{\min}$	$\nu_{\max}$	Det. 4 $\nu_{\min}$	$\nu_{\max}$	$\delta\nu$
1470.9	38	38/-1/n	6877.6	6765.0	6909.9	6871.9	6861.1	6825.0	6815.7	6781.5	6772.8	6740.4	7.2
1475.3	38	38/-1/i	6856.4	6744.5	6887.5	6850.3	6839.9	6804.6	6794.9	6761.3	6752.7	6720.9	7.1
1504.9	38	38/1/n	6718.2	6611.1	6742.6	6709.2	6699.7	6668.0	6660.0	6630.0	6622.1	6594.1	6.6
1508.9	38	38/1/i	6700.2	6593.7	6723.1	6690.3	6681.4	6650.3	6641.9	6612.9	6605.0	6577.6	6.5
1510.7	37	37/-1/n	6697.0	6585.9	6727.7	6690.8	6680.5	6645.4	6636.1	6602.8	6594.1	6563.0	7.4
1515.2	37	37/-1/i	6676.5	6566.4	6706.5	6669.8	6660.0	6625.1	6615.9	6583.3	6575.1	6544.1	7.3
1545.5	37	37/1/n	6542.4	6437.1	6565.1	6533.0	6524.0	6493.1	6485.1	6455.8	6448.3	6421.0	6.8
1549.7	37	37/1/i	6524.0	6419.7	6546.2	6514.2	6505.3	6475.0	6467.1	6438.7	6431.3	6404.5	6.7
1552.6	36	36/-1/n	6516.8	6407.8	6546.2	6510.0	6500.3	6466.2	6457.0	6424.7	6416.4	6385.7	7.6
1557.3	36	36/-1/i	6496.5	6388.6	6524.9	6489.7	6479.6	6446.2	6437.5	6405.3	6397.1	6367.0	7.5
1588.4	36	36/1/n	6366.2	6262.9	6388.1	6356.5	6347.6	6317.5	6309.9	6281.4	6274.3	6247.7	7.0
1592.7	36	36/1/i	6348.4	6245.7	6369.4	6338.3	6329.9	6300.4	6292.5	6264.9	6257.4	6231.3	6.9
1597.0	35	35/-1/n	6335.9	6229.0	6364.2	6329.1	6319.5	6286.1	6277.5	6246.1	6237.9	6208.1	7.8
1601.8	35	35/-1/i	6316.7	6210.4	6343.6	6309.1	6299.6	6267.2	6258.6	6227.4	6219.3	6190.4	7.7
1633.8	35	35/1/n	6189.7	6088.3	6210.4	6179.7	6171.3	6142.1	6134.6	6106.9	6099.8	6073.9	7.2
1638.2	35	35/1/i	6172.5	6072.0	6192.3	6162.2	6153.8	6125.2	6117.7	6090.9	6083.8	6058.4	7.1
1644.0	34	34/-1/n	6155.4	6050.7	6182.0	6148.2	6138.7	6106.5	6097.9	6067.6	6059.5	6030.6	8.1
1649.0	34	34/-1/i	6136.1	6032.1	6162.2	6128.6	6119.6	6087.5	6079.4	6049.2	6041.6	6013.2	8.0
1681.8	34	34/1/n	6013.2	5914.0	6033.2	6003.5	5995.2	5966.9	5959.5	5932.6	5925.6	5900.7	7.4
1686.4	34	34/1/i	5996.3	5898.0	6015.4	5986.2	5978.0	5950.3	5942.8	5916.8	5909.8	5885.1	7.3
1693.8	33	33/-1/n	5974.8	5872.3	6000.2	5967.3	5958.4	5927.0	5918.6	5888.9	5881.3	5853.4	8.3
1698.9	33	33/-1/i	5956.6	5854.5	5981.2	5948.5	5939.7	5908.8	5900.7	5871.6	5864.1	5836.3	8.2
1732.8	33	33/1/n	5836.7	5739.9	5855.5	5826.5	5818.7	5791.1	5784.0	5758.0	5751.4	5727.0	7.6
1737.4	33	33/1/i	5820.7	5724.4	5839.1	5810.2	5802.5	5775.7	5768.3	5742.8	5736.2	5712.3	7.5
1746.8	32	32/-1/n	5794.1	5693.5	5818.4	5786.4	5777.3	5747.1	5739.2	5710.4	5702.9	5675.7	8.6
1752.1	32	32/-1/i	5776.0	5676.3	5799.5	5768.0	5759.4	5729.3	5721.5	5693.5	5686.0	5659.3	8.5

Table 5d: Reference wavelengths, λ_{ref}, in nm for the standard wavelength settings, defined as the wavelength at pixel 512 of the 3rd detector. Order number ($\mathcal{O}$), internal wavelength identification (ID), unvignetted spectral range and coverage in vacuum wavenumber (ν, expressed in cm^{-1}) for each of the four detectors are also given. The last column lists the mean dispersion, $\delta\nu$ in 10^{-3} cm^{-1}/pixel, for detector 3. A ^{c} indicates that the order number must also be specified as a parameter. Illumination outside of the unvignetted spectral range is affected by lack of reproducibility at more than 1% level, for a 0.2 arcsec slit: wavenumber values given in italic fall outside the unvignetted range. The accuracy on the positioning of the reference wavelength is ≈ 30 pixels. *See Table 4a-4h for spectral ranges in wavelength.*

λ_{ref}	$\mathcal{O}$	ID	Unvign. range $\nu_{\min}$	$\nu_{\max}$	Det. 1 $\nu_{\min}$	$\nu_{\max}$	Det. 2 $\nu_{\min}$	$\nu_{\max}$	Det. 3 $\nu_{\min}$	$\nu_{\max}$	Det. 4 $\nu_{\min}$	$\nu_{\max}$	$\delta\nu$
1786.9	32	32/1/n	5660.3	5565.4	*5678.3*	5650.4	5642.4	5615.8	5608.8	5583.8	5577.2	*5553.7*	7.8
1791.7	32	32/1/i	5644.6	5550.6	*5661.9*	5634.4	5626.8	5600.4	5593.5	5568.9	5562.7	*5539.2*	7.7
1803.1	31	31/-1/n	5613.6	5515.4	*5636.7*	5605.7	5597.2	5567.6	5559.9	5532.2	5524.9	*5498.4*	8.8
1808.6	31	31/-1/i	5596.0	5498.7	*5618.3*	5587.8	5579.4	5550.3	5542.9	5515.4	5508.4	*5482.5*	8.7
1844.6	31	31/1/n	5483.7	5391.1	*5500.6*	5473.5	5466.0	5440.1	5433.3	5409.2	5402.8	*5379.8*	8.1
1849.5	31	31/1/i	5468.7	5376.9	*5484.9*	5458.2	5450.8	5425.3	5418.9	5394.9	5388.8	*5366.2*	8.0
1863.3	30	30/-1/n	5432.7	5336.7	*5454.3*	5424.5	5416.2	5387.9	5380.4	5353.3	5346.4	*5320.8*	9.1
1868.9	30	30/-1/i	5415.9	5320.8	*5436.9*	5407.5	5399.3	5371.4	5363.9	5337.6	5330.5	*5305.6*	9.0
1906.0	30	30/1/n	5307.3	5217.3	*5323.4*	5297.2	5289.9	5264.8	5258.5	5234.8	5228.8	*5206.7*	8.3
1911.1	30	30/1/i	5292.7	5203.2	*5308.1*	5282.3	5275.1	5250.7	5244.1	5221.1	5215.1	*5193.2*	8.2
1927.5	29	29/-1/n	5252.1	5158.6	*5272.9*	5243.8	5235.9	5208.3	5201.0	5175.2	5168.2	*5143.8*	9.4
1933.4	29	29/-1/i	5235.6	5143.0	*5255.7*	5227.1	5219.2	5192.1	5185.1	5159.4	5152.8	*5128.7*	9.3
1971.7	29	29/1/n	5130.8	5043.1	*5146.2*	5120.6	5113.5	5089.6	5083.1	5060.5	5054.6	*5033.0*	8.6
1977.0	29	29/1/i	5116.7	5029.4	*5131.4*	5106.2	5099.2	5075.6	5069.5	5046.9	5041.1	*5020.1*	8.5
1996.4	28	28/-1/n	5071.3	4980.3	*5090.9*	5062.8	5055.1	5028.7	5021.6	4996.5	4990.0	*4966.2*	9.8
2002.4	28	28/-1/i	5055.6	4965.2	*5074.3*	5046.9	5039.3	5013.3	5006.3	4981.6	4975.1	*4952.0*	9.7
2042.1	28	28/1/n	4954.2	4868.8	*4968.7*	4944.1	4937.3	4914.0	4908.0	4885.9	4880.2	*4859.6*	8.9
2047.6	28	28/1/i	4940.5	4855.8	*4954.4*	4930.2	4923.4	4900.5	4894.5	4873.1	4867.4	*4847.1*	8.8
2070.4	27	27/-1/n	4890.5	4801.9	*4908.7*	4881.9	4874.5	4849.0	4842.1	4817.9	4811.6	*4788.8*	10.1
2076.6	27	27/-1/i	4875.4	4787.4	*4893.1*	4866.7	4859.3	4834.2	4827.4	4803.8	4797.5	*4775.1*	10.0
2117.7	27	27/1/n	4777.6	4694.6	*4791.3*	4767.6	4761.0	4738.7	4732.6	4711.4	4706.1	*4686.0*	9.3
2123.4	27	27/1/i	4764.4	4682.1	*4777.4*	4754.2	4747.7	4725.7	4719.9	4699.0	4693.5	*4674.0*	9.2
2150.0	26	26/-1/n	4709.9	4623.6	*4727.0*	4701.0	4694.0	4669.4	4662.9	4639.5	4633.5	*4611.5*	10.5
2156.5	26	26/-1/i	4695.1	4609.8	*4711.9*	4686.3	4679.2	4655.1	4648.6	4625.8	4619.8	*4598.1*	10.4
2199.1	26	26/1/n	4601.3	4520.6	*4614.0*	4591.2	4584.8	4563.3	4557.5	4537.2	4531.9	*4512.6*	9.6
2205.0	26	26/1/i	4588.4	4508.4	*4600.7*	4578.1	4572.1	4550.8	4545.2	4525.1	4520.0	*4501.1*	9.5

Table 5e: Reference wavelengths, λ_{ref}, in nm for the standard wavelength settings, defined as the wavelength at pixel 512 of the 3rd detector. Order number ($\mathcal{O}$), internal wavelength identification (ID), unvignetted spectral range and coverage in vacuum wavenumber (ν, expressed in cm^{-1}) for each of the four detectors are also given. The last column lists the mean dispersion, $\delta\nu$ in 10^{-3} cm^{-1} /pixel, for detector 3. A ^{c} indicates that the order number must also be specified as a parameter. Illumination outside of the unvignetted spectral range is affected by lack of reproducibility at more than 1% level, for a 0.2 arcsec slit: wavenumber values given in italic fall outside the unvignetted range. The accuracy on the positioning of the reference wavelength is ≈ 30 pixels. See Table 4a-4h for spectral ranges in wavelength.

λ_{ref}	$\mathcal{O}$	ID	Unvign. range $\nu_{\min}$	$\nu_{\max}$	Det. 1 $\nu_{\min}$	$\nu_{\max}$	Det. 2 $\nu_{\min}$	$\nu_{\max}$	Det. 3 $\nu_{\min}$	$\nu_{\max}$	Det. 4 $\nu_{\min}$	$\nu_{\max}$	$\delta\nu$
2236.1	25	25/-1/n	4529.0	4445.0	*4545.0*	*4520.2*	4513.2	4489.5	4483.3	4460.9	4455.1	*4433.8*	10.9
2242.8	25	25/-1/i	4514.9	4431.8	*4530.4*	*4505.9*	4499.2	4475.9	4469.7	4447.6	4441.9	*4421.3*	10.8
2287.1	25	25/1/n	4424.6	4346.1	*4436.4*	*4414.4*	4408.4	4387.7	4382.1	4362.6	4357.5	*4339.0*	10.0
2293.2	25	25/1/i	4412.5	4334.6	*4423.8*	*4402.2*	4396.2	4375.8	4370.4	4351.0	4346.1	*4327.9*	9.9
2329.3	24	24/-1/n	4348.2	4266.8	*4363.2*	*4339.1*	4332.6	4310.0	4303.9	4282.5	4276.8	*4256.4*	11.4
2336.3	24	24/-1/i	4334.8	4253.9	*4349.1*	*4325.6*	4319.1	4296.8	4290.9	4269.7	4264.2	*4244.3*	11.3
2382.3	24	24/1/n	4248.4	4171.9	*4259.1*	*4238.0*	4232.3	4212.3	4207.0	4188.1	4183.4	*4165.6*	10.4
2388.7	24	24/1/i	4236.6	4160.8	*4246.8*	*4226.2*	4220.5	4200.8	4195.7	4177.1	4172.4	*4154.9*	10.3
2430.6	23	23/-1/n	4167.7	4088.1	*4181.3*	*4158.4*	4152.0	4130.2	4124.6	4103.9	4098.5	*4079.1*	11.9
2437.9	23	23/-1/i	4154.9	4076.0	*4167.9*	*4145.2*	4139.1	4117.6	4112.0	4091.8	4086.5	*4067.4*	11.8
2485.8	23	23/1/n	4072.2	3997.6	*4081.8*	*4061.6*	4056.0	4037.0	4031.9	4013.8	4009.1	*3992.2*	10.9
2492.5	23	23/1/i	4060.9	3986.9	*4070.0*	*4050.1*	4044.7	4025.9	4020.9	4003.2	3998.6	*3981.8*	10.8
2512.4	22	22/-1/n	4034.4	3954.1	*4048.3*	*4025.1*	4018.6	3996.6	3990.7	3969.8	3964.3	*3944.6*	12.9
2520.3	22	22/-1/i	4021.4	3941.7	*4034.7*	*4011.9*	4005.6	3983.9	3978.0	3957.4	3952.1	*3932.7*	12.8
2570.0	22	22/0/n	3941.0	3865.6	*3951.3*	*3930.7*	3925.0	3905.5	3900.3	3881.8	3877.0	*3859.7*	11.9
2577.3	22	22/0/i	3929.6	3854.8	*3939.3*	*3919.0*	3913.4	3894.2	3889.1	3871.0	3866.2	*3849.1*	11.8
2627.6	22	22/1/n	3851.9	3781.0	*3858.3*	*3840.2*	3835.2	3818.3	3813.7	3797.8	3793.6	*3778.6*	10.8
2634.2^c	22	22/1/i	3841.9	3771.6	*3847.8*	*3830.1*	3825.3	3808.5	3804.0	3788.3	3784.3	*3769.5*	10.7
2632.1^c	21	21/-1/n	3852.1	3773.2	*3864.1*	*3842.0*	3835.8	3814.8	3809.2	3789.3	3784.0	*3765.2*	13.5
2640.5	21	21/-1/i	3839.5	3761.2	*3851.0*	*3829.2*	3823.2	3802.4	3796.9	3777.3	3772.2	*3753.6*	13.4
2692.4	21	21/0/n	3763.1	3688.8	*3771.7*	*3751.9*	3746.6	3727.9	3723.0	3705.4	3700.7	*3684.2*	12.5
2700.0	21	21/0/i	3752.2	3678.5	*3760.2*	*3741.0*	3735.5	3717.2	3712.4	3695.1	3690.6	*3674.2*	12.3
2752.6	21	21/1/n	3678.2	3608.2	*3683.1*	*3665.8*	3661.1	3644.8	3640.6	3625.3	3621.4	*3607.0*	11.3
2759.5	21	21/1/i	3668.6	3599.2	*3673.1*	*3656.2*	3651.5	3635.6	3631.3	3616.4	3612.5	*3598.3*	11.2
2763.9	20	20/-1/n	3669.9	3591.8	*3679.9*	*3658.8*	3653.0	3632.9	3627.7	3608.5	3603.6	*3585.6*	14.2
2772.7	20	20/-1/i	3657.9	3580.4	*3667.4*	*3646.7*	3640.9	3621.2	3616.0	3597.3	3592.3	*3574.7*	14.0

Table 5f: Reference wavelengths, λ_{ref}, in nm for the standard wavelength settings, defined as the wavelength at pixel 512 of the 3rd detector. Order number ($\mathcal{O}$), internal wavelength identification (ID), unvignetted spectral range and coverage in vacuum wavenumber (ν, expressed in cm^{-1}) for each of the four detectors are also given. The last column lists the mean dispersion, $\delta\nu$ in 10^{-3} cm^{-1}/pixel, for detector 3. A ^{c} indicates that the order number must also be specified as a parameter. Illumination outside of the unvignetted spectral range is affected by lack of reproducibility at more than 1% level, for a 0.2 arcsec slit: wavenumber values given in italic fall outside the unvignetted range. The accuracy on the positioning of the reference wavelength is ≈ 30 pixels. *See Table 4a-4h for spectral ranges in wavelength.*

λ_{ref}	$\mathcal{O}$	ID	Unvign. range ν_{min}	ν_{max}	Det. 1 ν_{min}	ν_{max}	Det. 2 ν_{min}	ν_{max}	Det. 3 ν_{min}	ν_{max}	Det. 4 ν_{min}	ν_{max}	$\delta\nu$
2827.0	20	20/0/n	3585.5	3511.7	*3592.1*	3573.3	3568.1	3550.4	3545.7	3529.0	3524.6	*3508.8*	13.1
2835.0	20	20/0/i	3575.0	3501.8	*3581.3*	3562.8	3557.7	3540.2	3535.6	3519.0	3514.8	*3499.2*	13.0
2890.0	20	20/1/n	3505.0	3435.1	*3508.0*	3491.6	3487.0	3471.6	3467.5	3452.9	3449.1	3435.5	11.9
2897.3	20	20/1/i	3495.8	3426.4	*3498.5*	3482.3	3477.9	3462.6	3458.7	3444.4	3440.6	3427.1	11.7
2909.6	19	19/-1/n	3488.0	3410.1	*3495.6*	3475.6	3470.1	3451.0	3445.9	3427.8	3423.1	*3406.1*	14.9
2918.8	19	19/-1/i	3476.7	3399.4	*3483.8*	3464.2	3458.7	3439.9	3435.0	3417.2	3412.6	*3395.8*	14.8
2975.8	19	19/0/n	3408.2	3334.1	*3412.5*	3394.7	3389.7	3372.9	3368.4	3352.4	3348.3	*3333.3*	13.8
2984.2	19	19/0/i	3398.4	3324.8	*3402.2*	3384.7	3379.7	3363.2	3358.9	3343.1	3339.0	*3324.2*	13.6
3041.9	19	19/1/n	3332.0	3261.5	*3332.8*	3317.2	3312.9	3298.3	3294.4	3280.5	3276.9	3263.9	12.5
3049.5	19	19/1/i	3323.5	3253.3	*3323.8*	3308.5	3304.3	3289.8	3286.0	3272.5	3268.8	3256.2	12.4
3071.5	18	18/-1/n	3306.7	3227.9	*3311.4*	3292.4	3287.1	3269.0	3264.3	3247.2	3242.8	*3226.5*	15.8
3081.3	18	18/-1/i	3295.9	3217.6	*3300.1*	3281.4	3276.2	3258.5	3253.8	3237.0	3232.6	*3216.7*	15.6
3141.1	18	18/0/n	3231.5	3156.2	*3232.9*	3216.1	3211.4	3195.4	3191.1	3176.0	3172.1	3157.9	14.6
3150.0	18	18/0/i	3222.2	3147.2	*3223.1*	3206.5	3201.9	3186.1	3182.1	3167.2	3163.4	3149.3	14.4
3210.6	18	18/1/n	3159.8	3087.5	3157.8	3143.0	3138.8	3124.9	3121.2	3108.1	3104.7	3092.3	13.2
3218.7	18	18/1/i	3151.6	3079.7	3149.1	3134.6	3130.6	3116.9	3113.3	3100.4	3097.0	3084.9	13.1
3252.6	17	17/-1/n	3125.9	3045.1	*3127.0*	3109.1	3104.0	3087.1	3082.5	3066.4	3062.2	3046.9	16.7
3262.9	17	17/-1/i	3115.8	3035.4	*3116.4*	3098.8	3093.9	3077.1	3072.7	3056.8	3052.7	3037.7	16.5
3325.8	17	17/0/n	3055.5	2977.6	3053.3	3037.4	3033.1	3018.0	3014.0	2999.7	2996.0	2982.5	15.4
3335.3	17	17/0/i	3046.6	2969.0	3044.0	3028.4	3024.0	3009.1	3005.3	2991.2	2987.6	2974.3	15.2
3399.1	17	17/1/n	2988.1	2912.8	2982.6	2968.7	2964.8	2951.6	2948.1	2935.7	2932.6	2920.9	14.0
3407.7	17	17/1/i	2980.4	2905.4	2974.5	2960.8	2957.0	2944.0	2940.7	2928.4	2925.3	2913.8	13.8
3456.3	16	16/-1/n	2945.9	2861.6	2942.6	2925.8	2921.1	2905.1	2900.9	2885.7	2881.8	2867.4	17.7
3467.2	16	16/-1/i	2936.4	2852.5	2932.7	2916.1	2911.5	2895.8	2891.7	2876.7	2872.8	2858.7	17.5
3533.7	16	16/0/n	2880.1	2798.3	2873.7	2858.7	2854.5	2840.3	2836.6	2823.2	2819.7	2807.0	16.4
3543.8	16	16/0/i	2871.7	2790.2	2864.9	2850.1	2846.1	2832.1	2828.5	2815.2	2811.8	2799.3	16.2

Table 5g: Reference wavelengths, λ_{ref}, in nm for the standard wavelength settings, defined as the wavelength at pixel 512 of the 3rd detector. Order number ($\mathcal{O}$), internal wavelength identification (ID), unvignetted spectral range and coverage in vacuum wavenumber (ν, expressed in cm^{-1}) for each of the four detectors are also given. The last column lists the mean dispersion, $\delta\nu$ in 10^{-3} cm^{-1}/pixel, for detector 3. A ^{c} indicates that the order number must also be specified as a parameter. Illumination outside of the unvignetted spectral range is affected by lack of reproducibility at more than 1% level, for a 0.2 arcsec slit: wavenumber values given in italic fall outside the unvignetted range. The accuracy on the positioning of the reference wavelength is ≈ 30 pixels. *See Table 4a-4h for spectral ranges in wavelength.*

λ_{ref}	$\mathcal{O}$	ID	Unvign. range $\nu_{\min}$	$\nu_{\max}$	Det. 1 $\nu_{\min}$	$\nu_{\max}$	Det. 2 $\nu_{\min}$	$\nu_{\max}$	Det. 3 $\nu_{\min}$	$\nu_{\max}$	Det. 4 $\nu_{\min}$	$\nu_{\max}$	$\delta\nu$
3611.1	16	16/1/n	2817.3	2737.6	2807.6	2794.4	2790.8	2778.3	2775.1	2763.4	2760.4	2749.4	14.9
3620.2	16	16/1/i	2810.1	2730.5	2799.9	2787.0	2783.4	2771.2	2768.0	2756.6	2753.5	2742.8	14.7
3646.3	15	15/-2/n	2798.2	2707.8	2791.3	2774.7	2770.1	2754.2	2750.0	2735.0	2731.0	2716.8	19.5
3658.4	15	15/-2/i	2788.9	2698.7	2781.5	2765.1	2760.6	2745.0	2740.9	2726.1	2722.2	2708.2	19.3
3728.3	15	15/-1/n	2735.8	2647.4	2725.8	2710.9	2706.8	2692.7	2688.9	2675.5	2672.0	2659.4	18.2
3739.5	15	15/-1/i	2727.5	2639.4	2717.1	2702.4	2698.3	2684.4	2680.7	2667.6	2664.1	2651.7	18.0
3810.3	15	15/1/n	2676.1	2589.5	2663.0	2649.8	2646.1	2633.7	2630.3	2618.6	2615.5	2604.4	16.7
3820.5	15	15/1/i	2668.9	2582.5	2655.3	2642.4	2638.7	2626.5	2623.2	2611.6	2608.7	2597.7	16.5
3892.2	15	15/2/n	2619.0	2534.0	2602.6	2591.1	2588.0	2577.2	2574.3	2564.2	2561.5	2552.0	15.0
3901.4	15	15/2/i	2612.7	2527.9	2596.0	2584.7	2581.6	2571.0	2568.2	2558.2	2555.6	2546.3	14.8
3908.0	14	14/-2/n	2617.4	2520.4	2604.4	2588.9	2584.6	2569.8	2565.9	2551.9	2548.2	2534.9	20.9
3920.9	14	14/-2/i	2608.7	2511.9	2595.2	2580.0	2575.7	2561.2	2557.3	2543.6	2539.9	2526.9	20.7
3995.0	14	14/-1/n	2559.8	2464.5	2543.8	2529.9	2526.1	2512.9	2509.4	2496.9	2493.6	2481.8	19.5
4007.0	14	14/-1/i	2552.1	2456.9	2535.7	2522.0	2518.2	2505.2	2501.8	2489.5	2486.3	2474.7	19.3
4082.0	14	14/1/n	2504.8	2410.9	2485.8	2473.4	2470.0	2458.3	2455.3	2444.3	2441.4	2431.1	17.9
4093.0	14	14/1/i	2498.0	2404.2	2478.6	2466.5	2463.1	2451.6	2448.6	2437.8	2435.0	2424.8	17.7
4169.1	14	14/2/n	2452.0	2359.3	2429.8	2419.1	2416.1	2406.0	2403.3	2393.8	2391.4	2382.5	16.1
4178.9	14	14/2/i	2446.2	2353.6	2423.7	2413.1	2410.2	2400.3	2397.6	2388.3	2385.9	2377.2	15.9
4210.3	13	13/-2/n	2437.4	2332.0	2417.3	2402.9	2398.9	2385.3	2381.6	2368.7	2365.2	2352.9	22.5
4224.2	13	13/-2/i	2429.4	2324.2	2408.8	2394.7	2390.7	2377.3	2373.7	2360.9	2357.6	2345.5	22.3
4302.9	13	13/-1/n	2384.7	2280.7	2361.8	2348.9	2345.3	2333.1	2329.8	2318.2	2315.2	2304.3	21.0
4315.8	13	13/-1/i	2377.6	2273.7	2354.2	2341.5	2338.0	2326.0	2322.8	2311.4	2308.4	2297.6	20.8
4395.5	13	13/1/n	2334.3	2231.4	2308.5	2297.0	2293.8	2283.0	2280.2	2269.9	2267.3	2257.6	19.3
4407.3	13	13/1/i	2328.0	2225.3	2301.8	2290.6	2287.4	2276.8	2274.0	2263.9	2261.3	2251.8	19.1
4488.1	13	13/2/n	2285.9	2184.2	2257.2	2247.2	2244.4	2235.0	2232.5	2223.7	2221.4	2213.1	17.4
4498.7	13	13/2/i	2280.4	2178.8	2251.4	2241.6	2238.9	2229.7	2227.2	2218.5	2216.3	2208.1	17.2

Table 5h: Reference wavelengths, λ_{ref}, in nm for the standard wavelength settings, defined as the wavelength at pixel 512 of the 3rd detector. Order number ($\mathcal{O}$), internal wavelength identification (ID), unvignetted spectral range and coverage in vacuum wavenumber (ν, expressed in cm^{-1}) for each of the four detectors are also given. The last column lists the mean dispersion, $\delta\nu$ in 10^{-3} cm^{-1}/pixel, for detector 3. A ^{c} indicates that the order number must also be specified as a parameter. Illumination outside of the unvignetted spectral range is affected by lack of reproducibility at more than 1% level, for a 0.2 arcsec slit: wavenumber values given in italic fall outside the unvignetted range. The accuracy on the positioning of the reference wavelength is ≈ 30 pixels. *See Table 4a-4h for spectral ranges in wavelength.*

λ_{ref}	$\mathcal{O}$	ID	Unvign. range ν_{min}	ν_{max}	Det. 1 ν_{min}	ν_{max}	Det. 2 ν_{min}	ν_{max}	Det. 3 ν_{min}	ν_{max}	Det. 4 ν_{min}	ν_{max}	$\delta\nu$
4563.6	12	12/-2/n	2258.1	2142.9	2230.1	2216.9	2213.2	2200.6	2197.2	2185.3	2182.2	2170.8	24.3
4578.6	12	12/-2/i	2250.7	2135.7	2222.3	2209.3	2205.7	2193.3	2190.0	2178.2	2175.1	2164.0	24.1
4662.3	12	12/-1/n	2210.3	2096.3	2179.7	2167.8	2164.5	2153.2	2150.2	2139.5	2136.8	2126.6	22.7
4676.2	12	12/-1/i	2203.7	2090.0	2172.8	2161.0	2157.8	2146.7	2143.8	2133.2	2130.5	2120.6	22.5
4761.0	12	12/1/n	2164.4	2051.7	2131.3	2120.7	2117.8	2107.7	2105.1	2095.7	2093.2	2084.3	20.9
4773.8	12	12/1/i	2158.6	2046.0	2125.1	2114.7	2111.8	2102.0	2099.4	2090.1	2087.7	2079.0	20.7
4859.6	12	12/2/n	2120.4	2008.8	2084.7	2075.5	2072.9	2064.2	2061.9	2053.7	2051.5	2043.9	18.9
4871.1	12	12/2/i	2115.5	2003.8	2079.4	2070.3	2067.8	2059.2	2056.9	2048.9	2046.8	2039.3	18.7
4929.6	11	11/-2/n	2101.3	1974.7	2065.9	2053.2	2049.6	2037.5	2034.3	2022.8	2019.8	2008.9	27.3
4946.5	11	11/-2/i	2094.2	1967.7	2058.4	2045.8	2042.4	2030.5	2027.3	2016.0	2013.0	2002.3	27.0
5034.8	11	11/-1/n	2057.5	1932.2	2019.9	2008.4	2005.2	1994.3	1991.4	1981.0	1978.3	1968.5	25.6
5050.6	11	11/-1/i	2051.1	1926.0	2013.1	2001.8	1998.6	1987.9	1985.1	1974.9	1972.2	1962.6	25.4
5139.9	11	11/0/n	2015.5	1891.5	1975.7	1965.4	1962.5	1952.7	1950.2	1941.0	1938.5	1929.8	23.8
5154.6	11	11/0/i	2009.8	1885.9	1969.7	1959.5	1956.7	1947.1	1944.5	1935.5	1933.1	1924.6	23.6
5245.1	11	11/1/n	1974.5	1853.0	1933.2	1924.0	1921.5	1912.9	1910.6	1902.5	1900.4	1892.8	21.8
5258.4	11	11/1/i	1969.2	1848.4	1927.9	1918.9	1916.4	1907.9	1905.7	1897.7	1895.7	1888.2	21.5
5350.2	11	11/2/n	1933.5	1817.3	1892.1	1884.2	1882.0	1874.5	1872.6	1865.6	1863.8	1857.3	19.5
5362.1	11	11/2/i	1929.0	1813.3	1887.5	1879.7	1877.6	1870.3	1868.4	1861.5	1859.7	1853.3	19.2

16 Free wavelength settings

Table 6a: Available ranges of the reference wavelength λ_{ref} for the free settings. Values should be rounded to the closest 0.1 nm. A ^{c} besides an order number indicates that some reference wavelengths in that order are common to an adjacent order (see Table 7), in which case the order number must also be specified as a template parameter.

$\mathcal{O}$	$\lambda_{\text{ref}}^{min}$	$\lambda_{\text{ref}}^{max}$
59	958.3	961.0
58	974.8	977.6
57	991.9	994.8
56	1009.6	1012.5
55	1028.0	1030.9
54	1047.0	1050.0
53	1066.8	1069.8
52	1087.3	1090.4
51	1108.6	1111.8
50	1130.8	1134.0
49	1153.9	1157.2
48	1177.9	1181.3
47	1203.0	1206.4
46	1229.1	1232.6
45	1256.4	1260.0
44	1285.0	1288.7
43^c	1299.8	1333.5
42^c	1330.8	1365.2
41^c	1363.3	1398.5
40^c	1397.3	1433.5
39^c	1433.2	1470.2
38	1470.9	1508.9
37	1510.7	1549.7
36	1552.6	1592.7
35	1597.0	1638.2

Table 6b: Available ranges of the reference wavelength λ_{ref} for the free settings. Values should be rounded to the closest 0.1 nm. A ^{c} besides an order number indicates that some reference wavelengths in that order are common to an adjacent order (see Table 7), in which case the order number must also be specified as template parameter.

$\mathcal{O}$	$\lambda_{\mathrm{ref}}^{min}$	$\lambda_{\mathrm{ref}}^{max}$
34	1644.0	1686.4
33	1693.8	1737.4
32	1746.8	1791.7
31	1803.1	1849.5
30	1863.3	1911.1
29	1927.5	1977.0
28	1996.4	2047.6
27	2070.4	2123.4
26	2150.0	2205.0
25	2236.1	2293.2
24	2329.3	2388.7
23	2430.6	2492.5
22^c	2512.4	2634.2
21^c	2632.1	2759.5
20	2763.9	2897.3
19	2909.6	3049.5
18	3071.5	3218.7
17	3252.6	3407.7
16	3456.3	3620.2
15	3646.3	3901.4
14	3908.0	4178.9
13	4210.3	4498.7
12	4563.6	4871.1
11	4929.6	5362.1

17 Reference wavelengths common to different orders

Table 7: Ranges of reference wavelengths that are common to 2 successive orders: for wavelength in these ranges (inclusive), it is mandatory to specify the grating order as a template parameter. This is valid for both standard and free wavelength settings.

Common ranges		Orders
$\lambda_{\min}$	$\lambda_{\max}$	
1330.8	1333.5	42, 43
1363.2	1365.3	41, 42
1397.3	1398.5	40, 41
1433.2	1433.5	39, 40
2632.1	2634.2	21, 22

18 Calibration source for wavelength calibration

The table given below lists the recommended calibration source required by the wavelength calibration template attached immediately before or after a science template. Such a template is required if a wavelength calibration more accurate than ≈ 3 pixels is needed; otherwise, the internal model of the instrument is sufficient.

If the entry is *sky emission lines* or *sky absorption lines*, then neither the ThAr lamp nor the Halogen + N_2O or Halogen + CO gas cells provides enough lines for any useful wavelength calibration: the wavelength calibration must therefore be made using the science data themselves. Obviously, the *sky emission lines* cover the whole slit length, while the *sky absorption lines* are only useful in front of objects showing a continuum. The Halogen + CO gas cell is a good option for settings in order 24.

Note that sky emission lines can also be used red-ward of ≈ 2500 nm, instead of the Halogen+N_2O gas cell. The exposure time calculator (ETC) also allows one to determine the density of sky emission lines, sky absorption lines or of lines from the Halogen lamp + N_2O gas cell. A ThAr line list for the wavelength range covered by CRIRES is part of the static tables available at http://www.eso.org/observing/dfo/quality/CRIRES/pipeline/pipe_calib.html. However, a new table providing twice as many identified lines should be available shortly (see §7.2.1).

The CRIRES team is considering various solutions to provide accurate wavelength calibration in the spectral regions not yet covered by the current scheme. Updates will be posted in the instrument web page: http://www.eso.org/instruments/crires/. Potential users should email their respective contacts (§1.4).

Table 8a: Recommended wavelength calibration source.

Order	Source	Comment
59	ThAr	full range
58	ThAr	full range
57	ThAr	full range
56	ThAr	full range
55	ThAr	full range
54	ThAr	full range
53	ThAr	full range
52	ThAr	full range
51	ThAr	full range
50	ThAr	full range
49	ThAr	full range
48	ThAr	full range
47	ThAr	full range
46	ThAr	full range
45	ThAr	full range
44	ThAr	full range
43	ThAr	full range
42	ThAr	full range
41	ThAr	full range
40	ThAr	full range
39	ThAr	full range
38	ThAr	no lines in range $[1514, 1520]$
37	ThAr	no lines in range $[1514, 1523]$
36	ThAr	no lines in range $[1583, 1594]$
35	ThAr	no lines in range $[1583, 1594]$
34	ThAr	no lines in range $[1659, 1672]$
33	ThAr	no lines in ranges $[1659, 1672]$, $[1698, 1701]$
32	ThAr	no lines in ranges $[1730, 1739]$, $[1738, 1747]$, $[1764, 1784]$, $[1803, 1811]$
31	ThAr	no lines in ranges $[1764, 1784]$, $[1803, 1811]$, $[1816, 1825]$
30	ThAr	no lines in range $[1880, 1890]$

Table 8b: Recommended wavelength calibration source.

Order	Source	Comment
29	ThAr	few lines
28	ThAr	few lines
27	ThAr	few lines
26	ThAr	few lines
25	sky absorption lines	full range
24	HALOGEN+CO	full range
23	sky absorption lines	full range
22	HALOGEN+N$_2$O	useful ranges $[2581.0, 2640.6]$, $[2645.4, 2652.7]$
21	HALOGEN+N$_2$O	useful range $[2651.2, 2698.3]$
20	HALOGEN+N$_2$O	useful ranges $[2742.3, 2781.3]$, $[2847.8, 2917.7]$
19	HALOGEN+N$_2$O	useful range $[2860.6, 3016.7]$
18	sky emission lines	full range
17	sky emission lines	full range
16	HALOGEN+N$_2$O	useful range $[3533.8, 3629.9]$
15	HALOGEN+N$_2$O	useful ranges $[3581.6, 3629.5]$, $[3831.8, 3927.0]$
14	HALOGEN+N$_2$O	useful ranges $[3831.8, 4145.9]$, $[4161.9, 4177.9]$
13	HALOGEN+N$_2$O	useful ranges $[4136.7, 4145.9]$, $[4161.9, 4177.9]$, $[4234.3, 4368.8]$ $[4411.7, 4528.6]$
12	HALOGEN+N$_2$O	useful range $[4484.0, 4702.4]$
11	HALOGEN+N$_2$O	useful range $[5250.0, 5395.6]$

Part V

Tips for successful observations

19   Checklist

In this section, we provide a number of recommendations in order to increase the chances that a program is executed successfully.

19.1   Phase 1

Before submitting an ESO proposal involving CRIRES, the following points should be taken into account:

1. Tables 4a-4h and 5a-5h provide the current best estimate of the unvignetted spectral ranges for each standard setting, i.e, the one for which illumination should be reproducible to the 1% level. If the interesting spectral features are affected by detector glow or vignetting in a standard setting, a free wavelength setting may be chosen to optimize their location on the detectors. See also § 7.1.

2. The expected S/N for each object should be given in the time justification; it must be stated if it corresponds to the S/N per pixel or per resolution element. For extended objects, it is important to state if it corresponds to the S/N per pixel in the spatial direction or over the whole expected extension along the spatial direction.

3. Overheads can only be reasonably estimated if the DIT has been appropriately chosen. Although long DITs allow to reduce overheads, it is important to note that (a) the total object plus sky spectrum should not have more than about 10,000 ADUs ($\approx 70,000 \mathrm{e}^{-1}$); this is particularly relevant for observations in the L or M bands; (b) for observations of relatively faint targets in the J, H or K bands, the choice of long DITs (≥ 60s) should be balanced with the increased noise brought by the detector glow and the advantage that multiple exposures allow a better flat-field correction, in particular if some jitter is introduced.

4. *Service mode* programmes are executed using Observing Blocks (OBs) that should last less than 1 hour. Except for an associated telluric OB, a science OB is the typical unit of observation that should be completely independent of other OBs of the same programme. Indeed, different OBs of a given programme are usually observed in different nights. As a consequence:

   (a) The amount of time to request has to take into account all overheads, in particular, the ones associated with preset and acquisition for each OB.

   (b) Typically, each science OB should have one associated telluric OB. Some exceptions occur: for example, when targeting a specific line located away from any telluric absorption features. The amount of time to request has to take into account the time to execute all associated telluric OBs. In particular, one should *not* assume that one telluric OB will be useful for several science OBs.

19.2   Phase 2

1. If the slit orientation on the sky is not important for the science objective, the ELEV mode is strongly recommended. This avoids slit losses due to atmospheric refraction.

2. In the choice of wavelength settings, the interesting science features should avoid the vignetted and detector glow areas: the latter point is particularly critical for DITs longer than 60s. The wavelength coverage of the chosen wavelength settings can be compared with the output spectra of the CRIRES ETC. The position of the science features can be compared with Fig. 13 and the unvignetted range in Tables 4a-4h or 5a-5h. If the interesting spectral features are affected by detector glow or vignetting in a standard setting, a free wavelength setting may be chosen to optimize their location on the detectors. See also § 7.1

3. The selection of the DIT value does not only depend on the brightness of the target but also on the brightness of the infrared sky. The longer the wavelength, the brighter the sky, the shorter the DIT (to avoid saturation of the sky). This should be carefully checked with the help of the ETC.

4. In case the target is not the SV guide star (or the pointing position is located between two or more targets in the slit), special care has to be taken to correctly define the offsets. See §14.1.1 for definitions and conventions.

5. It is worth noting that the default telescope pointing is not centered on the 31″ slit (see Fig. 17). The distance to the North and South edge are 12″ and 19″, respectively. Therefore the nodding throw and jitter width should be chosen carefully, such that the targets stay in the slit area at all nodding/jittering positions. This is especially important when an extended object or multiple targets are in the slit.

6. Telluric standards should be chosen close in right ascension and airmass to the target. To avoid any confusion in the assignment of a telluric to a science target, it is recommended to name the telluric OB according to the science OB, i.e. 'CAL_<science OB name>'.

7. Finding charts should be created from infrared images (e.g. 2MASS) and should clearly indicate the location of the target, AO star and SVGS. The necessary information on the target, AO and SV stars should be given in the Instrument Comments field of each OB.

8. More detailed information on Phase 2 requirements can be found in §11 and at http://www.eso.org/sci/observing/phase2/P2PP/P2PPTool.html.